

UCSF

UC San Francisco Electronic Theses and Dissertations

Title

Genetic Analysis Uncovers Functions of Atypical Polyubiquitin Chains

Permalink

<https://escholarship.org/uc/item/0d50q2gw>

Author

Meza Gutierrez, Fernando

Publication Date

2018

Peer reviewed|Thesis/dissertation

Genetic Analysis Uncovers Functions of Atypical Polyubiquitin
Chains

by

Fernando Meza Gutierrez

DISSERTATION

Submitted in partial satisfaction of the requirements for the degree of

DOCTOR OF PHILOSOPHY

in

Biochemistry and Molecular Biology

in the

GRADUATE DIVISION

of the

UNIVERSITY OF CALIFORNIA, SAN FRANCISCO

Acknowledgements

I reach the end of my doctoral studies filled with gratitude towards all those who have contributed to making this possible. Earning a doctorate in biochemistry and molecular biology was quite unlikely given my personal background. The unwavering support and confidence provided by remarkable teachers and mentors allowed me to reach beyond what I thought were my limitations and complete my graduate studies. In particular, I would like to thank Dr. Leilani Miller, Professor of Biology at Santa Clara University and my undergraduate research advisor, for her scientific mentorship and friendship for almost a decade. Dr. David P. Toczyski, Professor of Biochemistry and Biophysics at the University of California San Francisco and my doctoral thesis advisor, pushed me to become the best scientist possible, supported me personally, and created an amazing laboratory environment that allowed me to pursue my scientific interests freely and fully.

I would like to thank Dr. Deniz Simsek, who performed the genetic interaction screen that served as the foundation of my doctoral research. My dissertation would also not have been possible without great collaborators, especially the laboratories of Drs. Nevan Krogan and David O. Morgan. I would like to acknowledge my colleagues in the Toczyski Laboratory. Together, we created an enriching, collaborative, supportive, and respectful environment that allowed me to focus fully on pursuing my scientific curiosity. To the members of my thesis committee, which over the years included Drs. Jeffrey Cox, Robert Edwards, David O. Morgan, and James Fraser, I extend my deepest gratitude for their mentorship, advice, support, and engagement in my research.

The financial support provided by the UC-MEXUS Doctoral Fellowship, Mexico's Consejo Nacional de Ciencia y Tecnología (CONACYT), and the Discovery Fellows Program was invaluable in permitting me to pursue my doctoral research free from financial concerns or limitations, and allowed me to expand my training by participating in scientific conferences.

The pursuit of a doctorate degree is an intense, challenging, and time-consuming endeavor. My friends and family grounded me, provided perspective, and supported me throughout the process. My partner, Karina Perlaza, supported me through my challenges and failures with love, understanding, and compassion. She also pushed me to become a better scientist and to pursue my goals fearlessly. My family has supported me throughout my academic career and given me the space to pursue my interests.

Chapter 1 is reproduced from a manuscript that is currently in preparation for submission. Co-authors of the manuscript include Deniz Simsek, Arda Mizrak, Jeffrey Johnson, Adam Deutschbauer, Hannes Braberg, Jiewei Xu, Michael Shales, Michelle Nguyen, Raquel Tamse-Kuehn, Curt Palm, David O. Morgan, Lars Steinmetz, Nevan J. Krogan, David P. Toczyski

Chapter 2 is reproduced from an article that is currently in preparation in collaboration with Deniz Simsek and David P. Toczyski. The article will be contributed to a volume of the publication *Methods in Enzymology*.

Genetic Analysis Uncovers Functions of Atypical Polyubiquitin Chains

Fernando Meza Gutierrez

Abstract

Polyubiquitination, the covalent attachment of a chain of ubiquitin to lysine (K) residues on proteins, is a highly conserved and abundant post-translational modification. It most commonly targets proteins for degradation but also has non-proteolytic functions. Polyubiquitin chains linked by each of the seven lysines on ubiquitin adopt distinct conformations. This structural variation is thought to explain the functional diversity of polyubiquitination. Although the functions of K48 and K63-linked chains are well understood, the functions of chains linked by the remaining ubiquitin lysine residues remain to be discovered. The aim of the dissertation work described here was to elucidate the functions of atypical polyubiquitin chains in *Saccharomyces cerevisiae*. In Chapters 1 and 2, a high-throughput genetic screen that served to uncover the genetic interactions of six of the seven ubiquitin-chain types is described. This genetic screen led to the discovery of two novel functions in amino acid homeostasis and cell cycle regulation by polyubiquitin chains linked through lysine 11 of ubiquitin. Chapter 3 details a novel method that is currently being developed to comprehensively identify substrates of specific polyubiquitin chain types using top-down proteomics. Altogether, the present work has advanced our understanding of the functions of polyubiquitin and provided novel methodologies to study the ubiquitin-proteasome system.

Table of Contents

Chapter 1: Genetic Analysis uncovers functions of atypical polyubiquitin chains.....	1
References for Chapter 1.....	21
Chapter 2: A genetic approach to study polyubiquitination in <i>Saccharomyces cerevisiae</i>	85
References for Chapter 2.....	103
Chapter 3: A top-down mass spectrometry-based method to identify substrates of polyubiquitin chains.....	111
References for Chapter 3.....	120

List of Figures

Chapter 1

Figure 1: The ubiquitin linkage SGA reveals the genetic interactome of polyubiquitin chain types and functional relationships between lysines of ubiquitin.....	59
Figure 2: Genetic interactions of individual ubiquitin linkage types.....	60
Figure 3: K11 linkages are functionally redundant with threonine biosynthesis and promote threonine import.....	61
Figure 4: K11 linkages contribute to APC-substrate turnover.....	62
Figure 1-figure supplement 1: Engineering of <i>ubi2-4</i>	63
Figure 1-figure supplement 2: Analysis of ubiquitin levels engineered strains.....	64
Figure 1-figure supplement 3: Engineering of strains expressing low levels of ubiquitin, and K48R ubiquitin mutants.....	65
Figure 1-figure supplement 4: The ubiquitin allele SGA protocol.....	66
Figure 1-figure supplement 5: Genetic modifications modestly increase the sporulation efficiency of the S288C yeast strain.....	67
Figure 1-figure supplement 6: Deletion of <i>UBI1</i> in K-to-R ubiquitin mutant strains and the in the SK1 gene deletion array.....	68
Figure 3-figure supplement 1: Gnp1 is a major threonine permease.....	69
Figure 4-figure supplement 1: Cell cycle profiling by FACS.....	70

Chapter 2

Figure 1: A plot of all the S-scores in the 4-marker ubiquitin SGA.	94
Figure 2: The conditional nature of some genetic interactions.	102

Chapter 3

Figure 1: The proteolysis of a K63-polyubiquitinated substrate with Lys-C /N.....	112
Figure 2: Digestion of total ubiquitin with Lys-C.....	116
Figure 3: Determination of activity of Lys-N from commercial sources.	117
Figure 4: Digestion of purified Sna3 with Lys-N.....	119

List of Tables

Chapter 1

Table S1: Plasmids used in this study.....	71
Table S2: Strains used in this study.....	72
Table S3: Oligonucleotides used in this study.....	77

Chapter 1

Genetic Analysis Reveals Functions of Atypical Polyubiquitin Chains

Fernando Meza-Gutierrez*, Deniz Simsek*, Arda Mizrak, Adam Deutschbauer, Hannes Braberg, Jeffrey Johnson, Jiewei Xu, Michael Shales, Michelle Nguyen, Raquel Tamse-Kuehn, Curt Palm, David O. Morgan, Lars Steinmetz, Nevan J. Krogan, David P.

Toczyski

Although polyubiquitin chains linked through all lysines of ubiquitin exist, specific functions are well-established only for lysine-48 and lysine-63 linkages in *Saccharomyces cerevisiae*. To identify pathways that are regulated by distinct polyubiquitin chains, strains with lysine-to-arginine ubiquitin mutations were crossed to a gene deletion array. Double mutant strains were analyzed to identify genes having genetic interactions with specific linkage types. The K11R mutant had strong genetic interactions with threonine biosynthetic genes. Consistently, we found that K11R mutants import threonine poorly. The K11R mutant also exhibited a strong genetic interaction with a subunit of the anaphase-promoting complex, suggesting a role in cell cycle regulation. K11-linkages are important for vertebrate APC function, but this was not thought to be the case in yeast. We show that the yeast APC also modifies substrates with K11-linkages *in vitro*, and that those chains contribute to normal APC-substrate turnover *in vivo*. This study reveals comprehensive genetic interactomes of polyubiquitin chains, and characterizes the role of K11-chains in two biological pathways.

*These authors contributed equally to this work.

Introduction

The ubiquitination of proteins is a highly conserved posttranslational modification that can alter the stability, localization, and function of proteins [1]. Ubiquitination regulates a broad range of important cellular pathways including, among many others, the DNA damage response [2,3], apoptosis [4], cell cycle progression [5], immune and inflammatory responses [6], and transcription [7]. Three enzyme classes mediate the covalent attachment of ubiquitin, a 76 amino acid protein, to target proteins: An E1 ubiquitin-activating enzyme activates ubiquitin for transfer to an E2 ubiquitin-conjugating enzyme, which then interacts with an E3 ubiquitin ligase to transfer ubiquitin to lysine residues on the target protein [8]. This enzymatic cascade can also transfer ubiquitin onto lysine residues of ubiquitin itself, thereby generating chains of polyubiquitin on target proteins [8].

Ubiquitin has seven acceptor lysines (K6, K11, K27 K29, K33, K48, and K63), all of which are used *in vivo* to generate polyubiquitin chains [9]. Polyubiquitin can also be linked through the N-terminal amino group of methionine 1 in ubiquitin, termed linear ubiquitin chains. K48 and K11 are the most abundant ubiquitin linkage types—each accounting for about a third of ubiquitin linkages in yeast—while the remaining five are present in relatively lower amounts [9]. Ubiquitin chains vary in their three-dimensional conformations. K48-linked chains, for example, adopt a closed conformation wherein ubiquitin's hydrophobic patch is sequestered in the interface between two adjacent ubiquitin protomers [10]. In contrast, K63-linked chains assume an extended conformation devoid of non-covalent contacts between ubiquitin monomers [11].

The structural diversity of polyubiquitin chains gives rise to disparate fates for protein targets [10]. K48-linked chains, for example, specify proteins for proteasomal degradation [12], while K63-linked chains have non-degradative roles in various signaling pathways including the DNA damage response [3,9,13–15], protein trafficking [16,17], mitophagy [18], inflammation [19–21], and immune responses [22]. Degradative functions of K11 linkages in endoplasmic reticulum biology [9], as well as Hedgehog signaling in fruit flies have been described [23], while the critical role of K11-linkages in mitotic progression in metazoans has been studied in detail [24–29]. Although K6, K27, K29, and K33 ubiquitin linkages are especially rare in cells [9,30], important observations have contributed to an increasing recognition of their physiological relevance [31]. K6-linked polyubiquitin chains, for example, are reported to function in the DNA damage response through the BRCA1-BARD1 E3 ligase in a proteolysis-independent manner [32,33], as well as in mitophagy through the E3 ligase, Parkin [18,34]. K27-linkages have also been linked to mitophagy, as some Parkin substrates are reportedly decorated with K27-linked ubiquitin chains [35,36]. mRNA stability is regulated by K29-linked ubiquitin chains on HuR, an mRNA binding protein, via an interaction with UBXD8, an adaptor for the essential p97 ATPase [37]. Finally, K33-linked ubiquitin chains have been suggested to regulate post-Golgi protein trafficking by mediating the interaction of Coronin-7 with Eps15, a *trans*-golgi network protein [38].

Notwithstanding these and other intriguing observations [39–41], a comprehensive examination of the roles of K6, K11, K27, K29, and K33 ubiquitin linkages, particularly in yeast, is lacking. This is owed to both the partial redundancy of ubiquitin acceptor lysines [9], and the technical limitations of current protein analysis

methods [42,43]. A high-throughput approach to uncover physiologically important functions of specific ubiquitin linkage types would significantly advance current understanding of the ubiquitin-proteasome system. Genetic interaction analysis, namely the study of the phenotypic effects of combining mutations, has long been a powerful tool for discovering novel gene-functions by revealing functional relationships between genes [44–51].

This report describes a comprehensive genetic analysis to uncover pathways that are regulated by specific ubiquitin linkage types. In a high-throughput manner, single deletions of non-essential genes were combined with mutations eliminating specific ubiquitin linkages. The growth phenotypes of double mutant strains were quantified to identify thousands of candidate genetic interactions. The genetic interactome of K11 linkages was of special interest due to that linkage type's relatively high abundance in yeast [9], and its known functions in the metazoan cell cycle [24]. Genetic and molecular analysis led to the discovery of novel physiological functions of K11 linkages in promoting amino acid import and contributing to cell cycle progression.

Results

The ubiquitin linkage synthetic genetic array

A synthetic genetic array analysis (SGA) was undertaken to identify pathways that are regulated by specific polyubiquitin chain types [46]. Yeast strains constitutively expressing single, double, and triple lysine-to-arginine (K-to-R) mutant ubiquitin alleles were engineered by modifying all four loci from which ubiquitin is normally expressed in yeast [1] (**Figure 1A, Materials and Methods, Figure 1-figure supplement 1**). The engineered yeast strains express ubiquitin at levels comparable to wild type yeast

(**Figure 1-figure supplement 2**). A strain expressing low levels of wild type ubiquitin (lacking ubiquitin expression at the modified *ubi4* locus) was also included in the ubiquitin SGA to control for possible non-specific effects of perturbing ubiquitin levels (**Figure 1-figure supplement 2, Figure 1-figure supplement 3A, Materials and Methods**). Because lysine 48 of ubiquitin is essential [52], strains expressing K48R ubiquitin also contained 20% wild type ubiquitin (**Figure 1-figure supplement 3B, Materials and Methods**). K63R ubiquitin mutants were initially included, but analysis of the data was not possible due to their extreme hypersensitivity to canavanine (data not shown), a toxic arginine analog used in the SGA protocol, even in the context of the deletion of the *CAN1* sensitivity gene (**Figure 1-figure supplement 4**). Linear ubiquitin chains were not analyzed in this study. The lysine-to-arginine ubiquitin mutant strains were systematically mated to a gene deletion library. The resulting diploid cells underwent sporulation to generate haploid double mutant cells expressing mutant ubiquitin alleles, and carrying single gene deletions (**Figure 1-figure supplement 4**). Colony sizes of the approximately forty-five thousand pairwise combinations of single gene deletions and ubiquitin K-to-R mutants were measured to identify genetic interactions.

Previous SGA screens have examined the synthetic phenotype of two [46–48,50,53,54], or in a few cases three [55], mutations, whereas the ubiquitin SGA necessitates examining five loci. During conventional SGA analysis in the S288C strain, heterozygous diploids are sporulated to generate haploid cells, a subset of which contains the double mutant to be examined. The haploid selection steps require the co-segregation of an additional three haploid selectable markers to efficiently eliminate unsporulated

diploid cells that would otherwise generate background [54]. The desired haploid spores are relatively abundant since only five total loci are under selection; hence, the low sporulation efficiency exhibited by S288C is acceptable [56]. In contrast, the final haploid cells in the ubiquitin SGA must contain all modified ubiquitin loci, haploid selectable markers, and a gene deletion, meaning that an exceedingly small percentage of spores will have the desired genotype. A strategy to ameliorate this problem would be to increase the efficiency of sporulation, thereby both reducing the number of unsporulated diploid cells (background), and increasing the number of correct haploid spores. Overexpression of Ime2, a positive regulator of sporulation [57], was able to increase the sporulation efficiency of S288C moderately, from 12% in wild type diploids to 38% (**Figure 1-figure supplement 5**). Other genetic manipulations similarly led to only modest increases in sporulation efficiency (**Figure 1-figure supplement 5**). The SK1 strain background provided a more efficient and physiologic solution, as it exhibits 92% sporulation efficiency [56][58]. The high sporulation efficiency also allowed for the omission of one haploid selection step commonly used in SGA studies, *lyp1Δ* selection (**Figure 1-figure supplement 4, Materials and Methods**). Hence, all K-to-R ubiquitin mutant strains and a novel single gene deletion library were generated in the SK1 strain background (**Figure 1A, Materials and Methods**). To further reduce the number of selections in the ubiquitin SGA protocol, and increase the percentage of spores carrying all desired mutations following sporulation, a *ubi1* allele lacking the ubiquitin gene was crossed into both the ubiquitin K-to-R strains and the gene deletion array, thereby eliminating an additional selection step (**Figure 1A, Figure 1-figure supplement 6A-B, Materials and Methods**).

The study of quantitative genetic interactions has proven to be a powerful approach to uncover novel functions of genes [47,48,50]. Negative (synthetic) genetic interactions, which arise when a double mutant exhibits a more severe phenotype than expected from the corresponding single mutant phenotypes, often occur when the gene pair functions in parallel or redundant pathways. Positive genetic interactions, defined as situations in which a double mutant has a phenotype equal to (epistasis), or less severe than the sickest single mutant (suppression), can occur when both genes function in the same pathway.

The ubiquitin SGA identified thousands of candidate genetic interactions between gene deletions and K-to-R ubiquitin mutations (**Figure 1B**). While several other large SGA screens have analyzed genetic interactions between large sets of gene deletions with known functional relationships, the ubiquitin SGA was carried out using a small number of ubiquitin mutants and an unbiased gene deletion array. Because genes with known related functions are more likely to have genetic interactions, it was expected that the ubiquitin SGA to have a lower density of true genetic interactions relative to other studies, which would have the effect of decreasing the reproducibility that any single genetic interaction score. Nonetheless, two biological replicates of the ubiquitin SGA had a correlation coefficient of 0.42, in line with other large genetic interaction screens (**Figure 1C**).

To characterize the robustness of the ubiquitin SGA further, the correlation between genetic and known physical interactions among genes was analyzed. Genes whose protein products are known to physically interact are generally also more likely to share genetic interactions, and thus tend to have highly correlated genetic interaction

profiles. The enrichment of genetic interaction similarities among gene pairs whose products physically interact was compared to protein pairs that have not been reported to interact. As expected, the median correlation coefficient within physically interacting gene pairs is significantly higher than among non-interacting gene pairs (**Figure 1D**). Although the genetic profiles of gene deletions in the ubiquitin SGA include only 17 scores, the screen is similarly enriched for genetic similarity within physically interacting gene pairs as the published chromosome biology E-MAP, wherein the genetic interaction profiles contain 754 scores and is biased for genes with known related functions (**Figure 1D**). Altogether, these analyses demonstrate the robustness and biological significance of the ubiquitin SGA.

Unbiased hierarchical clustering orders the mutant strains in the ubiquitin SGA relative to each other based on the similarity of their genetic interactions (**Figure 1B**). Genes that function in the same pathways or have similar functions generally have common genetic interactions. As expected, the ubiquitin SGA identified known gene modules based on their genetic interactions with the K-to-R ubiquitin mutants. For example, *rim101Δ*, *rim21Δ*, *ygr122wΔ*, and *dfg16Δ* form a cluster in the ubiquitin SGA (**Figure 1B**). All four genes are members of the Rim101 pathway, whose eponymous gene is a transcription factor that is activated in response to alkaline conditions in a manner dependent on Rim21, Ygr122Wp, and Dfg16 [59]. Other examples of known gene modules that were clustered by the ubiquitin linkage SGA include (**Figure 1B**): Three subunits of the chromatin-remodeling SWR-complex, *SWC2*, *SWC3*, and the catalytic subunit *SWR1* [60]; several genes in the MTC-gene cluster (*MTC4*, *MTC6*, *MAY24*) that was recently implicated in trafficking through the secretory pathway [50],

as well as genes with related functions in N-linked glycosylation (*OST6*, *ALG8*) [61,62], endocytic protein trafficking (*VFA1*) [63], or lipid biosynthesis (*YOR302W*) [64]; several members of the transcription and translation-regulating Elongator complex (*ELP2*, *3*, *6*) and *KTI12*, a known binding partner [65,66], as well as two genes, *NNF2* and *PSP2*, with putative related roles in transcription and splicing, respectively [67,68]; four genes, *PEX4*, *8*, *6*, *15* that function in peroxisome biogenesis and trafficking of proteins between peroxisomes and the cytosol [69]; and finally, two genes, *HOM2* and *HOM3*, that participate in the homoserine biosynthesis pathway [70].

The K-to-R ubiquitin mutants were also clustered based on the similarity of their genetic interactions with the gene deletion array. As expected, clustering of strains with common K-to-R mutations is generally observed (**Figure 1E**). For example, strains carrying the K33R mutation are clustered and have high correlation coefficients among each other. The same can be said of strains carrying the K6R and K48R mutations (**Figure 1E**). Interestingly, the K6R and K33R clusters are most similar to each other, suggesting similar physiological effects of mutating those ubiquitin lysines (**Figure 1E**). A surprising feature of the ubiquitin allele *SGA* is that the K11R mutation, despite the high abundance of K11 linkages in cells [9], does not drive clustering of double and triple mutants carrying K11 mutations (**Figure 1E**). Clustering is driven by a combination of the number and strength of common interactions between K-to-R mutants. Indeed, the K11R ubiquitin mutant has relatively few strong genetic interactions, suggesting that K11 linkages have a narrow set of functions in yeast (**Figure 1F**).

The ubiquitin *SGA* uncovered thousands of candidate genetic interactions between gene deletions and ubiquitin lysine mutations. To examine a few interactions in

more detail, gene deletion strains were mated to all single lysine-to-arginine mutants, as well as wild type ubiquitin strains. Following tetrad dissection, the growth phenotypes of single and double mutant cells were assessed. K63R mutants are included in this targeted analysis. Genes exhibiting genetic interactions with a single linkage type were examined first. The negative genetic interactions observed between *ubc4*Δ and K27R and between *hom2*Δ and K11R proved to be reproducible, and specific (**Figure 2A, 2B**). Next, *CDC26*, a gene whose deletion exhibited genetic interactions with multiple linkages (K48R>>K11≥K33R), was analyzed. Deletion of *CDC26* in combination with mutation of ubiquitin's K11 or K48 caused significant synthetic growth defects, whereas only a mild negative interaction was observed in *cdc26*Δ and K33R double mutant cells (**Figure 2C**). Having demonstrated the robustness and reproducibility of the ubiquitin SGA, the physiological functions of ubiquitin linkage types were explored.

K11 ubiquitin linkages promote amino acid homeostasis

The K11R mutant was of special interest due to the fact that K11-linkages are the most abundant non-K48 linkages in *S. cerevisiae* [9], and because of their important function in metazoan cell cycle regulation [24,26,27]. Characterization of the K11R mutant genetic interactome using gene ontology (GO) term enrichment analysis revealed a striking enrichment of genes involved in amino acid biosynthesis (**Figure 3A**) [71,72], suggesting a possible role of K11 linkages in amino acid homeostasis. To identify genes that had interactions specifically with K11R and not with other K-to-R ubiquitin mutations, the K11R mutant genetic interactome was compared to the averaged interactome of all single and double mutant strains not containing the K11R mutation (**Figure 3B**). Deletions of *HOM2* or *HOM3*, two genes involved in the biosynthesis of

homoserine, a threonine and methionine precursor [70], and to a lesser extent deletion of *GLY1*, which encodes an enzyme that generates threonine and glycine [73], exhibited strong genetic interactions specifically with the K11R ubiquitin mutants (**Figure 3B, 3C**). These genetic interactions suggested the existence of functional redundancy between K11 linkages and threonine or methionine biosynthesis. To determine whether perturbations of threonine or methionine levels was the basis for the synthetic growth defect observed in K11R and *hom2Δ* or *hom3Δ* double mutant cells, the growth medium was supplemented with homoserine, excess threonine, or methionine. Rescue—by either homoserine or threonine—of the synthetic growth defect caused by deletion of *HOM2* or *HOM3* in K11R mutant cells, suggested K11-linked polyubiquitin chains function redundantly with threonine biosynthesis (**Figure 3D**).

Whereas negative genetic interactions point to redundancy between genes and ubiquitin linkage types, the deletions of genes that function in the same pathway as a specific ubiquitin linkage are likely to have genetic interactions that are similar to that linkage type. Comparison of a comprehensive yeast genetic interaction network to the genetic interactome of the K11R ubiquitin mutant revealed that it is most similar to deletions of *GNP1* [74], a high-affinity threonine permease (**Figure 3-figure supplement 1A**) [75], and *YDR509W*, a dubious open reading frame that overlaps the N-terminus of *GNP1* and is thus likely to also abrogate *GNP1* expression [76] (**Figure 3E**). The similarity between the K11R mutant and *gnp1Δ* genetic interactomes suggested that K11 linkages play a role in promoting threonine import. To assess that model, the import of radioactively labeled threonine into wild type and K11R ubiquitin cells was measured, revealing a significant defect in the K11R ubiquitin mutant, and thus showing

that K11 linkages promote threonine import (**Figure 3F**). This previously unreported function of K11-linked polyubiquitin chains in amino acid import is likely the underlying basis of the synthetic growth defect observed in K11R and *hom2Δ* or *hom3Δ* double mutant cells.

Polyubiquitin chains are synthesized by E3 ubiquitin ligases [8]. If a particular E3 ligase were involved in the K11-mediated import of threonine, it would be expected to also have negative genetic interactions with *hom2Δ* or *hom3Δ*, an endoplasmic reticulum-resident E3 ubiquitin ligase [77], is responsible for approximately 50% of K11 linkages in yeast cells [9]. Deletion of *DOA10* in combination with *hom2Δ* also led to a synthetic growth defect that was rescued by homoserine (**Figure 3G**), suggesting that Doa10, along with K11 ubiquitin chains, contribute to threonine import. These results suggested that the Doa10-mediated ubiquitination of a substrate, or a set of substrates, might regulate amino acid import. The Doa10-dependent ubiquitinome was analyzed using quantitative mass spectrometry and ubiquitin-remnant enrichment. While known Doa10 substrates are less ubiquitinated in cells lacking Doa10, Ubc6, Ubc7, or Ubc6 and Ubc7, the substrate responsible for the role of Doa10 in amino acid homeostasis remains unknown (data not shown). Nonetheless, the discovery that Doa10 is the E3 ligase that mediates the role of K11-linkages in amino acid import is a significant discovery that counters models suggesting the observed amino acid import defect is due to non-specific perturbations of ubiquitin.

K11 ubiquitin linkages contribute to mitotic progression

The anaphase promoting complex (APC) is a highly conserved and essential E3 ubiquitin ligase that governs the metaphase to anaphase transition and mitotic exit by ubiquitinating several substrates, including securin and S and M-phase cyclins [78–80]. In yeast, the APC cooperates with two E2 ubiquitin conjugases, Ubc4 and Ubc1, to decorate its substrates with polyubiquitin chains and target them for proteasomal degradation [81]. Ubc4 is a promiscuous E2 that monoubiquitinates or initiates short ubiquitin chains on substrates [82,83]. Ubc1 subsequently extends those initial modifications with long and homogenous K48-linked ubiquitin chains [81,84]. K48 of ubiquitin is necessary for processive APC-substrate ubiquitination *in vitro* [81], and is the only linkage type required for normal cell cycle progression *in vivo* [84]. At high temperatures, a non-essential subunit of the APC, Cdc26, aids in the assembly, and promotes the stability, of the APC holoenzyme [85,86]. As expected, given the well-established role of K48 linkages in APC-mediated proteasomal degradation, K48R ubiquitin mutant cells lacking Cdc26 exhibit a significant growth defect (**Figure 2C**). Interestingly, deletion of *CDC26* in K11R mutant cells also leads to a strong synthetic growth defect (**Figure 2C**), suggesting a possible contribution of K11 linkages to APC function.

Although K11-linked polyubiquitin chains had not been previously reported to function in APC-substrate degradation in yeast, their role in metazoan APC-substrate turnover is well understood [24–29]. Analogous to the yeast APC, the metazoan APC interacts with two E2 enzymes, Ube2C and Ube2S, that sequentially ubiquitinate substrates [27,87]: Ube2c initially modifies substrates with monoubiquitin or short chains

that are then elongated by Ube2S with K11-linked chains [27]. The negative genetic interaction between K11R and *cdc26Δ* suggested that K11 linkages might also be important for the regulation of APC substrates in yeast. Indeed, cell cycle analysis experiments with cells lacking Cdc26 revealed that the cell cycle-regulated levels of securin and several cyclins were altered in K11R ubiquitin mutants relative to cells expressing wild type ubiquitin (**Figure 4A, Figure 4-figure supplement 1A**). For example, the mitotic cyclin Clb2 persisted much longer during mitosis in K11R cells, with its disappearance being delayed by almost 30 minutes (**Figure 4A**). The levels of the S/M cyclin, Clb3, and of the Separase-inhibitor, Securin (Pds1), were also misregulated in K11R mutant cells, although to a lesser extent than Clb2 (**Figure 4A**). Clb5, an S-phase cyclin, is normally targeted for degradation during the M and G1 phases by the APC [88,89]. Its expression during both M and G1 was elevated in K11R mutant cells, suggesting that K11 was required for complete turnover of this substrate (**Figure 4A**).

To ascertain whether the misregulation of APC substrates was caused by a defect in their turnover, and not due to other effects of mutating K11, *cdc26Δ* cells were synchronized in the G1 phase, and the half life of APC substrates was examined 60 minutes after release from G1, when the APC was active, as evidenced by securin turnover in **Figure 4A**. The turnover of all examined substrates is delayed in K11R mutant cells (**Figure 4B, C**). Interestingly, the turnover of substrates stalls after approximately 10 minutes in cycloheximide, likely due to degradation of APC substrate adaptors [90]. The half-lives of the substrates were estimated by fitting a second order polynomial trendline to the data and subsequently calculating the slope of the tangent line

at $t = 2.5\text{min}$, prior to the observed stalling of substrate turnover. On average, the half-lives of examined substrates were extended by approximately 3 fold in the K11R ubiquitin mutant (**Figure 4B, C**). Because defects in cell cycle progression in K11R mutant cells could explain the delay in APC substrate turnover, it was necessary to determine the half-lives of APC substrates independently of cell cycle progression. Ectopic expression of Clb2 in G1-arrested cells, which have active APC [91], permitted the analysis of the Clb2 half-life in cells that were in the same cell cycle stage. The half-life of Clb2 was analyzed after addition of cycloheximide to halt its translation, revealing a delay in Clb2 turnover in K11R mutant cells (**Figure 4D, Figure 4-figure supplement 1B**).

Finally, the capacity of the yeast APC to modify substrates with K11-linked polyubiquitin chains was analyzed *in vitro*. Briefly, the ubiquitination of an *in vitro*-translated fragment of the APC substrate Hsl1, by APC-Cdh1 and Ubc4, the initiating APC-cognate E2, was assayed in the presence of either WT, K0 (K6,11,27,29,33,48,63R), or K11-only (K6,27,29,33,48,63R) ubiquitin. Under these conditions, Hsl1 is strongly ubiquitinated in the presence of WT ubiquitin and, to a slightly lesser extent, in reactions containing K11-only ubiquitin (**Figure 4E**). In contrast, Hsl1 ubiquitination is significantly reduced in reactions containing K0 ubiquitin, as compared to K11-only. The ubiquitin smear observed when Hsl1 is incubated with K0 ubiquitin likely represents the attachment of monoubiquitins to several of the 21 lysines in the Hsl1 fragment used in the experiments. Therefore, the slower electrophoretic mobility of Hsl1 modified with K11-only ubiquitin relative to K0 ubiquitin shows that

the yeast APC extends monoubiquitin modifications of Hsl1 with K11-linked ubiquitin chains *in vitro*.

To ascertain the length of homogenous K11-linked chains generated by the yeast APC, all lysines of Hsl1 were mutated to arginine, except for 2 lysines that constitute two KEN-box degrons and K747 of Hsl1, which has been previously reported to be ubiquitinated. This mutant form of Hsl1, termed Hsl1-3K, allowed for the detection of Hsl1ubiquitination at a single lysine residue (K747). The observation that Hsl1-3K is decorated with a single monoubiquitin in reactions containing K0 ubiquitin confirmed that a one lysine, likely K747, is ubiquitinated by the APC in Hsl1-3K (**Figure 4F**). However, the reduced level of ubiquitination observed for Hsl1-3K related to WT Hsl1 (compare lane 5 in Figures 4G and 4H) suggests that recognition of this substrate by the APC is strongly compromised. Nonetheless, the substrate is polyubiquitinated in the presence WT ubiquitin (**Figure 4F**). Significantly, the monoubiquitination of Hsl1-3K in the presence of K11-only ubiquitin is extended with at least two further ubiquitins, leading to a chain composed of at least 3 ubiquitin protomers that are necessarily linked through lysine-11 of ubiquitin (**Figure 4F**). The higher level of Hsl1-3K ubiquitination seen with WT relative to K11-only ubiquitin (Figure 4F, lanes 3 and 4) could either represent ubiquitin chain branches or the combinatorial effect of a highly mutated ubiquitin and substrate. Altogether, our results show that K11 linkages contribute to APC-substrate turnover in yeast.

Discussion

Although some large-scale proteomics studies have advanced our understanding of the physiological roles of specific polyubiquitin chain types, much of the progress has

occurred through the study of single pathways. A significant challenge for the ubiquitin field has been the partial redundancy between ubiquitin linkage types [9]. The analysis of genetic interactions, however, reveals phenotypic functional relationships between genes, thereby facilitating the discovery of physiologically important functions of genes. The synthetic genetic array (SGA) reported here represents the first comprehensive genetic analysis of lysine-to-arginine ubiquitin mutant alleles. This SGA leverages the power of yeast genetics to uncover physiologically important functional relationships between ubiquitin linkage types and thousands of genes.

The ubiquitin linkage SGA necessitated the development of a novel SGA protocol and reagents to permit the analysis of genetic interactions in cells carrying five mutations, as well as haploid selectable markers. The large number of loci under selection meant that an extremely small number of spores carried the desired genotype for SGA analysis. To increase the number of spores, the ubiquitin linkage SGA was carried out in the SK1 strain background, which exhibits about 8-fold higher sporulation efficiency relative to S288C [56], the yeast strain most commonly used in SGA studies. This also permitted the omission of a haploid selection step by decreasing background unsporulated diploids. The ubiquitin linkage SGA therefore required the development of a new gene deletion library in the SK1 background. To increase the percentage of spores carrying the desired genotype for SGA analysis, the *UBI1* locus was replaced in the entire SK1 deletion library, as well as in the panel of K-to-R ubiquitin mutant strains, thereby reducing the loci under selection. Ultimately, the technical advancements described here reduced, from eight to six, the number of loci under selection, thereby making the ubiquitin linkage SGA feasible.

A novel role of K11 linkages in promoting amino acid import adds to already well-established roles of the ubiquitin-proteasome system in that process. First, expression of amino acid permeases is promoted by the transcription factors Stp1/2, which are proteolytically processed into their active forms in a ubiquitin-dependent process utilizing K48 ubiquitin linkages [92,93]. Our unpublished results show that neither this pathway nor the levels or localization of the threonine permease Gnp1 are affected by the K11R ubiquitin mutation (data not shown). Conversely, downregulation of permeases occurs when an essential E3 ligase, Rsp5, modifies their intracellular domains with monoubiquitin and short K63-linked polyubiquitin chains, thereby triggering endocytosis and vacuolar targeting [17,94,95]. The observed enrichment of threonine biosynthesis genes in the genetic interactions of the K11R ubiquitin mutant would suggest a specific function in threonine import. A more likely model, however, is that threonine homeostasis is more susceptible to perturbations, perhaps due to relatively low redundancy in its modes of import [75]. Thus, our data may point to a role for K11 linkages with many importers whose functional impairment is not phenotypic.

The ubiquitin allele SGA also revealed a previously unreported contribution of K11 linkages to cell cycle regulation. The genetic interaction between K48 linkages and *CDC26* was not unexpected, as it is understood that the yeast APC decorates its substrates with K48-linked ubiquitin chains [84]. The genetic interaction between K11 linkages and *CDC26* identified by the ubiquitin allele SGA led to the recognition that K11 linkages also contribute to APC-substrate turnover *in vivo*, and that the APC can directly modify a substrate with K11-linked polyubiquitin *in vitro*. These results suggest

that the metazoan APC, which modifies its substrates with K11-linked ubiquitin chains [24–29], and the yeast APC are more alike than previously appreciated.

The metazoan and yeast APC both interact with two E2 enzymes that sequentially modify substrates [24,27,81,96]. The initiating E2 enzymes, Ube2C in metazoans and Ubc4 in yeast, modify substrates with single ubiquitins and short chains [83]. Because initiating E2s must be able to modify lysines on substrates, which can exist in diverse structural and chemical environments, they necessarily lack strong lysine preference [82,83]. Ubc4 or Ube2c-mediated modifications are then elongated by Ube2S in metazoans, or Ubc1 in yeast. In contrast to initiating E2s, Ube2S and Ubc1 exhibit a strong preference for ubiquitin's lysine 11 and 48, respectively [84,97], and are unable to efficiently modify lysines on substrates [27,81].

In light of preceding APC studies, the genetic, molecular, and biochemical studies presented here suggest that the yeast APC modifies its substrates with a base of Ubc4-mediated short K11-linked chains that are functionally important [83]. Ubc1 then extends those initial modifications with long K48-linked polyubiquitin chains [81,84]. This model (**Figure 4G**) differs from the well-established mechanism of the metazoan APC, which modifies substrates with a base of short chains with K48 and other linkages, which then branch into long K11-linked chains. The fact that the contribution of K11 linkages to APC-substrate turnover is appreciable only in cells without Cdc26 suggests a nuanced role of K11 linkages in yeast, similar to metazoans, wherein disruption of the K11-specific E2, Ube2s, is not lethal. Pivotal work has shown that K11/K48 branched chains significantly enhance substrate degradation in mammalian cells [24,29]. Whether this

holds true in yeast has not been studied, but would provide an appealing explanation for the conditional requirement for K11-linkages in APC function.

Detailed analysis of genetic interactions uncovered by the ubiquitin linkage SGA analysis has enabled the discovery of two novel physiological functions of K11 ubiquitin linkages in two essential processes: amino acid homeostasis and cell cycle regulation. Altogether, the ubiquitin allele SGA has broadened our global understanding of the functions of polyubiquitin chain types by revealing their genetic interactomes, and demonstrated the utility of genetic analysis for interrogating the complexity of the ubiquitin-proteasome system.

References

1. Finley D, Ulrich HD, Sommer T, Kaiser P. The Ubiquitin-Proteasome System of *Saccharomyces cerevisiae*. *Genetics*. 2012;192: 319–360.
doi:10.1534/genetics.112.140467
2. Jackson SP, Durocher D. Regulation of DNA Damage Responses by Ubiquitin and SUMO. *Mol Cell*. 2013;49: 795–807. doi:10.1016/j.molcel.2013.01.017
3. Harper JW, Elledge SJ. The DNA Damage Response: Ten Years After. *Mol Cell*. 2007;28: 739–745. doi:10.1016/j.molcel.2007.11.015
4. Broemer M, Meier P. Ubiquitin-mediated regulation of apoptosis. *Trends Cell Biol*. 2009;19: 130–140. doi:10.1016/j.tcb.2009.01.004
5. Borg NA, Dixit VM. Ubiquitin in Cell-Cycle Regulation and Dysregulation in Cancer. *Annu Rev Cancer Biol*. 2017;1: 59–77. doi:10.1146/annurev-cancerbio-040716-075607
6. Wertz IE, Dixit VM. Signaling to NF- κ B: Regulation by Ubiquitination. *Cold Spring Harb Perspect Biol*. 2010;2. doi:10.1101/cshperspect.a003350
7. Geng F, Wenzel S, Tansey WP. Ubiquitin and Proteasomes in Transcription. *Annu Rev Biochem*. 2012;81: 177–201. doi:10.1146/annurev-biochem-052110-120012
8. Hershko A, Ciechanover A. The ubiquitin system. *Annu Rev Biochem*. 1998;67: 425–479. doi:10.1146/annurev.biochem.67.1.425

9. Xu P, Duong DM, Seyfried NT, Cheng D, Xie Y, Robert J, et al. Quantitative Proteomics Reveals the Function of Unconventional Ubiquitin Chains in Proteasomal Degradation. *Cell*. 2009;137: 133–145. doi:10.1016/j.cell.2009.01.041
10. Komander D, Rape M. The ubiquitin code. *Annu Rev Biochem*. 2012;81: 203–229. doi:10.1146/annurev-biochem-060310-170328
11. Datta AB, Hura GL, Wolberger C. The Structure and conformation of Lys-63 linked tetraubiquitin. *J Mol Biol*. 2009;392: 1117–1124. doi:10.1016/j.jmb.2009.07.090
12. Chau V, Tobias JW, Bachmair A, Marriott D, Ecker DJ, Gonda DK, et al. A multiubiquitin chain is confined to specific lysine in a targeted short-lived protein. *Science*. 1989;243: 1576–1583.
12. Ulrich HD. The RAD6 Pathway: Control of DNA Damage Bypass and Mutagenesis by Ubiquitin and SUMO. *ChemBioChem*. 2005;6: 1735–1743. doi:10.1002/cbic.200500139
14. Spence J, Sadis S, Haas AL, Finley D. A ubiquitin mutant with specific defects in DNA repair and multiubiquitination. *Mol Cell Biol*. 1995;15: 1265–1273.
15. Wang B, Elledge SJ. Ubc13/Rnf8 ubiquitin ligases control foci formation of the Rap80/Abraxas/Brc1/Brcc36 complex in response to DNA damage. *Proc Natl Acad Sci U S A*. 2007;104: 20759–20763. doi:10.1073/pnas.0710061104

16. Lauwers E, Jacob C, André B. K63-linked ubiquitin chains as a specific signal for protein sorting into the multivesicular body pathway. *J Cell Biol.* 2009;185: 493–502. doi:10.1083/jcb.200810114
17. MacGurn JA, Hsu P-C, Emr SD. Ubiquitin and membrane protein turnover: from cradle to grave. *Annu Rev Biochem.* 2012;81: 231–259. doi:10.1146/annurev-biochem-060210-093619
18. Ordureau A, Heo J-M, Duda DM, Paulo JA, Olszewski JL, Yanishevski D, et al. Defining roles of PARKIN and ubiquitin phosphorylation by PINK1 in mitochondrial quality control using a ubiquitin replacement strategy. *Proc Natl Acad Sci U S A.* 2015;112: 6637–6642. doi:10.1073/pnas.1506593112
19. Deng L, Wang C, Spencer E, Yang L, Braun A, You J, et al. Activation of the I κ B kinase complex by TRAF6 requires a dimeric ubiquitin-conjugating enzyme complex and a unique polyubiquitin chain. *Cell.* 2000;103: 351–361.
20. Grabbe C, Husnjak K, Dikic I. The spatial and temporal organization of ubiquitin networks. *Nat Rev Mol Cell Biol.* 2011;12: 295–307. doi:10.1038/nrm3099
21. Wang C, Deng L, Hong M, Akkaraju GR, Inoue J, Chen ZJ. TAK1 is a ubiquitin-dependent kinase of MKK and IKK. *Nature.* 2001;412: 346–351. doi:10.1038/35085597
22. Manzanillo PS, Ayres JS, Watson RO, Collins AC, Souza G, Rae CS, et al. The ubiquitin ligase parkin mediates resistance to intracellular pathogens. *Nature.* 2013;501: 512–516. doi:10.1038/nature12566

23. Zhang Z, Lv X, Yin W, Zhang X, Feng J, Wu W, et al. Ter94 ATPase Complex Targets K11-Linked Ubiquitinated Ci to Proteasomes for Partial Degradation. *Dev Cell*. 2013;25: 636–644. doi:10.1016/j.devcel.2013.05.006
24. Meyer H-J, Rape M. Enhanced protein degradation by branched ubiquitin chains. *Cell*. 2014;157: 910–921. doi:10.1016/j.cell.2014.03.037
25. Williamson A, Wickliffe KE, Mellone BG, Song L, Karpen GH, Rape M. Identification of a physiological E2 module for the human anaphase-promoting complex. *Proc Natl Acad Sci U S A*. 2009;106: 18213–18218. doi:10.1073/pnas.0907887106
26. Matsumoto ML, Wickliffe KE, Dong KC, Yu C, Bosanac I, Bustos D, et al. K11-linked polyubiquitination in cell cycle control revealed by a K11 linkage-specific antibody. *Mol Cell*. 2010;39: 477–484. doi:10.1016/j.molcel.2010.07.001
27. Wu T, Merbl Y, Huo Y, Gallop JL, Tzur A, Kirschner MW. UBE2S drives elongation of K11-linked ubiquitin chains by the anaphase-promoting complex. *Proc Natl Acad Sci U S A*. 2010;107: 1355–1360. doi:10.1073/pnas.0912802107
28. Jin L, Williamson A, Banerjee S, Philipp I, Rape M. Mechanism of ubiquitin-chain formation by the human anaphase-promoting complex. *Cell*. 2008;133: 653–665. doi:10.1016/j.cell.2008.04.012
29. Yau RG, Doerner K, Castellanos ER, Haakonsen DL, Werner A, Wang N, et al. Assembly and Function of Heterotypic Ubiquitin Chains in Cell-Cycle and Protein Quality Control. *Cell*. 2017; doi:10.1016/j.cell.2017.09.040

30. Dammer EB, Na CH, Xu P, Seyfried NT, Duong DM, Cheng D, et al. Polyubiquitin Linkage Profiles in Three Models of Proteolytic Stress Suggest the Etiology of Alzheimer Disease. *J Biol Chem.* 2011;286: 10457–10465.
doi:10.1074/jbc.M110.149633
31. Akutsu M, Dikic I, Bremm A. Ubiquitin chain diversity at a glance. *J Cell Sci.* 2016;129: 875–880. doi:10.1242/jcs.183954
32. Nishikawa H, Ooka S, Sato K, Arima K, Okamoto J, Klevit RE, et al. Mass spectrometric and mutational analyses reveal Lys-6-linked polyubiquitin chains catalyzed by BRCA1-BARD1 ubiquitin ligase. *J Biol Chem.* 2004;279: 3916–3924.
doi:10.1074/jbc.M308540200
33. Christensen DE, Brzovic PS, Klevit RE. E2-BRCA1 RING interactions dictate synthesis of mono- or specific polyubiquitin chain linkages. *Nat Struct Mol Biol.* 2007;14: 941–948. doi:10.1038/nsmb1295
34. Ordureau A, Sarraf SA, Duda DM, Heo J-M, Jedrychowski MP, Sviderskiy VO, et al. Quantitative Proteomics Reveal a Feedforward Mechanism for Mitochondrial PARKIN Translocation and Ubiquitin Chain Synthesis. *Mol Cell.* 2014;56: 360–375.
doi:10.1016/j.molcel.2014.09.007
35. Birsa N, Norkett R, Wauer T, Mevissen TET, Wu H-C, Foltynie T, et al. Lysine 27 ubiquitination of the mitochondrial transport protein Miro is dependent on serine 65 of the Parkin ubiquitin ligase. *J Biol Chem.* 2014;289: 14569–14582.
doi:10.1074/jbc.M114.563031

36. Geisler S, Holmström KM, Skujat D, Fiesel FC, Rothfuss OC, Kahle PJ, et al. PINK1/Parkin-mediated mitophagy is dependent on VDAC1 and p62/SQSTM1. *Nat Cell Biol.* 2010;12: ncb2012. doi:10.1038/ncb2012
37. Zhou H-L, Geng C, Luo G, Lou H. The p97–UBXD8 complex destabilizes mRNA by promoting release of ubiquitinated HuR from mRNP. *Genes Dev.* 2013;27: 1046–1058. doi:10.1101/gad.215681.113
38. Yuan W-C, Lee Y-R, Lin S-Y, Chang L-Y, Tan YP, Hung C-C, et al. K33-Linked Polyubiquitination of Coronin 7 by Cul3-KLHL20 Ubiquitin E3 Ligase Regulates Protein Trafficking. *Mol Cell.* 2014;54: 586–600. doi:10.1016/j.molcel.2014.03.035
39. Silva GM, Finley D, Vogel C. K63 polyubiquitination is a new modulator of the oxidative stress response. *Nat Struct Mol Biol.* 2015;22: nsmb.2955. doi:10.1038/nsmb.2955
40. Song EJ, Werner SL, Neubauer J, Stegmeier F, Aspden J, Rio D, et al. The Prp19 complex and the Usp4Sart3 deubiquitinating enzyme control reversible ubiquitination at the spliceosome. *Genes Dev.* 2010;24: 1434–1447. doi:10.1101/gad.1925010
41. Elia AEH, Boardman AP, Wang DC, Huttlin EL, Everley RA, Dephoure N, et al. Quantitative Proteomic Atlas of Ubiquitination and Acetylation in the DNA Damage Response. *Mol Cell.* 2015;59: 867–881. doi:10.1016/j.molcel.2015.05.006
42. Swatek KN, Komander D. Ubiquitin modifications. *Cell Res.* 2016;26: 399–422. doi:10.1038/cr.2016.39

43. Carrano AC, Bennett EJ. Using the Ubiquitin-modified Proteome to Monitor Protein Homeostasis Function. *Mol Cell Proteomics MCP*. 2013;12: 3521–3531.
doi:10.1074/mcp.R113.029744
44. Dixon SJ, Costanzo M, Baryshnikova A, Andrews B, Boone C. Systematic mapping of genetic interaction networks. *Annu Rev Genet*. 2009;43: 601–625.
doi:10.1146/annurev.genet.39.073003.114751
45. Tong AH, Evangelista M, Parsons AB, Xu H, Bader GD, Pagé N, et al. Systematic genetic analysis with ordered arrays of yeast deletion mutants. *Science*. 2001;294: 2364–2368. doi:10.1126/science.1065810
46. Tong AHY, Lesage G, Bader GD, Ding H, Xu H, Xin X, et al. Global Mapping of the Yeast Genetic Interaction Network. *Science*. 2004;303: 808–813.
doi:10.1126/science.1091317
47. Schuldiner M, Collins SR, Thompson NJ, Denic V, Bhamidipati A, Punna T, et al. Exploration of the Function and Organization of the Yeast Early Secretory Pathway through an Epistatic Miniarray Profile. *Cell*. 2005;123: 507–519.
doi:10.1016/j.cell.2005.08.031
48. Braberg H, Jin H, Moehle EA, Chan YA, Wang S, Shales M, et al. From Structure to Systems: High-Resolution, Quantitative Genetic Analysis of RNA Polymerase II. *Cell*. 2013;154: 775–788. doi:10.1016/j.cell.2013.07.033
49. Costanzo M, Baryshnikova A, Bellay J, Kim Y, Spear ED, Sevier CS, Ding H, Koh JL, Toufighi K, Mostafavi S, Prinz J, St Onge RP, VanderSluis B, Makhnevych T,

Vizeacoumar FJ, Alizadeh S, Bahr S, Brost RL, Chen Y, Cokol M, Deshpande R, Li Z, Lin ZY, Liang W, Marback M, Paw J, San Luis BJ, Shuteriqi E, Tong AH, van Dyk N, Wallace IM, Whitney JA, Weirauch MT, Zhong G, Zhu H, Houry WA, Brudno M, Ragibizadeh S, Papp B, Pál C, Roth FP, Giaever G, Nislow C, Troyanskaya OG, Bussey H, Bader GD, Gingras AC, Morris QD, Kim PM, Kaiser CA, Myers CL, Andrews BJ, Boone C. The genetic landscape of a cell. *Science*. 2010;327: 425–431. doi:10.1126/science.1180823

50. Costanzo M, VanderSluis B, Koch EN, Baryshnikova A, Pons C, Tan G, Wang W, Usaj M, Hanchard J, Lee SD, Pelechano V, Styles EB, Billmann M, van Leeuwen J, van Dyk N, Lin ZY, Kuzmin E, Nelson J, Piotrowski JS, Srikumar T, Bahr S, Chen Y, Deshpande R, Kurat CF, Li SC, Li Z, Usaj MM, Okada H, Pascoe N, San Luis BJ, Sharifpoor S, Shuteriqi E, Simpkins SW, Snider J, Suresh HG, Tan Y, Zhu H, Malod-Dognin N, Janjic V, Przulj N, Troyanskaya OG, Stagljar I, Xia T, Ohya Y, Gingras AC, Raught B, Boutros M, Steinmetz LM, Moore CL, Rosebrock AP, Caudy AA, Myers CL, Andrews B, Boone C. A global genetic interaction network maps a wiring diagram of cellular function. *Science*. 2016;353. doi:10.1126/science.aaf1420
51. Sarin S, Ross KE, Boucher L, Green Y, Tyers M, Cohen-Fix O. Uncovering Novel Cell Cycle Players Through the Inactivation of Securin in Budding Yeast. *Genetics*. 2004;168: 1763–1771. doi:10.1534/genetics.104.029033
52. Finley D, Sadis S, Monia BP, Boucher P, Ecker DJ, Crooke ST, et al. Inhibition of proteolysis and cell cycle progression in a multiubiquitination-deficient yeast mutant. *Mol Cell Biol*. 1994;14: 5501–5509.

53. Tong AHY, Boone C. Synthetic genetic array analysis in *Saccharomyces cerevisiae*. *Methods Mol Biol Clifton NJ*. 2006;313: 171–192.
54. Collins SR, Roguev A, Krogan NJ. Quantitative Genetic Interaction Mapping Using the E-MAP Approach. *Methods Enzymol*. 2010;470: 205–231. doi:10.1016/S0076-6879(10)70009-4
55. Haber JE, Braberg H, Wu Q, Alexander R, Haase J, Ryan C, et al. Systematic Triple-Mutant Analysis Uncovers Functional Connectivity between Pathways Involved in Chromosome Regulation. *Cell Rep*. 2013;3: 2168–2178. doi:10.1016/j.celrep.2013.05.007
56. Deutschbauer AM, Davis RW. Quantitative trait loci mapped to single-nucleotide resolution in yeast. *Nat Genet*. 2005;37: ng1674. doi:10.1038/ng1674
57. Neiman AM. Sporulation in the Budding Yeast *Saccharomyces cerevisiae*. *Genetics*. 2011;189: 737–765. doi:10.1534/genetics.111.127126
58. Ben-Ari G, Zenvirth D, Sherman A, David L, Klutstein M, Lavi U, et al. Four Linked Genes Participate in Controlling Sporulation Efficiency in Budding Yeast. *PLoS Genet*. 2006;2. doi:10.1371/journal.pgen.0020195
59. Maeda T. The signaling mechanism of ambient pH sensing and adaptation in yeast and fungi. *FEBS J*. 2012;279: 1407–1413. doi:10.1111/j.1742-4658.2012.08548.x
60. Rando OJ, Winston F. Chromatin and Transcription in Yeast. *Genetics*. 2012;190: 351–387. doi:10.1534/genetics.111.132266

61. Knauer R, Lehle L. The oligosaccharyltransferase complex from *Saccharomyces cerevisiae*. Isolation of the OST6 gene, its synthetic interaction with OST3, and analysis of the native complex. *J Biol Chem*. 1999;274: 17249–17256.
62. Stagljar I, te Heesen S, Aebi M. New phenotype of mutations deficient in glucosylation of the lipid-linked oligosaccharide: cloning of the ALG8 locus. *Proc Natl Acad Sci U S A*. 1994;91: 5977–5981.
63. Arlt H, Perz A, Ungermann C. An overexpression screen in *Saccharomyces cerevisiae* identifies novel genes that affect endocytic protein trafficking. *Traffic Cph Den*. 2011;12: 1592–1603. doi:10.1111/j.1600-0854.2011.01252.x
64. Delbecq P, Calvo O, Filipkowski RK, Piérard A, Messenguy F. Functional analysis of the leader peptide of the yeast gene CPA1 and heterologous regulation by other fungal peptides. *Curr Genet*. 2000;38: 105–112.
65. Krogan NJ, Greenblatt JF. Characterization of a Six-Subunit Holo-Elongator Complex Required for the Regulated Expression of a Group of Genes in *Saccharomyces cerevisiae*. *Mol Cell Biol*. 2001;21: 8203–8212.
doi:10.1128/MCB.21.23.8203-8212.2001
66. Petrakis TG, Søggaard TMM, Erdjument-Bromage H, Tempst P, Svejstrup JQ. Physical and functional interaction between Elongator and the chromatin-associated Kti12 protein. *J Biol Chem*. 2005;280: 19454–19460. doi:10.1074/jbc.M413373200

67. Briand J-F, Navarro F, Rematier P, Boschiero C, Labarre S, Werner M, et al. Partners of Rpb8p, a Small Subunit Shared by Yeast RNA Polymerases I, II, and III. *Mol Cell Biol.* 2001;21: 6056–6065. doi:10.1128/MCB.21.17.6056-6065.2001
68. Waldherr M, Ragnini A, Jank B, Teply R, Wiesenberger G, Schweyen RJ. A multitude of suppressors of group II intron-splicing defects in yeast. *Curr Genet.* 1993;24: 301–306.
69. Sibirny AA. Yeast peroxisomes: structure, functions and biotechnological opportunities. *FEMS Yeast Res.* 2016;16. doi:10.1093/femsyr/fow038
70. Mountain HA, Byström AS, Larsen JT, Korch C. Four major transcriptional responses in the methionine/threonine biosynthetic pathway of *Saccharomyces cerevisiae*. *Yeast.* 1991;7: 781–803. doi:10.1002/yea.320070804
71. Huang DW, Sherman BT, Lempicki RA. Systematic and integrative analysis of large gene lists using DAVID bioinformatics resources. *Nat Protoc.* 2009;4: 44–57. doi:10.1038/nprot.2008.211
72. Huang DW, Sherman BT, Lempicki RA. Bioinformatics enrichment tools: paths toward the comprehensive functional analysis of large gene lists. *Nucleic Acids Res.* 2009;37: 1–13. doi:10.1093/nar/gkn923
73. Liu JQ, Nagata S, Dairi T, Misono H, Shimizu S, Yamada H. The GLY1 gene of *Saccharomyces cerevisiae* encodes a low-specific L-threonine aldolase that catalyzes cleavage of L-allo-threonine and L-threonine to glycine--expression of the gene in

Escherichia coli and purification and characterization of the enzyme. *Eur J Biochem.* 1997;245: 289–293.

74. Ryan CJ, Roguev A, Patrick K, Xu J, Jahari H, Tong Z, et al. Hierarchical Modularity and the Evolution of Genetic Interactomes across Species. *Mol Cell.* 2012;46: 691–704. doi:10.1016/j.molcel.2012.05.028

75. Regenberg B, Düring-Olsen L, Kielland-Brandt MC, Holmberg S. Substrate specificity and gene expression of the amino-acid permeases in *Saccharomyces cerevisiae*. *Curr Genet.* 1999;36: 317–328.

76. Fisk DG, Ball CA, Dolinski K, Engel SR, Hong EL, Issel-Tarver L, et al. *Saccharomyces cerevisiae* S288C genome annotation: a working hypothesis. *Yeast Chichester Engl.* 2006;23: 857–865. doi:10.1002/yea.1400

77. Zattas D, Hochstrasser M. Ubiquitin-dependent protein degradation at the yeast endoplasmic reticulum and nuclear envelope. *Crit Rev Biochem Mol Biol.* 2015;50: 1–17. doi:10.3109/10409238.2014.959889

74. Sumara I, Maerki S, Peter M. E3 ubiquitin ligases and mitosis: embracing the complexity. *Trends Cell Biol.* 2008;18: 84–94. doi:10.1016/j.tcb.2007.12.001

79. Tyers M, Jorgensen P. Proteolysis and the cell cycle: with this RING I do thee destroy. *Curr Opin Genet Dev.* 2000;10: 54–64. doi:10.1016/S0959-437X(99)00049-0

80. Thornton BR, Toczyski DP. Securin and B-cyclin/CDK are the only essential targets of the APC. *Nat Cell Biol.* 2003;5: 1090–1094. doi:10.1038/ncb1066
81. Rodrigo-Brenni MC, Morgan DO. Sequential E2s Drive Polyubiquitin Chain Assembly on APC Targets. *Cell.* 2007;130: 127–139. doi:10.1016/j.cell.2007.05.027
82. Arnason T, Ellison MJ. Stress resistance in *Saccharomyces cerevisiae* is strongly correlated with assembly of a novel type of multiubiquitin chain. *Mol Cell Biol.* 1994;14: 7876–7883.
83. Kirkpatrick DS, Hathaway NA, Hanna J, Elsasser S, Rush J, Finley D, et al. Quantitative analysis of in vitro ubiquitinated cyclin B1 reveals complex chain topology. *Nat Cell Biol.* 2006;8: 700–710. doi:10.1038/ncb1436
84. Rodrigo-Brenni MC, Foster SA, Morgan DO. Catalysis of lysine 48-specific ubiquitin chain assembly by residues in E2 and ubiquitin. *Mol Cell.* 2010;39: 548–559. doi:10.1016/j.molcel.2010.07.027
85. Schwickart M, Havlis J, Habermann B, Bogdanova A, Camasses A, Oelschlaegel T, et al. Swm1/Apc13 Is an Evolutionarily Conserved Subunit of the Anaphase-Promoting Complex Stabilizing the Association of Cdc16 and Cdc27. *Mol Cell Biol.* 2004;24: 3562–3576. doi:10.1128/MCB.24.8.3562-3576.2004
86. Zachariae W, Shevchenko A, Andrews PD, Ciosk R, Galova M, Stark MJR, et al. Mass Spectrometric Analysis of the Anaphase-Promoting Complex from Yeast: Identification of a Subunit Related to Cullins. *Science.* 1998;279: 1216–1219. doi:10.1126/science.279.5354.1216

87. Brown NG, VanderLinden R, Watson ER, Weissmann F, Ordureau A, Wu K-P, et al. Dual RING E3 Architectures Regulate Multiubiquitination and Ubiquitin Chain Elongation by APC/C. *Cell*. 2016;165: 1440–1453. doi:10.1016/j.cell.2016.05.037
88. Ostapenko D, Burton JL, Solomon MJ. The Ubp15 deubiquitinase promotes timely entry into S phase in *Saccharomyces cerevisiae*. *Mol Biol Cell*. 2015;26: 2205–2216. doi:10.1091/mbc.E14-09-1400
89. Shirayama M, Tóth A, Gálová M, Nasmyth K. APCCdc20 promotes exit from mitosis by destroying the anaphase inhibitor Pds1 and cyclin Clb5. *Nature*. 1999;402: 203–207. doi:10.1038/46080
90. Foe IT, Foster SA, Cheung SK, DeLuca SZ, Morgan DO, Toczyski DP. Ubiquitination of Cdc20 by the APC occurs through an intramolecular mechanism. *Curr Biol CB*. 2011;21: 1870–1877. doi:10.1016/j.cub.2011.09.051
91. Zachariae W, Schwab M, Nasmyth K, Seufert W. Control of Cyclin Ubiquitination by CDK-Regulated Binding of Hct1 to the Anaphase Promoting Complex. *Science*. 1998;282: 1721–1724. doi:10.1126/science.282.5394.1721
92. Ljungdahl PO. Amino-acid-induced signalling via the SPS-sensing pathway in yeast. *Biochem Soc Trans*. 2009;37: 242–247. doi:10.1042/BST0370242
93. Petroski MD, Deshaies RJ. Mechanism of Lysine 48-Linked Ubiquitin-Chain Synthesis by the Cullin-RING Ubiquitin-Ligase Complex SCF-Cdc34. *Cell*. 2005;123: 1107–1120. doi:10.1016/j.cell.2005.09.033

94. Lauwers E, Erpapazoglou Z, Haguenaer-Tsapis R, André B. The ubiquitin code of yeast permease trafficking. *Trends Cell Biol.* 2010;20: 196–204.
doi:10.1016/j.tcb.2010.01.004
95. Kim HC, Huibregtse JM. Polyubiquitination by HECT E3s and the Determinants of Chain Type Specificity. *Mol Cell Biol.* 2009;29: 3307–3318.
doi:10.1128/MCB.00240-09
96. Garnett MJ, Mansfeld J, Godwin C, Matsusaka T, Wu J, Russell P, et al. UBE2S elongates ubiquitin chains on APC/C substrates to promote mitotic exit. *Nat Cell Biol.* 2009;11: 1363–1369. doi:10.1038/ncb1983
97. Wickliffe KE, Lorenz S, Wemmer DE, Kuriyan J, Rape M. The Mechanism of Linkage-Specific Ubiquitin Chain Elongation by a Single-Subunit E2. *Cell.* 2011;144: 769–781. doi:10.1016/j.cell.2011.01.035
98. Boeke JD, LaCroute F, Fink GR. A positive selection for mutants lacking orotidine-5'-phosphate decarboxylase activity in yeast: 5-fluoro-orotic acid resistance. *Mol Gen Genet MGG.* 1984;197: 345–346.
99. Hanna J, Leggett DS, Finley D. Ubiquitin depletion as a key mediator of toxicity by translational inhibitors. *Mol Cell Biol.* 2003;23: 9251–9261.
100. Partow S, Siewers V, Bjørn S, Nielsen J, Maury J. Characterization of different promoters for designing a new expression vector in *Saccharomyces cerevisiae*. *Yeast Chichester Engl.* 2010;27: 955–964. doi:10.1002/yea.1806

101. Finley D, Bartel B, Varshavsky A. The tails of ubiquitin precursors are ribosomal proteins whose fusion to ubiquitin facilitates ribosome biogenesis. *Nature*. 1989;338: 394–401. doi:10.1038/338394a0
102. Ozkaynak E, Finley D, Solomon MJ, Varshavsky A. The yeast ubiquitin genes: a family of natural gene fusions. *EMBO J*. 1987;6: 1429–1439.
103. Schuldiner M, Collins SR, Weissman JS, Krogan NJ. Quantitative genetic analysis in *Saccharomyces cerevisiae* using epistatic miniarray profiles (E-MAPs) and its application to chromatin functions. *Methods San Diego Calif*. 2006;40: 344–352. doi:10.1016/j.ymeth.2006.07.034
104. Collins SR, Schuldiner M, Krogan NJ, Weissman JS. A strategy for extracting and analyzing large-scale quantitative epistatic interaction data. *Genome Biol*. 2006;7: R63. doi:10.1186/gb-2006-7-7-r63
105. Collins SR, Miller KM, Maas NL, Roguev A, Fillingham J, Chu CS, et al. Functional dissection of protein complexes involved in yeast chromosome biology using a genetic interaction map. *Nature*. 2007;446: 806–810. doi:10.1038/nature05649
106. Cox J, Mann M. MaxQuant enables high peptide identification rates, individualized p.p.b.-range mass accuracies and proteome-wide protein quantification. *Nat Biotechnol*. 2008;26: 1367–1372. doi:10.1038/nbt.1511

107. Hashash N, Johnson AL, Cha RS. Regulation of fragile sites expression in budding yeast by MEC1, RRM3 and hydroxyurea. *J Cell Sci.* 2011;124: 181–185.
doi:10.1242/jcs.077313

108. Hashash N, Johnson AL, Cha RS. Topoisomerase II– and Condensin-Dependent Breakage of MEC1ATR-Sensitive Fragile Sites Occurs Independently of Spindle Tension, Anaphase, or Cytokinesis. *PLOS Genet.* 2012;8: e1002978.
doi:10.1371/journal.pgen.1002978

Materials and Methods

Generation of an SK1 gene deletion library

SK1 diploids of genotype *his3/his3 ura3/ura3 CAN1/can1::STE2pr-SpHIS5* were transformed with a PCR-generated cassette containing the KanMX4 module flanked by ORF-specific homology. Transformants were selected by their dominant resistance to geneticin (G148). Correct replacement of the target locus with the KanMX4 module was verified by the appearance of PCR products of expected size. The resulting heterozygotes were sporulated at 25°C for 2 days. To select for haploids of MAT_a, and carrying the STE2pr-SpHIS5 at the *can1* locus, cells were pinned onto SD + canavanine + uracil – histidine plates and incubated at 30°C for 2 days. To select for cells carrying single gene deletions, haploids were then transferred to plates containing 400 mg/L G418 plates and incubated at 30°C for 24 hours.

Deletion of *UBI1*

The ubiquitin linkage SGA required the analysis of genetic interactions in cells carrying mutations in all four ubiquitin loci, a single gene deletion, as well as haploid selectable markers. To decrease the number of loci under selection, and thereby increase the percentage of spores with the desired genotype, the *UBI1* locus was deleted in all strains in the SK1 Deletion library, as well as in the panel of K-to-R ubiquitin mutant strains (see below). *UBI1* was replaced with a construct expressing the ribosomal protein Rpl40A from the constitutive GPD promoter (**Figure 1-figure supplement 6**). This decreased the number of selection steps required for the ubiquitin linkage SGA to 6: 3 ubiquitin loci, 1 gene deletion, 2 haploid and mating type selection markers.

As outlined in **Figure 1-figure supplement 6**, a 500 μ L liquid culture of strain DS1 of the genotype Mat alpha; *his3*; *ura3*; CAN1; *ubi1 Δ ::LoxP-GAL1pr-Cre-URA3-LoxP-GPDpr-RPL40A* was spread on a C-uracil plate to generate a lawn of cells that was subsequently pinned into the 384 format to allow mating to the SK1 gene deletion library. It is worth noting that the GAL1pr-Cre construct could not be maintained in bacteria due to leakiness of the promoter, and was therefore amplified from yeast genomic DNA directly. After mating to the SK1 gene deletion array on YPAD medium, diploids were selected using C-uracil + G418 plates. After sporulation for 2 days, haploids were selected first on C-uracil for 24 hours; then on C-uracil + G418 for 2 days. Then, haploids were plated on 2% galactose containing plates for 2 days to induce Cre recombinase that deleted the endogenous ubiquitin in *UBI1*, as well as *URA3* and the Cre recombinase due to the position of the LoxP sites. The modified library was plated on 5-fluoro-orotic acid (FOA) plates and incubated at 30°C for 24 hours. This serves as a negative selection for the *URA3* auxotrophic marker, such that cells containing a functional *URA3* gene will die on FOA plates [98]. FOA negative selection was performed consecutively three times to ensure *URA3* deletion, and the final plate was replica plated on C-uracil plates. The modified *ubi1* locus was amplified from the library using primers outside the homology arms and sequenced to confirm the successful recombination event. Deletion of *UBI1* did not result in changes in the total ubiquitin levels (**Figure 1-figure supplement 6C**), agreeing with a previous report [99] or any changes in the doubling time.

Generation of K-to-R ubiquitin mutant strains

To express K-to-R mutant ubiquitin alleles from a strong, constitutive promoter, *TEF1*, *HYP2*, *PYK1*, *PDC1*, and GPD promoters were analyzed, and the GPD promoter was chosen since it resulted in the highest ubiquitin expression in agreement with a previous report [100].

Plasmids generated, and the relevant cloning information, are listed in **Table S1**. Generation of the *ubi1* allele is discussed above.

The *UBI2* locus was replaced with two tandem copies of the GPD promoter driving expression of the ribosomal protein Rpl40A (**Figure 1-figure supplement 1**). The modified locus was marked with the Hygromycin resistance gene. Deletion of *UBI2* resulted in a doubling time of 2 hours, compared to 1.6 hours for wild type cells, in agreement with a previous report [2]. The modified *ubi2* locus with 2 tandem GPDpr-*RPL40A* copies exhibited a normal doubling time.

The endogenous *UBI3* locus encodes a hybrid of ubiquitin fused to the ribosomal protein gene *RPS31*. The locus was replaced with a construct expressing a polypeptide composed of three tandem ubiquitin copies fused to one *RPS31* copy, under the control of the GPD promoter. An additional *RPS31* gene was placed under the control of the GPD promoter at this locus (**Figure 1-figure supplement 1**). Several *UBI3* modifications were attempted prior to selecting this construct. Deletion of *UBI3* resulted in a doubling time of 7 hours, in agreement with a previous report [2]. Multiple *ubi3* alleles were generated with varying numbers of GPDpr-*RPS31* copies. Although there was a correlation between the number of *RPS31* copies and doubling time, even 5 copies of GPDpr-*RPS31* resulted in a slow doubling time of 3 hours. It is suggested the

ubiquitin fusion protein assists in ribosomal protein expression [101]. Therefore, given the possibility that ubiquitin acts as a chaperone for Rps31, 3 tandem copies of ubiquitin were fused to *RPS31*. An additional GPDpr-*RPS31* copy was integrated, and the *ubi3* locus was marked with *URA3* (**Figure 1-figure supplement 1**). The resulting *ubi3* allele led to growth rates similar to wild type.

The *UBI4* locus normally encodes 5 tandem copies of ubiquitin, expressed as single polypeptide. *UBI4* was replaced with a 2 copies of a construct expressing, under the control of the GPD promoter, ubiquitin including the C-terminal asparagine found in endogenous *UBI4* and which is proteolytically processed to release mature ubiquitin [1,102]. This locus was marked with a Nourseothricin (NAT) resistance cassette (**Figure 1-figure supplement 1**).

A strain expressing low levels of wild type ubiquitin was included to control for the potential effects of altered ubiquitin levels. The strain differs from other strains in this study at *ubi4*, which is replaced only with the NAT resistance cassette. Thus, ubiquitin is only expressed from *ubi3* (**Figure 1-figure supplement 3A**).

Lysine 48 of ubiquitin is essential, therefore, the K48R ubiquitin mutant strain was modified to express one copy of wild type ubiquitin from the GPD promoter-driven triple-ubiquitin fusion at *ubi3* (**Figure 1-figure supplement 3B**). Double mutants carrying the K48R mutation and another lysine mutation expressed one copy of double lysine mutant ubiquitin (K11R K48R, for example) and two copies of single mutant ubiquitin (K11R, for example) at *ubi3*. Double mutant ubiquitin was expressed from *ubi4*.

To integrate the constructs described above, a diploid strain homozygous for the engineered *ubi1* locus was transformed with the *ubi2*-targeting construct. Transformants were selected on hygromycin plates, and then transformed with the *ubi3*-targeting constructs carrying the various ubiquitin mutations. The resulting transformants were selected on plates lacking uracil, then sporulated. Triple mutant *ubi1; ubi2; ubi3* cells of mating type alpha were selected by growth on plates lacking uracil, and containing hygromycin. The *ubi4* targeting constructs carrying ubiquitin mutations were introduced into a wild type diploid strain. The strain was sporulated, and *ubi4* mutant haploids of mating type a were selected by their growth on nourseothricin-containing plates. *ubi1; ubi2; ubi3* cells were mated to cells carrying the *ubi4* mutant locus. Diploids were sporulated, and haploids carrying all modified ubiquitin loci were selected.

Optimization and establishment of the ubiquitin linkage SGA protocol

A detailed 4-marker SK1 SGA protocol is outlined in **Figure 1-figure supplement 4**, and is modified from the 2-marker s288c SGA protocol with the key optimization steps described below[103]. To ensure the quality of the genetic interaction screen, multiple optimizations were performed at various steps of the ubiquitin linkage SGA. During the pinning steps with a Singer ROTOR instrument, a mixed pinning set up was used to maximize the number of cells transferred. Linkage analysis was used in pilot screens to determine whether the selections were functional and recovered accurate genetic interactions. Specifically, since the SGA is selecting for haploid cells with modified ubiquitin loci, crossing all K-to-R ubiquitin strains to the *ubi2* deletion strain from the SK1 deletion library will result in lethality.

Sporulation of the SK1 strain is 90-100% efficient compared to the 10-16% sporulation efficiency of s288c strain [56]. Conventional SGA studies using S288C sporulate cells for 5 days. The high sporulation efficiency of SK1 allowed sporulation for 2 days at 25°C, thereby shortening the duration of the genetic screen significantly.

It is essential to determine the optimal concentration of G418, as this selection is required to select against the wild type allele of the K-to-R mutant strains and select for the specific gene deletion that comes from the library. Previous SGA studies have used between 100mg/L and 200mg/L G418 [54]. Titration of various G418 concentrations for SK1 indicated that this strain requires higher G418 concentrations. 350mg/L was used for the ubiquitin linkage SGA.

After sporulation, canavanine is used to kill the remaining diploids. In the S288C-SGA, since sporulation is inefficient, 50 mg/L Canavanine is included throughout the SGA workflow (following sporulation) (**Figure 1-figure supplement 4**) [7]. In the SK1 SGA, including 50 mg/L Canavanine along with the mutant selection steps (e.g. 50 mg/L Canavanine + 350 mg/L G418) resulted in sickness and changes in the colony sizes (data not shown). Titration of canavanine, in combination with the various selection drugs used in the SGA workflow, revealed that 10mg/L of canavanine was sufficient to kill diploids, without causing growth defects. 50mg/L of canavanine was still used for haploid selection following sporulation, and 10mg/L was included in all subsequent selection plates (**Figure 1-figure supplement 4**).

The K-to-R ubiquitin loci were selected prior to selecting for the deletion array, as linkage analysis with *ubi2* revealed that the reverse order did not efficiently select for cells carrying the modified ubiquitin loci. Haploid mutant selections were performed in

the following order: 1) C-uracil plates (*ubi3*), 200 mg/L hygromycin (*ubi2*); 2) 100mg/L Nourseothricin (*ubi4*); 3) 350 mg/L G418 (single gene deletions). In each drug selection step, the previous selection drug or condition was included to ensure precise mutant selections (**Figure 1-figure supplement 4**).

SGA data analysis

The final double mutant selection plates were grown at 30°C for 48 hours, and then photographed. Colony sizes were recorded and normalized, and genetic interaction scores (S-scores) were calculated using established SGA protocols [54,104]. Of the 2655 gene deletion strains used in the final analysis, 576 strains were analyzed based on three technical replicates, while the rest were analyzed based on 2 biological replicates, each with 3 technical replicates. The 2 biological replicates were used to compute the correlation coefficient between replicates of the screen. Hierarchical clustering of mutants was performed using the Gene Cluster 3.0 software, and data was visualized with TreeView. The Pearson correlation coefficient between the genetic interactions of the K-to-R ubiquitin mutants and the genetic interactions of thousands of single gene deletions was calculated using a combined budding yeast genetic interactome data set [74]. Correlation coefficients calculated from genetic interaction profiles with 500 or more genetic interaction pairs are graphed in **Figure 3E**. For analysis of gene ontology term enrichment, the genetic interactions of K-to-R ubiquitin mutants with S-scores of -2 or less were analyzed for the enrichment of biological process (BP_Direct) GO terms using the Database for Annotation, Visualization and Integrated Discovery (DAVID) tool [71,72].

Analysis of genetic similarity enrichment within physically interacting gene pairs

The degree of enrichment of genetic interaction profile similarity among gene pairs that physically interact was compared to gene pairs that are not known to physically interact. This comparison was carried out using the genetic interactions in the ubiquitin SGA, as well as the chromosome biology E-MAP [105]. The analysis was done for the 392 gene deletions that were present in both screens. Physical interaction data was obtained from Collins *et al*, 2007. A threshold of a PE score greater than 2 was used to determine gene pairs that physically interact. The Pearson correlation coefficient for all gene deletions was calculated based on the similarity of their genetic interaction profiles in each screen. The correlation coefficients of physically interacting and non-interacting genes were graphed.

Strains, cell culture conditions, and plasmids

Plasmids and strains used in this study are listed in Supplementary tables 1 and 2, respectively. All yeast strains in this study are in the SK1 background. Cells were cultured at 30°C, unless otherwise noted, on YM-1 media supplemented with 2% dextrose. Selective media lacking specific amino acids or nucleobases was made using Complete Supplement Mixture (CSM) from Sunrise Sciences, supplemented with yeast nitrogen base and 2% glucose. Cloning of constructs and transformations were done using standard techniques.

Validation of genetic interactions

K-to-R ubiquitin mutant strains (DS368-397, Supplementary Table 2) were mated to desired single gene deletions from the SK1 deletion library. Diploid cells were

sporulated at 23°C, and tetrads were dissected on YM-1 plates with 2% dextrose. Spores were then genotyped by replica-plating onto appropriate plates, and the desired mutant spores were selected. Petite colonies were identified by lack of growth on plates containing 3% glycerol as the carbon source and discarded. To analyze the growth of strains, overnight cultures were normalized to an OD600 value of 1, then 5-fold serial dilutions were spotted onto CSM plates supplemented with 2% glucose, unless otherwise indicated, grown for 3 days at 30°C and then scanned. It is worth noting that, as with all SGA analyses, a quantitative validation of genetic interactions requires the replication of the full SGA protocol (Figure 1-figure supplement 4) since the presence of any or all of the four selectable markers used could affect the genetic interaction.

Threonine uptake assay

Overnight cultures were diluted to OD600 of 0.05 in B-liquid, pH4.5, supplemented with 0.01mg/ml histidine, 0.02mg/ml uracil, and 0.1mM threonine. When cultures reached OD600 of 0.3, 6ml were collected for time point zero and placed on ice with 120ul of 1M NaN₃. The cells were incubated on ice for the duration of the experiment, then 0.5uCi of 3-3H L-threonine (American Radiolabeled Chemicals, ART 0330) were added to time point zero, and mixed by inverting once. Cells were then immediately collected by filtration with glass microfiber filters (Whatman, 934-AH), and then washed with 25ml of cold water. The filter was then placed in a scintillation vial and dried overnight at 55°C. To begin the time-course experiment, 3uCi of 3-3H L-threonine were added to each 34ml culture. For each indicated time point, 6ml were collected by filtration as described above. The OD600 of the cultures was recorded at each time point. Radioactivity was measured by liquid scintillation counting (Research Products

International, Bio-Safe NA; Beckman, LS6500) for 5 minutes. Experiments were performed in triplicate. The slope was calculated by linear regression, and a 2 sample T-test was performed to determine statistical significance.

Quantitative proteomics

The indicated strains were grown to mid-log phase in C-Lys media containing either ¹³C6, ¹⁵N2 (Cambridge Isotope Laboratories, Tewksbury MA), or unlabeled lysine, both at 0.06mg/ml. Sufficient incorporation of labeled lysine was attained by allowing cells grow for more than eight generations. Cells were collected by centrifugation, washed with cold HPLC-grade water and flash frozen. Cell pellets were then resuspended in lysis buffer (8M urea, 0.1M Tris-HCl pH 8, 150mM NaCl, Roche mini protease inhibitor tablet without EDTA) and lysed by bead beating (20 1-minute bursts with rests of 2 minutes following each cycle). Lysates were collected and incubated at room temperature with rotation. The lysates were then clarified by centrifugation at 17,000 x g for 10 minutes, followed by a second clarification cycle on the collected supernatant. The protein concentration in each sample was determined by BCA (Pierce) and samples were normalized accordingly. Disulfides were reduced with 4mM TCEP and cysteines alkylated with 10mM iodoacetamide, both for 30 minutes at room temperature in the dark. Excess iodoacetamide was quenched with 10mM DTT for 30 minutes at room temperature in the dark. The samples were diluted to reduce the urea concentration to 2M with 0.1M Tris-HCL pH 8. Trypsin (in 50mM acetic acid) was added at a ratio of 1mg of enzyme to 100mg of protein in the sample, and samples were incubated at room temperature overnight with end-to-end rotation.

After digestion 10 % TFA was added to a final concentration of 0.3-0.1 % TFA, with pH of final solution <3. Insoluble material was precipitated by centrifugation and peptides were loaded onto a Sep Pak tC18 column that had been activated with 1 mL 80 % ACN/0.1 % TFA and equilibrated with 3 x 1 mL 0.1 % TFA. Columns were washed with 5 x 1 mL 0.1 TFA and eluted with 1 mL 40 % ACN/0.1 % TFA prior to lyophilization. Diglycine-modified peptides were immunoprecipitated using an antibody specific for the K-GG motif characteristic of trypsinized, Ub-modified peptides (UbiScan, Cell Signaling Technology). Immunoprecipitates were then desalted using C18 Ultra MicroSpin columns (Nest Group), evaporated to dryness, and reconstituted in 0.1% formic acid for LC-MS/MS analysis.

Samples were analyzed on a Thermo Fisher Orbitrap Fusion mass spectrometry system equipped with a Easy nLC 1200 ultra-high pressure liquid chromatography system interfaced via a Nanospray Flex nanoelectrospray source. Samples were injected on a C18 reverse phase column (25 cm x 75 um packed with ReprosilPur C18 AQ 1.9 um particles). Peptides were separated by an organic gradient from 5% to 30% ACN in 0.1% formic acid over 120 minutes at a flow rate of 300 nl/min. The MS continuously acquired spectra in a data-dependent manner throughout the gradient, acquiring a full scan in the Orbitrap (at 120,000 resolution with an AGC target of 200,000 and a maximum injection time of 100 ms) followed by as many MS/MS scans as could be acquired on the most abundant ions in 3s in the dual linear ion trap (rapid scan type with an intensity threshold of 5000, HCD collision energy of 29%, AGC target of 10,000, a maximum injection time of 35 ms, and an isolation width of 1.6 m/z). Singly and unassigned charge states were

rejected. Dynamic exclusion was enabled with a repeat count of 1, an exclusion duration of 20 s, and an exclusion mass width of +/- 10 ppm.

Raw mass spectrometry data were assigned to *S. cerevisiae* protein sequences and MS1 intensities extracted with the MaxQuant software package (version 1.5.5.1) [106]. Data were searched against the SwissProt *S. cerevisiae* protein database. Variable modifications were allowed for N-terminal protein acetylation, methionine oxidation, and lysine diglycine modification. A static modification was indicated for carbamidomethyl cysteine. The 'Match between runs' feature was enabled to match within 2 minutes between runs. All other settings were left using MaxQuant default settings.

Cell cycle and half-life analysis experiments

Overnight cultures grown at room temperature were diluted to OD600 of 0.25, and then arrested with 15ug/ml alpha factor at room temperature for 4 hours. More alpha factor was added every 2 hours. To release cells from arrest, cells were washed and resuspended in fresh media, then shifted to 30°C. Small samples were taken for flow cytometry analysis. Alpha factor was added to cultures 45 minutes after release to prevent cells from re-entering the cell cycle following mitosis. For experiments analyzing the half-life of proteins, cycloheximide was added to cultures at 200ug/ml at the indicated time points. For experiments analyzing the half-life of proteins in G1-arrested cultures, cells growing in YM-1 media with 2% raffinose were arrested in G1 phase as described above. Cells were then collected by centrifugation, washed and resuspended in YM-1 media containing 4% galactose and 15ug/ml alpha factor for 1.5hrs, and shifted to 37°C. Cultures were then centrifuged and cells were resuspended in YM-1 containing 2% glucose, and 200ug/ml cycloheximide. Cell pellets were collected by centrifugation at the

indicated time points, washed with cold water, and then flash frozen. In all cases, the cell cycle was profiled using DNA content analysis by flow cytometry. Briefly, cells were fixed in 70% ethanol, then treated at 50°C with RNase A (0.25mg/ml in 50mM sodium citrate) and Proteinase K (0.063mg/ml in 50mM sodium citrate) for 1 hour each, followed by incubation with Sytox Green (1:10000) overnight at 4°C.

Western blots & antibodies

Cell pellets were resuspended in 100ul of Sina's loading buffer (50mM Tris pH7.5, 5mM EDTA, 10% glycerol, 5% SDS, 0.5% 2-mercaptoethanol, 0.1% w/v bromophenol blue) and 50ul of glass beads. Samples were incubated at 100°C for 7 minutes, then processed in bead beater for 3 minutes, followed by heating at 100°C for 7 minutes. Cell lysates were analyzed by SDS-PAGE using 4-20% gradient Tris-HCl gels (BioRad, #3450034). Proteins were transferred onto 0.2um nitrocellulose membrane. Membranes were blocked with 5% nonfat dry milk in PBS-T or Odyssey Blocking Buffer. Rabbit antibodies recognizing Clb2, Clb3, Clb5, and Pds1 were generous gifts from Adam Rudner. Cdc28 was analyzed with goat antibody from Santa Cruz Biotechnology (yC-20). Mouse anti-PSTAIR (P7962) and Flag epitope (F3165) were purchased from Millipore-Sigma. Rabbit anti ubiquitin antibody was purchased from Thermo-Fisher (PA3-16717) or Santa Cruz Biotechnology (sc-9133).

***In vitro* APC ubiquitination assay**

APC was immunopurified using rabbit IgG beads (Invitrogen 14301) from a yeast strain expressing Cdc16-TAP::HIS3 and lacking Cdh1 (*cdh1::LEU2*) in lysis buffer (25mM HEPES 7.5, 150mM KOAc, 5mM MgCl₂, 10% Glycerol, 0.2% Triton X, 1mM

DTT, 1mM PMSF) for 1.5 hours at 4°C following bead beating. Beads were washed 3X with 25mM HEPES 7.5, 150mM KOAc, 10% Glycerol, 0.1% Triton X.

Cdh1 was *in vitro* translated using Promega kit (Promega L1170). Cdh1 was then incubated with the APC on beads from the above step for 30 minutes at room temperature. Beads were washed 3X with 25mM HEPES 7.5, 150mM KOAc, 10% Glycerol, 0.1% Triton X.

Hsl1 (667-872)-TAP was *in vitro* translated using Promega kit (Promega L1170) using 35S-Methionine. After *in vitro* translation, the Hsl1 fragment was incubated with IgG-coupled magnetic beads for 30 minutes, and washed 3X with 25mM HEPES 7.5, 150mM KOAc, 10% Glycerol, 0.1% Triton X. Hsl1 was cleaved off the beads with TEV protease for 30 mins (AcTEV - Thermo Fisher 12575015).

Wild type (U-100Sc), K11-only (UM-K110) and K0 (UM-KOK) ubiquitin was purchased from Boston Biochem, INC. Uba1 and Ubc4 were expressed in *E. coli* and purified. Ubc4 was charged with ubiquitin using 0.2mg/ml Uba1, 2mg/ml Ubc4, 2mg/ml ATP, and 2mg/ml ubiquitin. The reaction was incubated at 37°C for at least 30 minutes. APC-Cdh1 was incubated with charged Ubc4 and TEV purified Hsl1 fragment at 25°C for 45 minutes. Reactions were terminated by adding 2X SDS loading dye and analyzed by SDS PAGE.

Figure Legends

Figure 1: The ubiquitin linkage SGA reveals the genetic interactome of polyubiquitin chain types and functional relationships between lysines of ubiquitin

A) *UBI1-UBI4* were modified to express lysine to arginine mutant ubiquitin alleles under the control of the constitutive GPD promoter. Ribosomal proteins, which are normally encoded at *UBI1-UBI3*, were also placed under the control of the GPD promoter individually, or as ubiquitin-fusions. **B)** *Top:* A clustered heat map of quantitative genetic interactions between ubiquitin K-to-R mutants and an array of single gene deletions. Each K-to-R is expressed as the only ubiquitin present in the cell, except for K48R, which is lethal and was therefore co-expressed with WT (20% of total). As indicated in the adjacent color legend, blue pixels represent negative genetic interaction scores, yellow pixels represent positive genetic interaction scores, and black pixels indicate no interaction. Grey pixels represent interactions displaying extremely low signal, which could represent either strong negative interactions or pinning errors. *Bottom:* Unbiased hierarchical clustering identifies known gene modules. Named genes are part of the complexes or pathways listed (bold), or have related functions. **C)** Scatter plot comparing the genetic interaction scores in two biological replicates of the ubiquitin SGA. The correlation coefficient between the two replicates was calculated. **D)** The correlation of genetic interaction profiles of physically interacting or non-interacting gene pairs in the ubiquitin SGA and the chromosome biology E-MAP [105]. **E)** The correlation between the genetic interactomes of K-to-R ubiquitin mutants is shown as a heat map of correlation coefficients, and a dendrogram showing hierarchical clustering.

As the color legend indicates, correlation coefficient values of 1 are shown as yellow pixels, while values of -1 are shown as blue pixels. **F)** A histogram showing the frequencies (Log2) of genetic interactions with the indicated S-scores for each single K-to-R ubiquitin mutant.

Figure 2: Gene deletions exhibit genetic interactions with specific ubiquitin linkage types

A-C) Left: The genetic interaction scores of K-to-R ubiquitin mutants with deletions of *UBC4* (**A**), *HOM2* (**B**), or *CDC26* (**C**); Scores less than zero represent varying degrees of negative genetic interactions (blue bars), while scores larger than zero indicate positive interactions (yellow bars). **Right:** Candidate genetic interactions were validated by 5-fold spot dilution assays of the indicated strains.

Figure 3: K11 linkages are functionally redundant with threonine biosynthesis and promote threonine import

A) Gene Ontology (GO) term enrichment analysis was performed on the genetic interactions of the K11R ubiquitin mutant having genetic interaction scores of -2 or less. The fold enrichment of biological function GO terms (BP_Direct) that were significantly enriched is shown. **B)** The genetic interaction scores of the K11R ubiquitin mutant were plotted against the averaged genetic interaction scores of all K-to-R strains not containing the K11R mutation. Highlighted genes had negative interactions specifically with the K11R ubiquitin mutant, and had related functions in amino acid biosynthesis. **C)** *HOM2* and *HOM3* are required for the biosynthesis of homoserine, a methionine and threonine precursor. **D)** The negative genetic interactions of the K11R ubiquitin mutant with deletions of *HOM2* or *HOM3* were validated by 5-fold spot dilution assays of the

indicated strains. Excess homoserine, threonine, or methionine was added to C-leu plates as noted. **E)** The correlation coefficient between the genetic interactions of the K11R ubiquitin mutant and single gene deletion strains was calculated. The genetic interactome of the K11R ubiquitin mutant is most similar to the genetic interactions of strains carrying deletions of *GNP1* or *YDR509W*. **F)** The import of tritiated threonine into wild type and K11R ubiquitin mutant cells was measured by scintillation counting. The Y-axis shows the measured counts per minute (CPM) divided by optical density (OD600) of the cell cultures (CPM/OD600). **G)** A negative genetic interaction between deletions of *HOM2* and *DOA10* is shown by spot dilution assays of the indicated strains. The genetic interaction is abrogated by addition of homoserine to C-leu plates.

Figure 4: K11 linkages contribute to APC-substrate turnover

A) Wild type and K11R ubiquitin mutant cells lacking Cdc26 were synchronized in G1 phase with α factor, then released into the cell cycle. Samples were taken at the specified times after release and analyzed by probing western blots for the indicated proteins. **B,** **C)** *cdc26* Δ cells expressing wild type or K11R ubiquitin were arrested in G1 with α -factor. Cells were washed in fresh media to release from the arrest and, after sixty minutes, protein synthesis was blocked by the addition of cycloheximide. The APC was active at this time point, as measured by Pds1 and Clb5 turnover (Panel 4A). Samples were taken at the specified times after cycloheximide addition and analyzed by probing western blots for the indicated proteins. Bands were quantified using the Licor Image Studio Software and were normalized to Cdc28 or PSTAIR as loading controls (n=3). **D)** Cells were synchronized in G1 phase with α factor. During the G1 arrest, Clb2-6xHis-3xFlag expression was induced by the addition of galactose, and cells were shifted to

37°C. Clb2 synthesis was then blocked by removal of galactose, and addition of glucose and cycloheximide. The levels of Clb2-6xHis-3xFlag in wild type and K11R ubiquitin cells lacking Cdc26 were analyzed by western blotting at the indicated times. Cdc28 was examined as a loading control using Anti-PSTAIR antibody. Bands were quantified as in Figure 4C. **E)** A radioactively-labeled fragment of Hsl1, amino acids 667-872, was incubated with APC, Cdh1, Ubc4, and the indicated forms of ubiquitin. The ubiquitination of Hsl1 was analyzed by SDS-PAGE and autoradiography. **F)** All lysine residues on Hsl1 (667-872) were mutated to arginine, except for 2 lysines (K775, 812) that are part of 2 KEN box degrons, and lysine 747, which has been previously reported as being ubiquitinated. This Hsl1 fragment is termed Hsl1-3K, and was analyzed as in 4E. **G)** A model describing the well-established role of K11 linkages in mammalian cells, and their function in yeast APC substrate degradation as suggested by the data presented here.

Figure Supplement Legends

Figure 1-figure supplement 1: Engineering of *ubi2-4* to express K-to-R mutant ubiquitin

A) *UBI2* was modified to express two copies of the ribosomal protein Rpl40A, each from a GPD promoter. The locus is marked with a hygromycin resistance cassette. **B)** The engineered *UBI3* locus is marked with a *URA3* cassette and expresses three tandem copies of ubiquitin fused to the ribosomal protein Rps31, under the control of the GPD promoter. An additional copy of Rps31 is expressed from its own GPD promoter. **C)** *UBI4* was modified to carry two copies of the GPD promoter, each driving expression of

mutant ubiquitin. The locus is marked with a nourseothricin (NAT) resistance cassette.

A-C) Asterisks indicate mutant ubiquitin alleles;

Figure 1-figure supplement 2: Analysis of ubiquitin levels in K-to-R ubiquitin mutants

The levels of ubiquitin were analyzed by western blotting. A wild type SK1 strain with endogenous *UBI1-4* was compared to the strains used in this study that express K-to-R mutant ubiquitin alleles, as well as wild type ubiquitin, from engineered ubiquitin loci. PSTAIR was used as loading control.

Figure 1-figure supplement 3: Engineering of strains expressing low levels of ubiquitin, and K48R ubiquitin mutants

A) A strain expressing ubiquitin at low levels was generated as described in Figure 1-figure supplement 1, with the notable difference that *UBI4* locus was replaced only with the NAT resistance cassette. Ubiquitin is therefore only expressed from *ubi3*. **B)** Strains expressing K48R ubiquitin were complemented with wild type ubiquitin to permit viability. At *ubi3* the first two ubiquitins are mutated at K48, while the third ubiquitin is wild type; at *ubi4*, K48R mutant ubiquitin is expressed. Asterisks indicate mutant ubiquitin alleles. Strains expressing ubiquitin with the K48R and another lysine mutation express one copy of double lysine mutant ubiquitin at *ubi3* and two copies at *ubi4*.

Figure 1-figure supplement 4: The ubiquitin allele SGA protocol

Ubiquitin K-to-R mutant strains were mated to an array of single gene deletion strains. Several selection steps allowed for the generation of haploid, MATa strains carrying a single gene deletion and expressing K-to-R mutant ubiquitin. The colony sizes of each

strain were recorded to identify genetic interactions. A detailed description of the ubiquitin allele protocol is included in the Materials and Methods section.

Figure 1-figure supplement 5: Genetic modifications modestly increase the sporulation efficiency of the S288C yeast strain

The sporulation efficiency of S288C diploid cells was recorded after 4 days in sporulation media at 23°C. Modest increases in sporulation efficiency were observed in cells lacking *RME1*, or carrying one or two extra copies of *IME1*, *IME2*, or *NDT80*, as indicated.

Figure 1-figure supplement 6: Deletion of *UBI1* in K-to-R ubiquitin mutant strains and the in the SK1 gene deletion array

A) *UBI1* was replaced with a construct expressing the ribosomal protein Rpl40a driven by the *GPD1* promoter. The final *ubi1* locus does not carry a marker. Initially, *UBI1* was replaced with a *URA3*-marked construct expressing the Cre recombinase protein from a galactose-inducible promoter, and flanked by LoxP recombination sites. After crossing this construct into the deletion collection, Cre was induced with galactose and the *URA3* marker and Gal1pr-Cre construct were excised from the genome by the Cre recombinase. This excision was extremely robust and was selected for in the *UBI1* backcrossed library with 5FOA **B)** The steps undertaken to modify *UBI1* in the entire SK1 gene deletion array are detailed. **C)** The levels of ubiquitin were analyzed by western blotting in the indicated strains.

Figure 3-figure supplement 1: Gnp1 is a major threonine permease

A) The import of tritiated threonine into wild type cells and cells lacking Gnp1 was measured by scintillation counting. The Y-axis shows the measured counts per minute (CPM) divided by optical density (OD600) of the cell cultures (CPM/OD600).

Figure 4-figure supplement 1: Cell cycle profiling by FACS

A) WT and K11R mutant cells were treated as in Figure 4A and analyzed by flow cytometry. **B)** WT and K11R mutant cells were treated as in Figure 4D and analyzed by flow cytometry. It is worth noting that the high flocculence of the SK1 strain renders difficult the interpretation of cell cycle profiles by FACS [107,108].

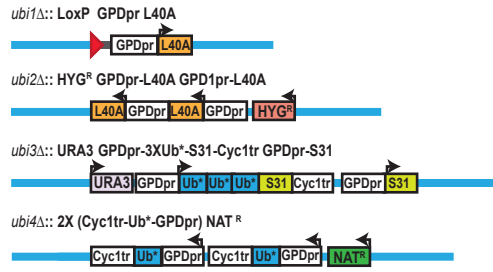
Table S1: Plasmids used in this study.

Table S2: Strains used in this study.

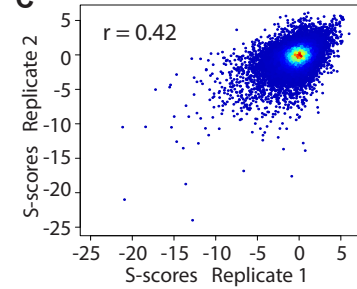
Table S3: Oligonucleotides used in this study.

Figure 1

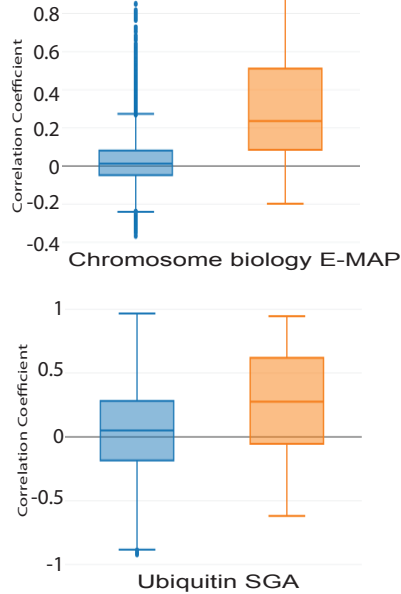
A



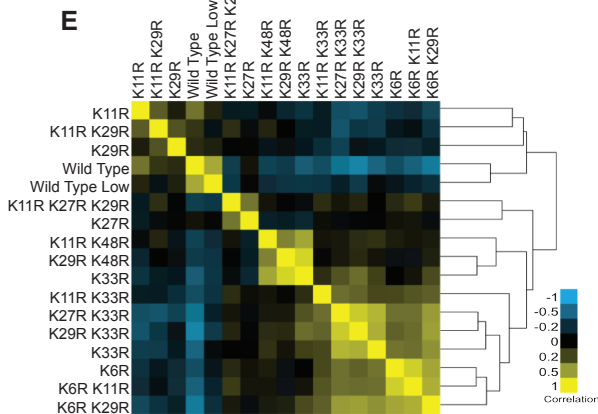
C



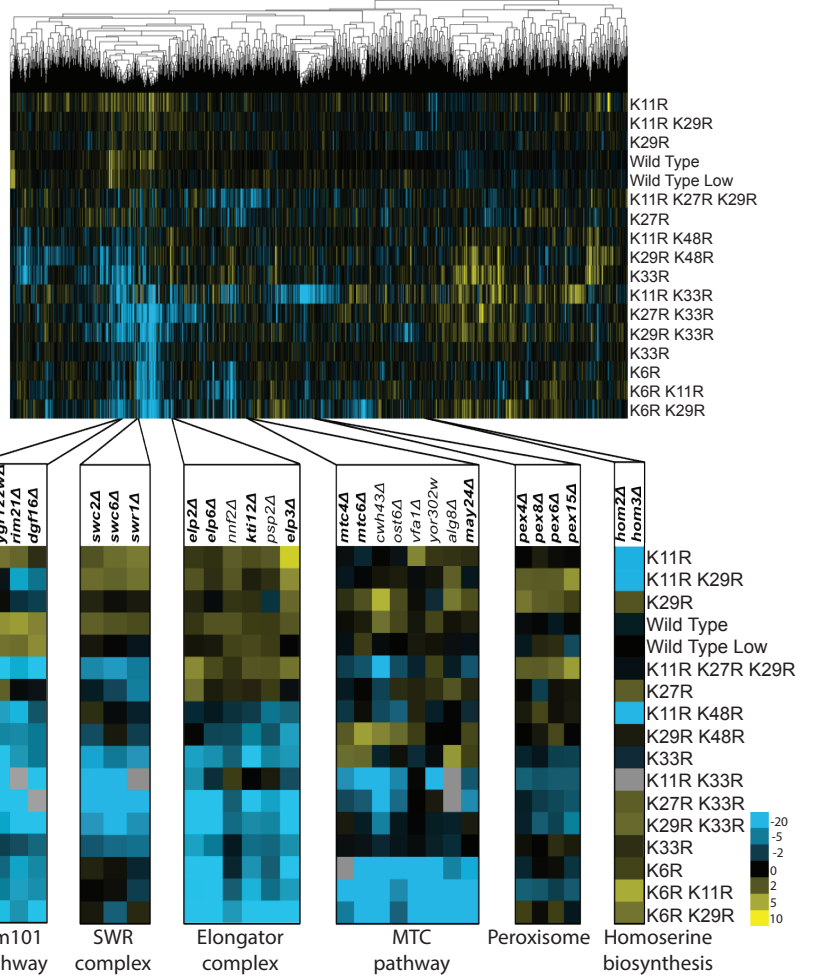
D Non-Interacting Interacting



E



B



F

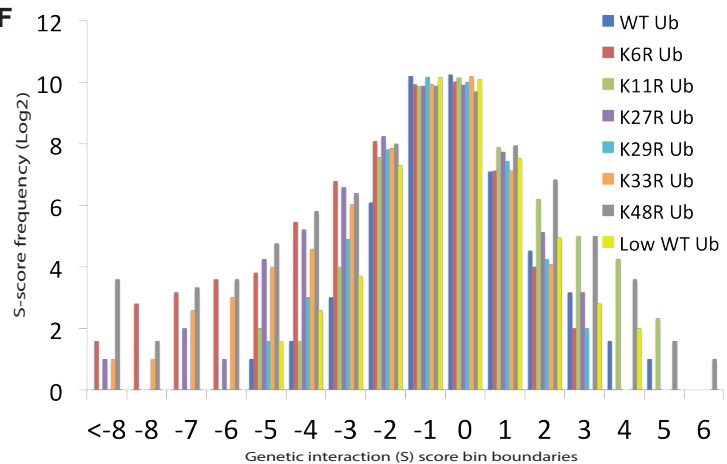


Figure 2

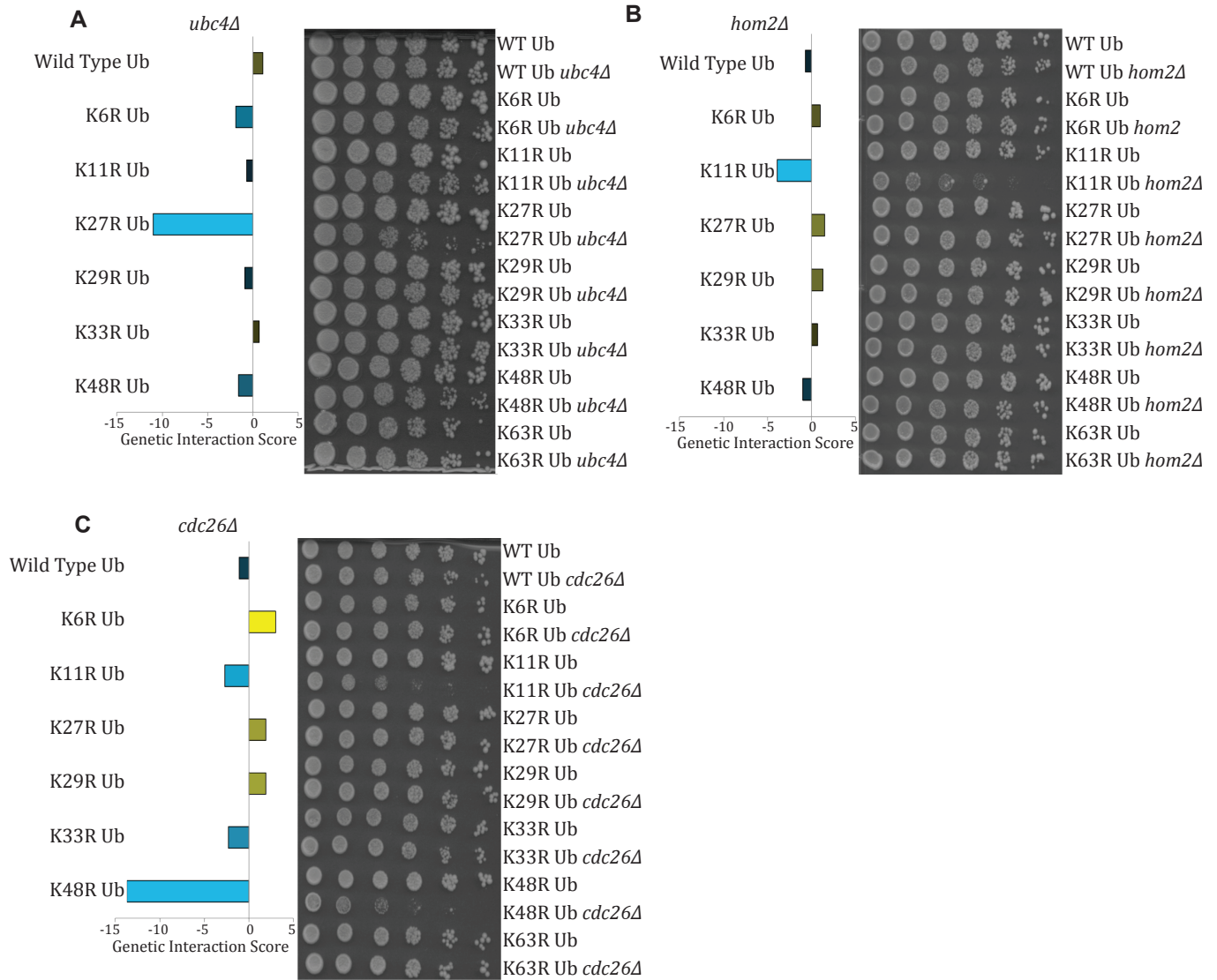


Figure 3

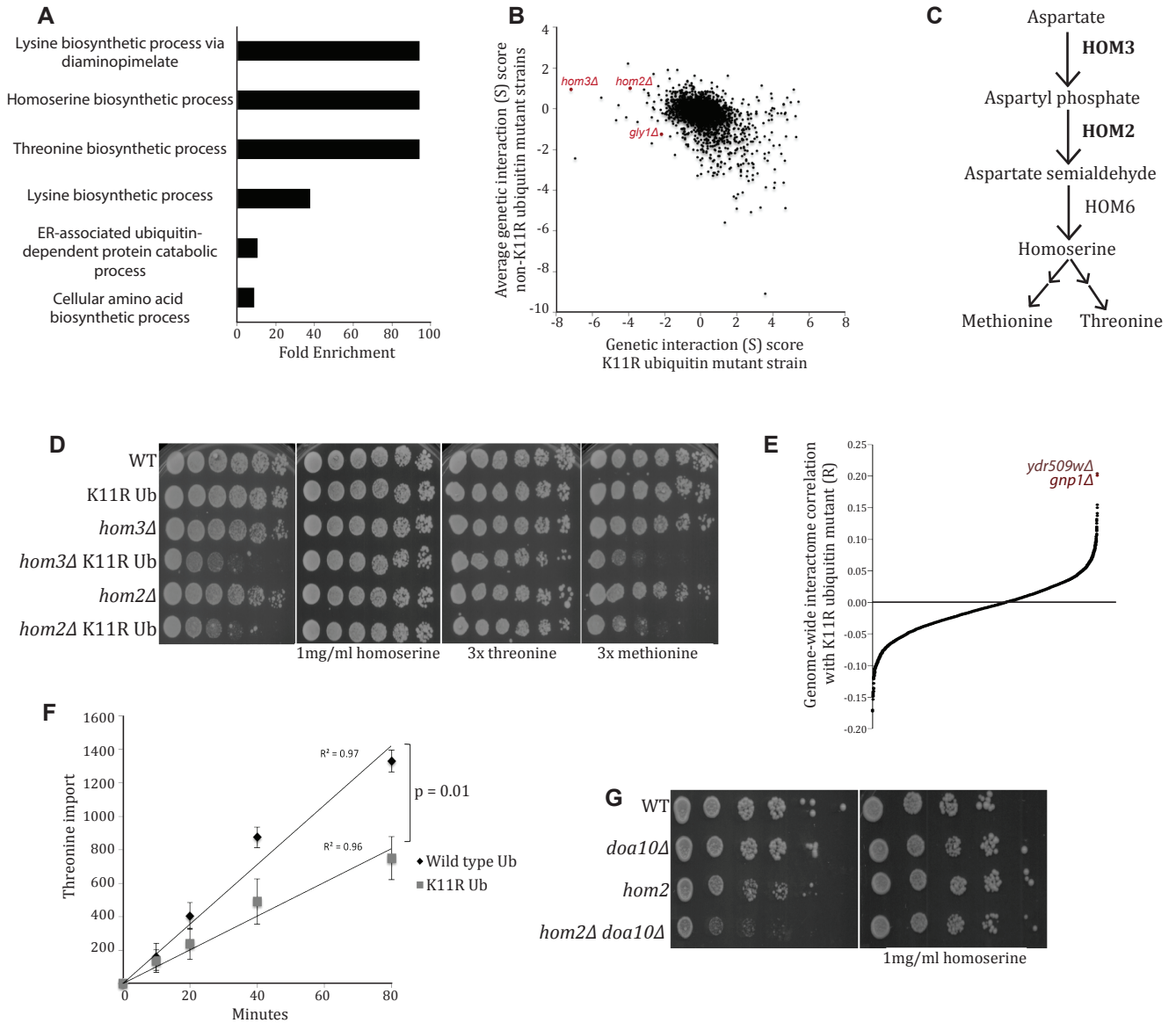


Figure 4

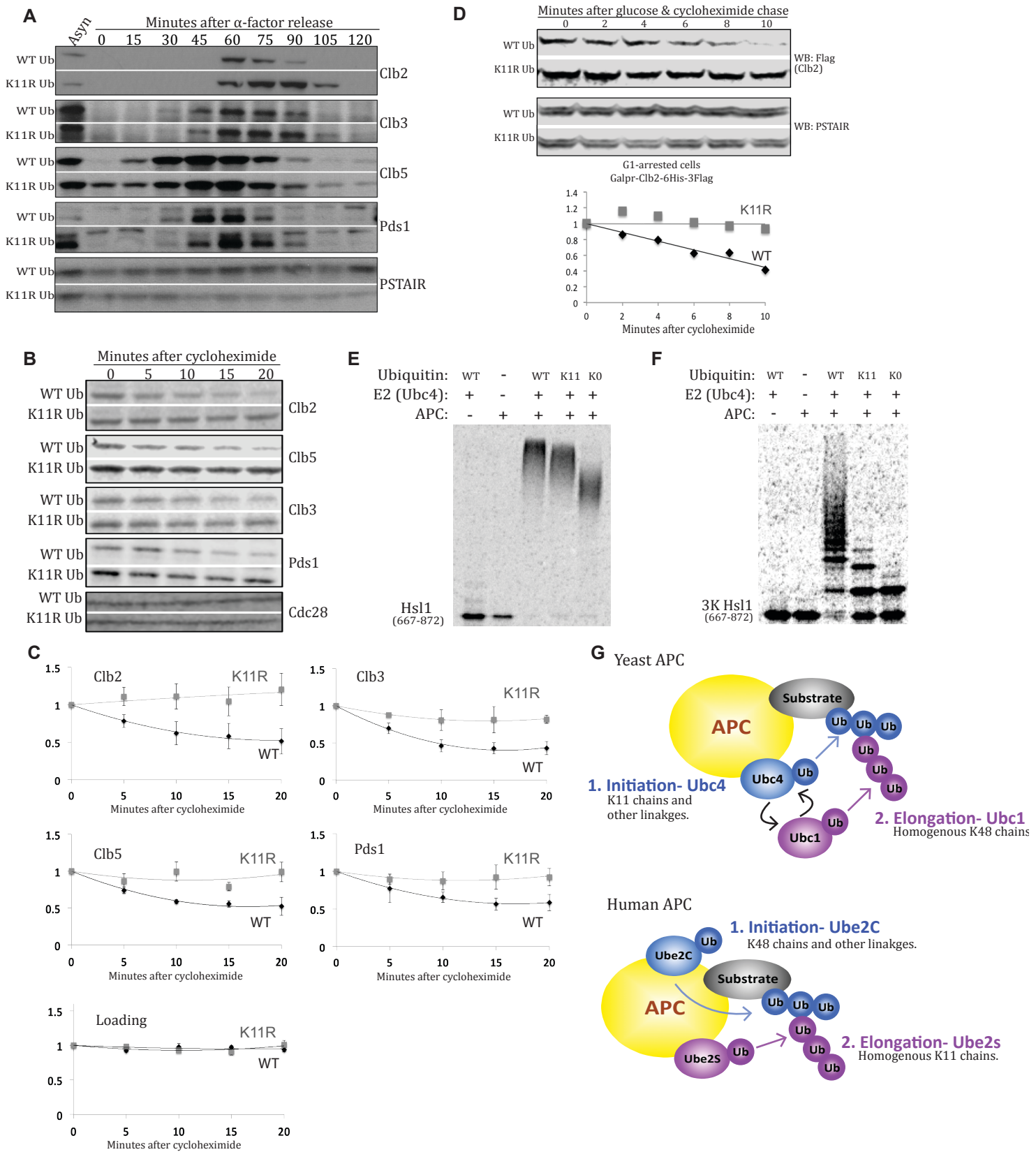


Figure 1-figure supplement 1

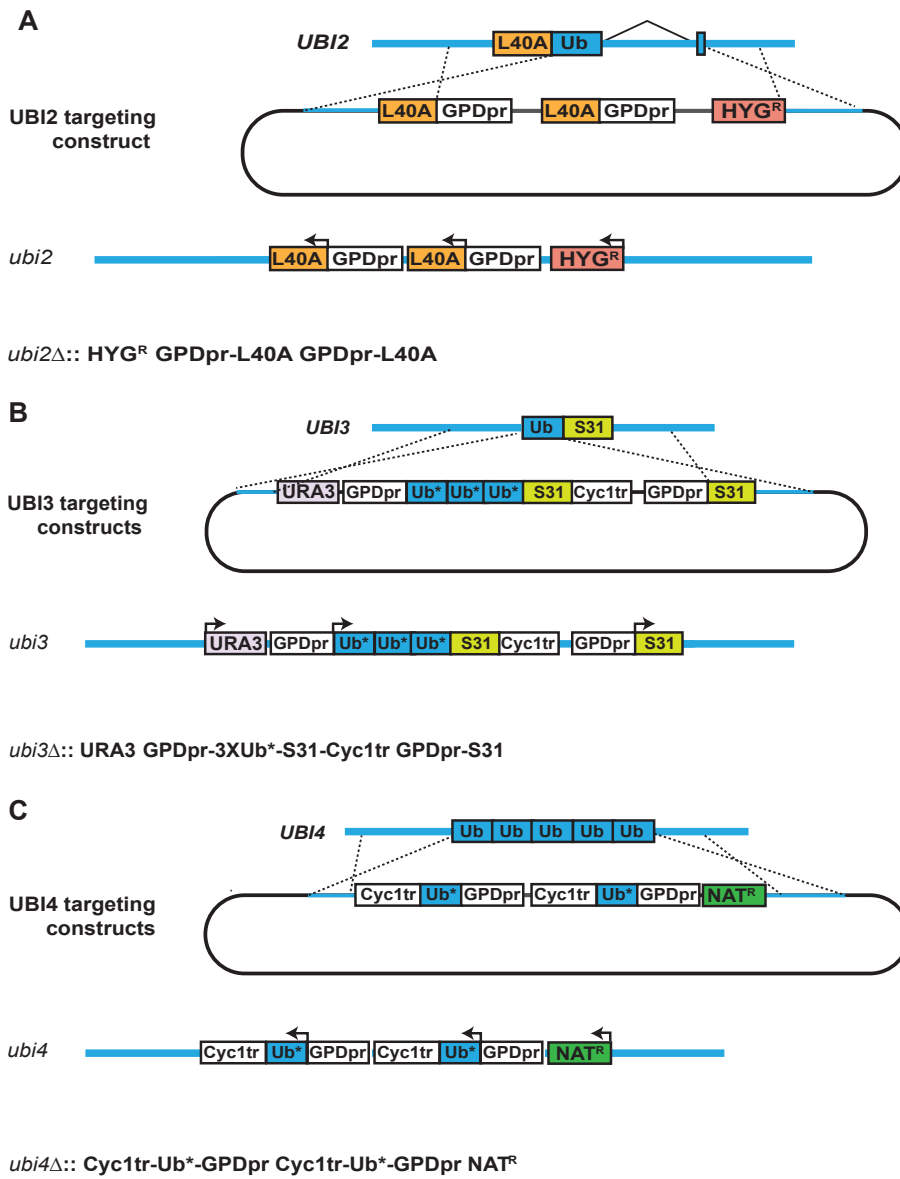


Figure 1-figure supplement 2

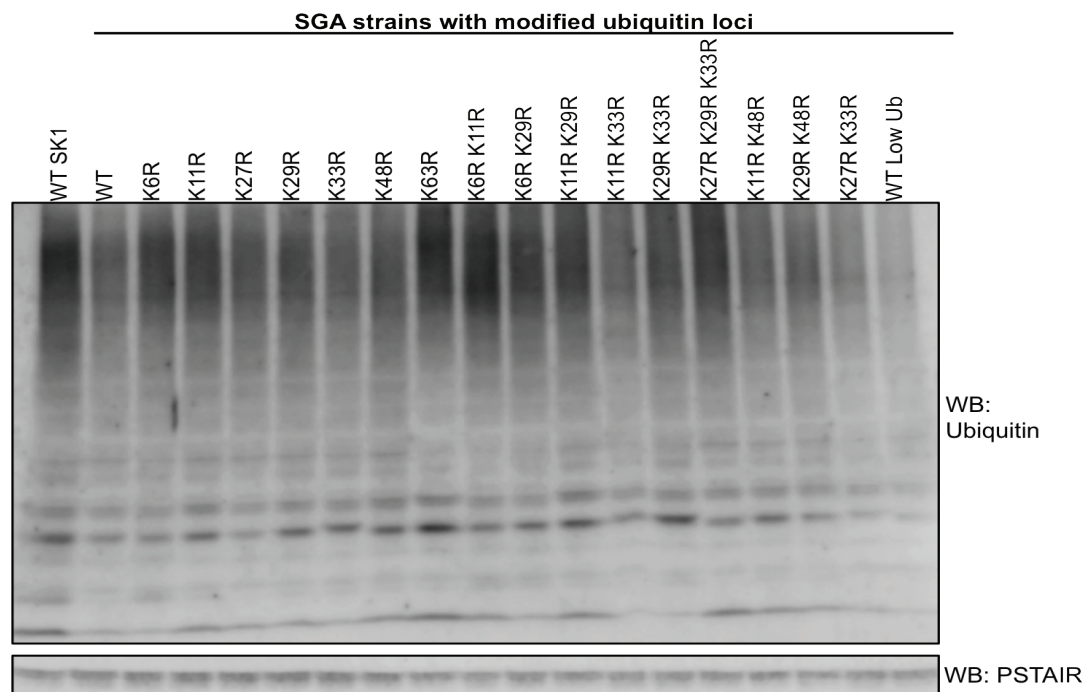


Figure 1-figure supplement 3

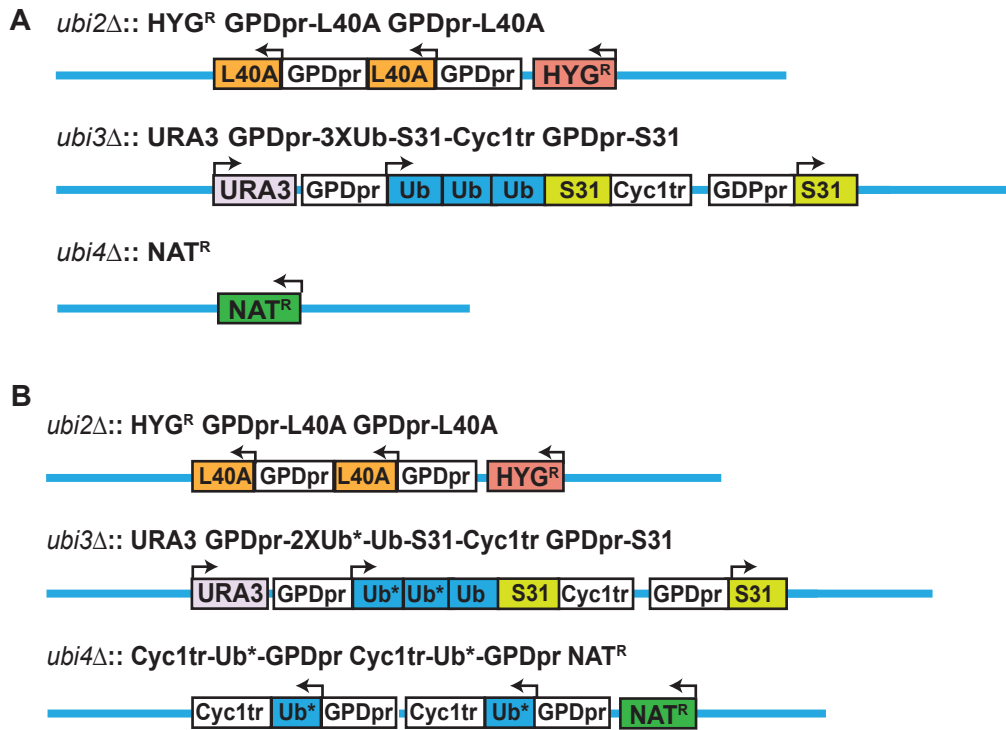


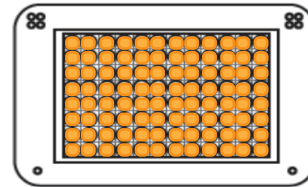
Figure 1-figure supplement 4

17 K-to-R Ub strains



MAT α ; *his3*; *ura3*; **CAN1**;
ubi1 Δ :: GPDpr-L40A;
ubi2 Δ :: HYG^R GPDpr-L40A GPDpr-L40A;
ubi3 Δ :: URA3 GPDpr-3XUb*-S31-Cyc1tr GPDpr-S31;
ubi4 Δ :: GPDpr-Ub*-Cyc1tr-GPDpr-Ub*-Cyc1tr NAT^R;
XXX

Haploid SK1 gene deletion library
 2655 gene knock outs



MAT a; *his3*; *ura3*; *can1 Δ* ::STE2pr-SpHIS5;
ubi1 Δ :: GPDpr-L40A;
UBI2;
UBI3;
UBI4;
xxx::KAN^R

X

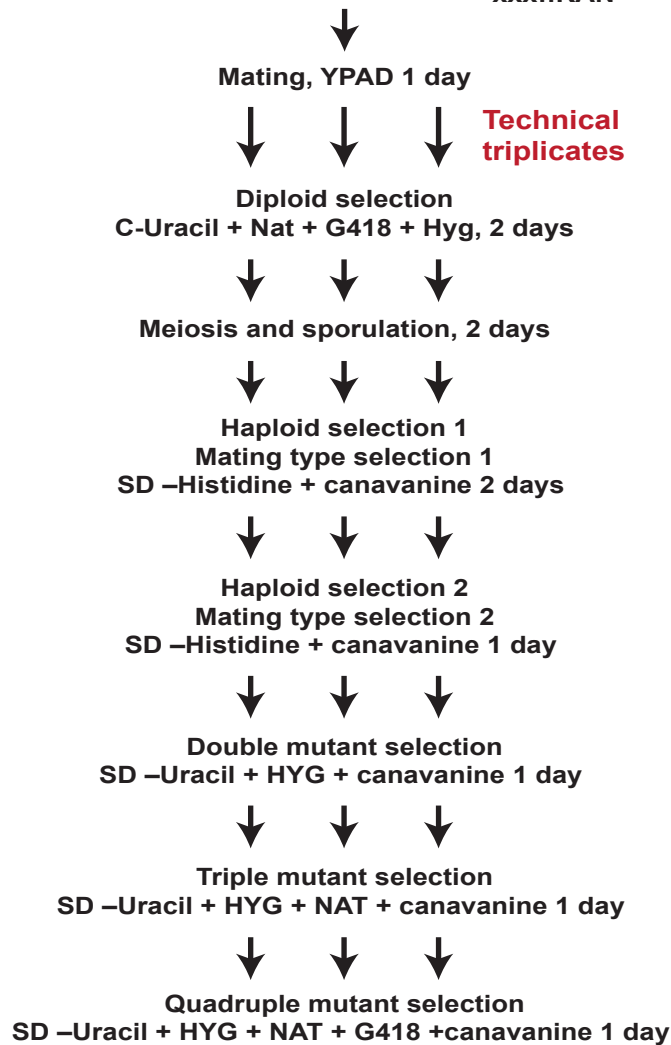


Figure 1-figure supplement 5

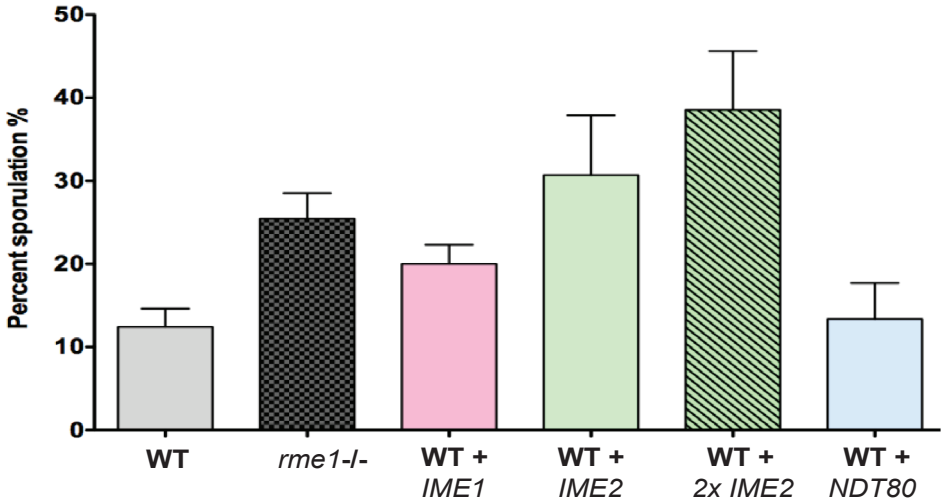


Figure 1-figure supplement 6

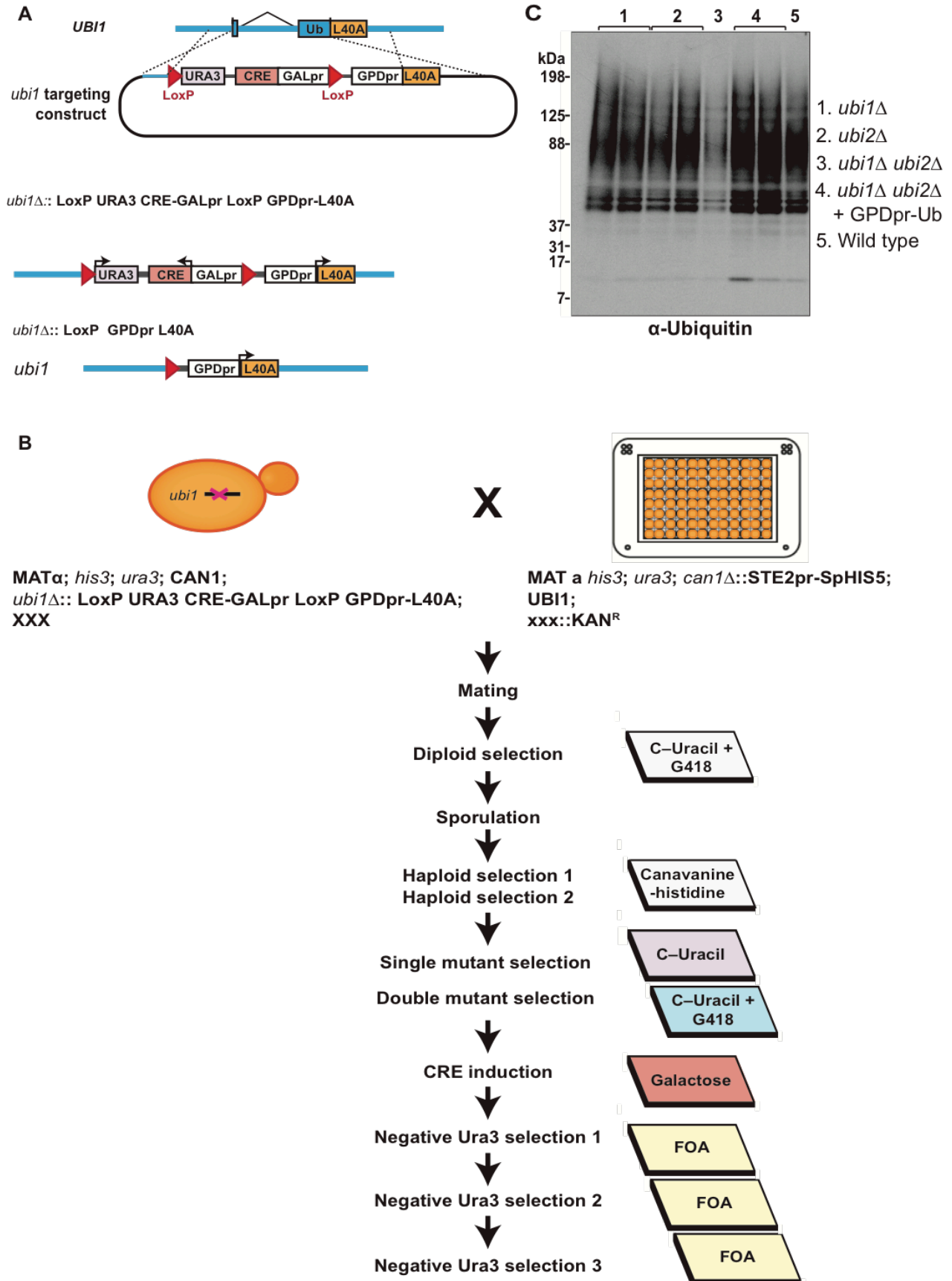


Figure 3-figure supplement 1

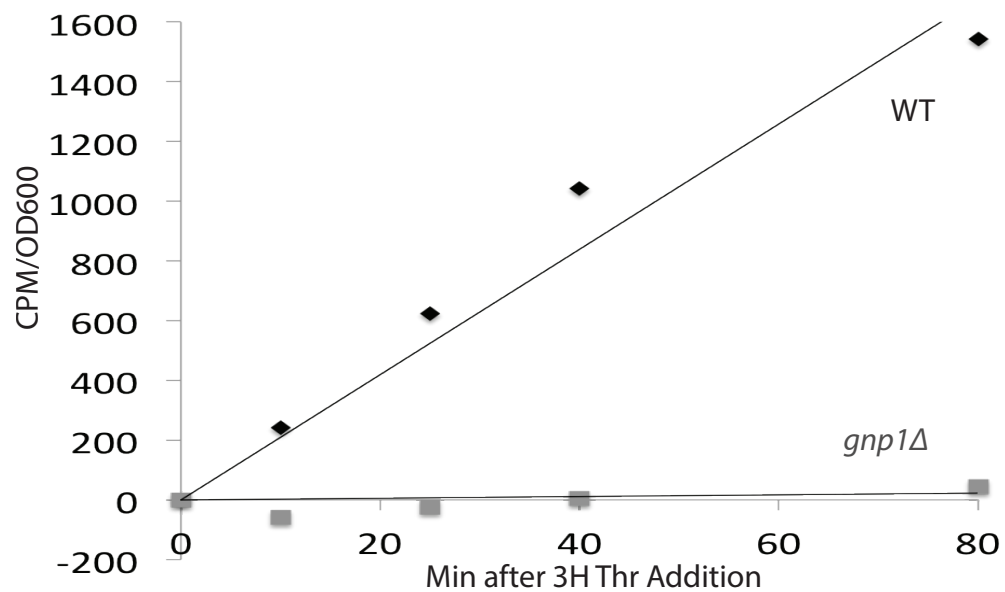
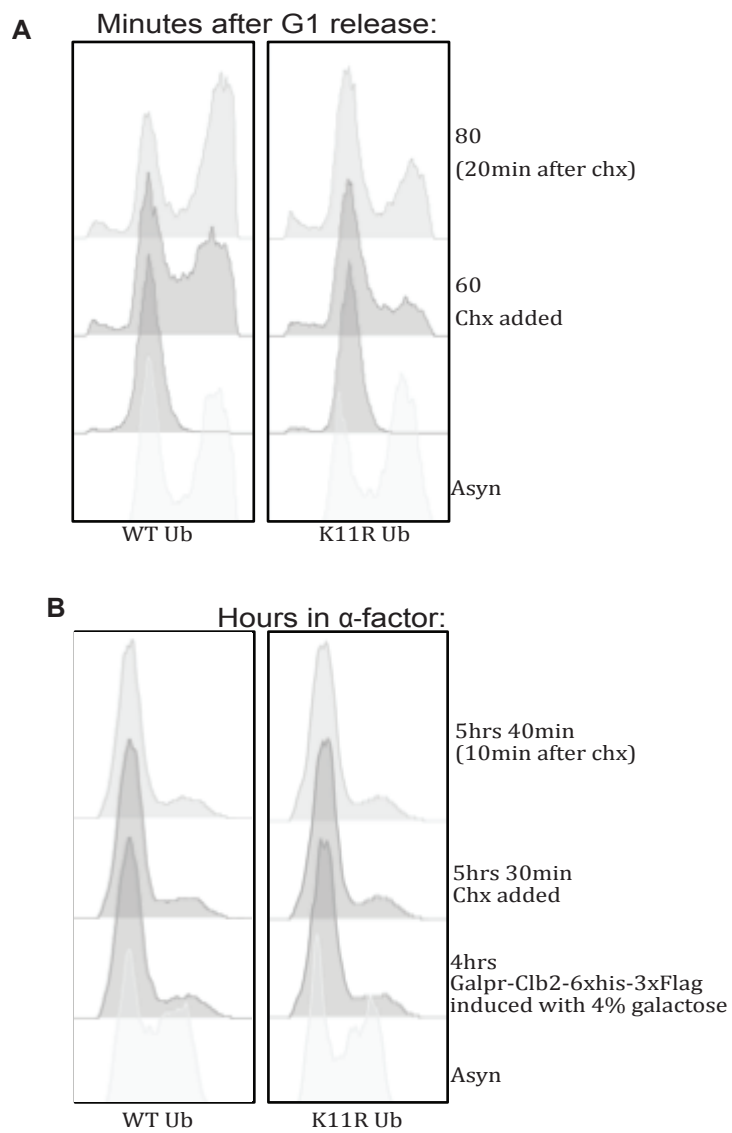


Figure 4-figure supplement 1



Supplementary table 1: Plasmids used in this study.

Plasmids	
Name	Description
DS199	Ubi1 targeting construct
DS200	Ubi2 targeting construct
DS203	WT Ub Ubi3 targeting construct
DS204	K6R Ub Ubi3 targeting construct
DS205	K11R Ub Ubi3 targeting construct
DS206	K27R Ub Ubi3 targeting construct
DS207	K29R Ub Ubi3 targeting construct
DS208	K33R Ub Ubi3 targeting construct
DS209	K48R Ub Ubi3 targeting construct
DS210	K6R K11R Ub Ubi3 targeting construct
DS211	K6R K29R Ub Ubi3 targeting construct
DS212	K11R K29R Ub Ubi3 targeting construct
DS213	K11R K33R Ub Ubi3 targeting construct
DS214	K27R K33R Ub Ubi3 targeting construct
DS215	K29R K33R Ub Ubi3 targeting construct
DS216	K11R K48R Ub Ubi3 targeting construct
DS217	K29R K48R Ub Ubi3 targeting construct
DS218	K11R K27R K29R Ub Ubi3 targeting construct
DS219	WT Ub Ubi4 targeting construct
DS220	K6R Ub Ubi4 targeting construct
DS221	K11R Ub Ubi4 targeting construct
DS222	K27R Ub Ubi4 targeting construct
DS223	K29R Ub Ubi4 targeting construct
DS224	K33R Ub Ubi4 targeting construct
DS225	K48R Ub Ubi4 targeting construct
DS226	K6R K11R Ub Ubi4 targeting construct
DS227	K6R K29R Ub Ubi4 targeting construct
DS228	K11R K29R Ub Ubi4 targeting construct
DS229	K11R K33R Ub Ubi4 targeting construct
DS230	K27R K33R Ub Ubi4 targeting construct
DS231	K29R K33R Ub Ubi4 targeting construct
DS232	K11R K48R Ub Ubi4 targeting construct
DS233	K29R K48R Ub Ubi4 targeting construct
DS234	K11R K27R K29R Ub Ubi4 targeting construct
DS235	Ubi4 targeting construct with no Ubiquitin
FMGp33	Prs413-Galpr-Clb2-6xHis-3xFlag

Supplementary Table 2: Strains used in this study.

Strain ID	#	Description	Genotype
DS	368	WT ubiquitin SGA strain	his3; ura3; ubi1Δ:: GPDpr-L40A; ubi2Δ:: HYGR GPDpr-L40A GPDpr-L40A; ubi3Δ:: URA3 GPDpr-3xUb-S31-Cyc1tr GPDpr-S31; ubi4Δ:: 2X (Cyc1tr-Ub-GDPpr) NATR; MAT α
DS	369	K6R ubiquitin SGA strain	his3; ura3; ubi1Δ:: GPDpr-L40A; ubi2Δ:: HYGR GPDpr-L40A GPDpr-L40A; ubi3Δ:: URA3 GPDpr-3xUb(K6R)-S31-Cyc1tr GPDpr-S31; ubi4Δ:: 2X (Cyc1tr-Ub(K6R)-GDPpr) NATR; MAT α
DS	370	K11R ubiquitin SGA strain	his3; ura3; ubi1Δ:: GPDpr-L40A; ubi2Δ:: HYGR GPDpr-L40A GPDpr-L40A; ubi3Δ:: URA3 GPDpr-3xUb(K11R)-S31-Cyc1tr GPDpr-S31; ubi4Δ:: 2X (Cyc1tr-Ub(K11R)-GDPpr) NATR; MAT α
DS	371	K27R ubiquitin SGA strain	his3; ura3; ubi1Δ:: GPDpr-L40A; ubi2Δ:: HYGR GPDpr-L40A GPDpr-L40A; ubi3Δ:: URA3 GPDpr-3xUb(K27R)-S31-Cyc1tr GPDpr-S31; ubi4Δ:: 2X (Cyc1tr-Ub(K27R)-GDPpr) NATR; MAT α
DS	372	K29R ubiquitin SGA strain	his3; ura3; ubi1Δ:: GPDpr-L40A; ubi2Δ:: HYGR GPDpr-L40A GPDpr-L40A; ubi3Δ:: URA3 GPDpr-3xUb(K29R)-S31-Cyc1tr GPDpr-S31; ubi4Δ:: 2X (Cyc1tr-Ub(K29R)-GDPpr) NATR; MAT α
DS	373	K33R ubiquitin SGA strain	his3; ura3; ubi1Δ:: GPDpr-L40A; ubi2Δ:: HYGR GPDpr-L40A GPDpr-L40A; ubi3Δ:: URA3 GPDpr-3xUb(K33R)-S31-Cyc1tr GPDpr-S31; ubi4Δ:: 2X (Cyc1tr-Ub(K33R)-GDPpr) NATR; MAT α
DS	374	K48R ubiquitin SGA strain	his3; ura3; ubi1Δ:: GPDpr-L40A; ubi2Δ:: HYGR GPDpr-L40A GPDpr-L40A; ubi3Δ:: URA3 GPDpr-2xUb(K48R)-Ub-S31-Cyc1tr GPDpr-S31; ubi4Δ:: 2X (Cyc1tr-Ub(K48R)-GDPpr) NATR; MAT α
DS	376	K63R ubiquitin SGA strain	his3; ura3; ubi1Δ:: GPDpr-L40A; ubi2Δ:: HYGR GPDpr-L40A GPDpr-L40A; ubi3Δ:: URA3 GPDpr-3xUb(K63R)-S31-Cyc1tr GPDpr-S31; ubi4Δ:: 2X (Cyc1tr-Ub(K63R)-GDPpr) NATR; MAT α
DS	377	K6R K11R ubiquitin SGA strain	his3; ura3; ubi1Δ:: GPDpr-L40A; ubi2Δ:: HYGR GPDpr-L40A GPDpr-L40A; ubi3Δ:: URA3 GPDpr-3xUb(K6R,K11R)-S31-Cyc1tr GPDpr-S31; ubi4Δ:: 2X (Cyc1tr-Ub(K6R,K11R)-GDPpr) NATR; MAT α
DS	378	K6R K29R ubiquitin SGA strain	his3; ura3; ubi1Δ:: GPDpr-L40A; ubi2Δ:: HYGR GPDpr-L40A GPDpr-L40A; ubi3Δ:: URA3 GPDpr-3xUb(K6R,K29R)-S31-Cyc1tr GPDpr-S31; ubi4Δ:: 2X (Cyc1tr-Ub(K6R,K29R)-GDPpr) NATR; MAT α
DS	381	K11R K29R ubiquitin SGA strain	his3; ura3; ubi1Δ:: GPDpr-L40A; ubi2Δ:: HYGR GPDpr-L40A GPDpr-L40A; ubi3Δ:: URA3 GPDpr-3xUb(K11R,K29R)-S31-Cyc1tr GPDpr-S31; ubi4Δ:: 2X (Cyc1tr-Ub(K11R,K29R)-GDPpr) NATR; MAT α
DS	382	K11R K33R ubiquitin SGA strain	his3; ura3; ubi1Δ:: GPDpr-L40A; ubi2Δ:: HYGR GPDpr-L40A GPDpr-L40A; ubi3Δ:: URA3 GPDpr-3xUb(K11R,K33R)-S31-Cyc1tr GPDpr-S31; ubi4Δ:: 2X (Cyc1tr-Ub(K11R,K33R)-GDPpr) NATR; MAT α
DS	384	WT-lower ubiquitin SGA strain	his3; ura3; ubi1Δ:: GPDpr-L40A; ubi2Δ:: HYGR GPDpr-L40A GPDpr-L40A; ubi3Δ:: URA3 GPDpr-3xUb-S31-Cyc1tr GPDpr-S31; ubi4Δ:: NATR; MAT α
DS	389	K29R K33R ubiquitin SGA strain	his3; ura3; ubi1Δ:: GPDpr-L40A; ubi2Δ:: HYGR GPDpr-L40A GPDpr-L40A; ubi3Δ:: URA3 GPDpr-3xUb(K29R,K33R)-S31-Cyc1tr GPDpr-S31; ubi4Δ:: 2X (Cyc1tr-Ub(K29R,K33R)-GDPpr) NATR; MAT α
DS	392	K11R K27R K29R ubiquitin SGA strain	his3; ura3; ubi1Δ:: GPDpr-L40A; ubi2Δ:: HYGR GPDpr-L40A GPDpr-L40A; ubi3Δ:: URA3 GPDpr-3xUb(K11R, K27R, K29R)-S31-Cyc1tr GPDpr-S31; ubi4Δ:: 2X (Cyc1tr-Ub(K11R, K27R, K29R)-GDPpr) NATR; MAT α

Supplementary Table 2, continued: Strains used in this study.

Strain ID	#	Description	Genotype
DS	394	K11R K48R ubiquitin SGA strain	his3; ura3; ubi1Δ:: GPDpr-L40A; ubi2Δ:: HYGR GPDpr-L40A GPDpr-L40A; ubi3Δ:: URA3 GPDpr-Ub(K11R,K48R)-2XUb(K11R)-S31-Cyc1tr GPDpr-S31; ubi4Δ:: 2X (Cyc1tr-Ub(K11R,K48R)-GDPpr) NATR; MAT α
DS	396	K29R K48R ubiquitin SGA strain	his3; ura3; ubi1Δ:: GPDpr-L40A; ubi2Δ:: HYGR GPDpr-L40A GPDpr-L40A; ubi3Δ:: URA3 GPDpr-Ub(K29R,K48R)-2XUb(K29R)-S31-Cyc1tr GPDpr-S31; ubi4Δ:: 2X (Cyc1tr-Ub(K29R,K48R)-GDPpr) NATR; MAT α
DS	397	K27R K33R ubiquitin SGA strain	his3; ura3; ubi1Δ:: GPDpr-L40A; ubi2Δ:: HYGR GPDpr-L40A GPDpr-L40A; ubi3Δ:: URA3 GPDpr-3xUb(K27R,K33R)-S31-Cyc1tr GPDpr-S31; ubi4Δ:: 2X (Cyc1tr-Ub(K27R,K33R)-GDPpr) NATR; MAT α
FMGy	91	WT ubiquitin SGA strain_5	his3; ura3; ubi1Δ:: GPDpr-L40A; ubi2Δ:: HYGR GPDpr-L40A GPDpr-L40A; ubi3Δ:: URA3 GPDpr-3xUb-S31-Cyc1tr GPDpr-S31; ubi4Δ:: 2X (Cyc1tr-Ub-GDPpr) NATR; MAT a
FMGy	92	K11R ubiquitin SGA strain_5	his3; ura3; ubi1Δ:: GPDpr-L40A; ubi2Δ:: HYGR GPDpr-L40A GPDpr-L40A; ubi3Δ:: URA3 GPDpr-3xUb(K11R)-S31-Cyc1tr GPDpr-S31; ubi4Δ:: 2X (Cyc1tr-Ub(K11R)-GDPpr) NATR; MAT a
FMGy	94	<i>hom2Δ</i> K11R ubiquitin SGA strain_2	his3; ura3; ubi1Δ:: GPDpr-L40A; ubi2Δ:: HYGR GPDpr-L40A GPDpr-L40A; ubi3Δ:: URA3 GPDpr-3xUb(K11R)-S31-Cyc1tr GPDpr-S31; ubi4Δ:: 2X (Cyc1tr-Ub(K11R)-GDPpr) NATR; <i>hom2Δ::KanR</i> ; MAT a
FMGy	95	<i>hom2Δ</i> WT ubiquitin SGA strain_2	his3; ura3; ubi1Δ:: GPDpr-L40A; ubi2Δ:: HYGR GPDpr-L40A GPDpr-L40A; ubi3Δ:: URA3 GPDpr-3xUb-S31-Cyc1tr GPDpr-S31; ubi4Δ:: 2X (Cyc1tr-Ub-GDPpr) NATR; <i>hom2Δ::KanR</i> ; MAT α
FMGy	98	<i>hom3Δ</i> K11R ubiquitin SGA strain	his3; ura3; ubi1Δ:: GPDpr-L40A; ubi2Δ:: HYGR GPDpr-L40A GPDpr-L40A; ubi3Δ:: URA3 GPDpr-3xUb(K11R)-S31-Cyc1tr GPDpr-S31; ubi4Δ:: 2X (Cyc1tr-Ub(K11R)-GDPpr) NATR; <i>hom3Δ::KanR</i> ; MAT α
FMGy	99	<i>hom3Δ</i> WT ubiquitin SGA strain	his3; ura3; ubi1Δ:: GPDpr-L40A; ubi2Δ:: HYGR GPDpr-L40A GPDpr-L40A; ubi3Δ:: URA3 GPDpr-3xUb-S31-Cyc1tr GPDpr-S31; ubi4Δ:: 2X (Cyc1tr-Ub-GDPpr) NATR; <i>hom3Δ::KanR</i> ; MAT a
FMGy	110	K11R ubiquitin SGA strain_1	his3; ura3; ubi1Δ:: GPDpr-L40A; ubi2Δ:: HYGR GPDpr-L40A GPDpr-L40A; ubi3Δ:: URA3 GPDpr-3xUb(K11R)-S31-Cyc1tr GPDpr-S31; ubi4Δ:: 2X (Cyc1tr-Ub(K11R)-GDPpr) NATR; MAT α
FMGy	126	K6R ubiquitin SGA strain_1	his3; ura3; ubi1Δ:: GPDpr-L40A; ubi2Δ:: HYGR GPDpr-L40A GPDpr-L40A; ubi3Δ:: URA3 GPDpr-3xUb(K6R)-S31-Cyc1tr GPDpr-S31; ubi4Δ:: 2X (Cyc1tr-Ub(K6R)-GDPpr) NATR; MAT α
FMGy	127	<i>hom2Δ</i> K6R ubiquitin SGA strain	his3; ura3; ubi1Δ:: GPDpr-L40A; ubi2Δ:: HYGR GPDpr-L40A GPDpr-L40A; ubi3Δ:: URA3 GPDpr-3xUb(K6R)-S31-Cyc1tr GPDpr-S31; ubi4Δ:: 2X (Cyc1tr-Ub(K6R)-GDPpr) NATR; <i>hom2Δ::KanR</i> ; MAT a
FMGy	181	K33R ubiquitin SGA strain_1	his3; ura3; ubi1Δ:: GPDpr-L40A; ubi2Δ:: HYGR GPDpr-L40A GPDpr-L40A; ubi3Δ:: URA3 GPDpr-3xUb(K33R)-S31-Cyc1tr GPDpr-S31; ubi4Δ:: 2X (Cyc1tr-Ub(K33R)-GDPpr) NATR; MAT α
FMGy	184	<i>hom2Δ</i> K33R ubiquitin SGA strain	his3; ura3; ubi1Δ:: GPDpr-L40A; ubi2Δ:: HYGR GPDpr-L40A GPDpr-L40A; ubi3Δ:: URA3 GPDpr-3xUb(K33R)-S31-Cyc1tr GPDpr-S31; ubi4Δ:: 2X (Cyc1tr-Ub(K33R)-GDPpr) NATR; <i>hom2Δ::KanR</i> ; MAT a
FMGy	190	K48R ubiquitin SGA strain_1	his3; ura3; ubi1Δ:: GPDpr-L40A; ubi2Δ:: HYGR GPDpr-L40A GPDpr-L40A; ubi3Δ:: URA3 GPDpr-2XUb(K48R)-Ub-S31-Cyc1tr GPDpr-S31; ubi4Δ:: 2X (Cyc1tr-Ub(K48R)-GDPpr) NATR; MAT a

Supplementary Table 2, continued: Strains used in this study.

Strain ID	#	Description	Genotype
FMGy	192	<i>hom2Δ</i> K48R ubiquitin SGA strain	his3; ura3; ubi1Δ:: GPDpr-L40A; ubi2Δ:: HYGR GPDpr-L40A GPDpr-L40A; ubi3Δ:: URA3 GPDpr-2XUb(K48R)-Ub-S31-Cyc1tr GPDpr-S31; ubi4Δ:: 2X (Cyc1tr-Ub(K48R)-GDPpr) NATR; <i>hom2Δ</i> ::KanR; MATα
FMGy	198	WT	his3; ura3; MAT a
FMGy	199	<i>hom2Δ doa10Δ</i>	his3; ura3; <i>doa10Δ</i> ::NATR; <i>hom2Δ</i> ::KanR; MAT α
FMGy	201	<i>doa10Δ</i>	his3; ura3; <i>doa10Δ</i> ::NATR; MAT a
FMGy	202	<i>hom2Δ</i>	his3; ura3; <i>hom2Δ</i> ::KanR; MAT a
FMGy	213	WT	his3; ura3; MAT α
FMGy	268	<i>hom2Δ</i> K11R ubiquitin SGA strain_1	his3; ura3; ubi1Δ:: GPDpr-L40A; ubi2Δ:: HYGR GPDpr-L40A GPDpr-L40A; ubi3Δ:: URA3 GPDpr-3xUb(K11R)-S31-Cyc1tr GPDpr-S31; ubi4Δ:: 2X (Cyc1tr-Ub(K11R)-GDPpr) NATR; <i>hom2Δ</i> ::KanR; MAT α
FMGy	327	WT ubiquitin SGA strain_1	his3; ura3; ubi1Δ:: GPDpr-L40A; ubi2Δ:: HYGR GPDpr-L40A GPDpr-L40A; ubi3Δ:: URA3 GPDpr-3xUb-S31-Cyc1tr GPDpr-S31; ubi4Δ:: 2X (Cyc1tr-Ub-GDPpr) NATR; MAT α
FMGy	328	K11R ubiquitin SGA strain_2	his3; ura3; ubi1Δ:: GPDpr-L40A; ubi2Δ:: HYGR GPDpr-L40A GPDpr-L40A; ubi3Δ:: URA3 GPDpr-3xUb(K11R)-S31-Cyc1tr GPDpr-S31; ubi4Δ:: 2X (Cyc1tr-Ub(K11R)-GDPpr) NATR; MAT a
FMGy	331	WT ubiquitin SGA strain_3	his3; ura3; ubi1Δ:: GPDpr-L40A; ubi2Δ:: HYGR GPDpr-L40A GPDpr-L40A; ubi3Δ:: URA3 GPDpr-3xUb-S31-Cyc1tr GPDpr-S31; ubi4Δ:: 2X (Cyc1tr-Ub-GDPpr) NATR; MAT α
FMGy	334	K11R ubiquitin SGA strain_3	his3; ura3; ubi1Δ:: GPDpr-L40A; ubi2Δ:: HYGR GPDpr-L40A GPDpr-L40A; ubi3Δ:: URA3 GPDpr-3xUb(K11R)-S31-Cyc1tr GPDpr-S31; ubi4Δ:: 2X (Cyc1tr-Ub(K11R)-GDPpr) NATR; MAT α
FMGy	338	WT ubiquitin SGA strain_4	his3; ura3; ubi1Δ:: GPDpr-L40A; ubi2Δ:: HYGR GPDpr-L40A GPDpr-L40A; ubi3Δ:: URA3 GPDpr-3xUb-S31-Cyc1tr GPDpr-S31; ubi4Δ:: 2X (Cyc1tr-Ub-GDPpr) NATR; MAT α
FMGy	341	K11R ubiquitin SGA strain_4	his3; ura3; ubi1Δ:: GPDpr-L40A; ubi2Δ:: HYGR GPDpr-L40A GPDpr-L40A; ubi3Δ:: URA3 GPDpr-3xUb(K11R)-S31-Cyc1tr GPDpr-S31; ubi4Δ:: 2X (Cyc1tr-Ub(K11R)-GDPpr) NATR; MAT a
FMGy	344	K6R ubiquitin SGA strain_2	his3; ura3; ubi1Δ:: GPDpr-L40A; ubi2Δ:: HYGR GPDpr-L40A GPDpr-L40A; ubi3Δ:: URA3 GPDpr-3xUb(K6R)-S31-Cyc1tr GPDpr-S31; ubi4Δ:: 2X (Cyc1tr-Ub(K6R)-GDPpr) NATR; MAT a
FMGy	347	K27R ubiquitin SGA strain_1	his3; ura3; ubi1Δ:: GPDpr-L40A; ubi2Δ:: HYGR GPDpr-L40A GPDpr-L40A; ubi3Δ:: URA3 GPDpr-3xUb(K27R)-S31-Cyc1tr GPDpr-S31; ubi4Δ:: 2X (Cyc1tr-Ub(K27R)-GDPpr) NATR; MAT a
FMGy	349	K29R ubiquitin SGA strain_1	his3; ura3; ubi1Δ:: GPDpr-L40A; ubi2Δ:: HYGR GPDpr-L40A GPDpr-L40A; ubi3Δ:: URA3 GPDpr-3xUb(K29R)-S31-Cyc1tr GPDpr-S31; ubi4Δ:: 2X (Cyc1tr-Ub(K29R)-GDPpr) NATR; MAT α
FMGy	352	K33R ubiquitin SGA strain_2	his3; ura3; ubi1Δ:: GPDpr-L40A; ubi2Δ:: HYGR GPDpr-L40A GPDpr-L40A; ubi3Δ:: URA3 GPDpr-3xUb(K33R)-S31-Cyc1tr GPDpr-S31; ubi4Δ:: 2X (Cyc1tr-Ub(K33R)-GDPpr) NATR; MAT α
FMGy	355	K48R ubiquitin SGA strain_2	his3; ura3; ubi1Δ:: GPDpr-L40A; ubi2Δ:: HYGR GPDpr-L40A GPDpr-L40A; ubi3Δ:: URA3 GPDpr-2XUb(K48R)-Ub-S31-Cyc1tr GPDpr-S31; ubi4Δ:: 2X (Cyc1tr-Ub(K48R)-GDPpr) NATR; MAT a
FMGy	375	K63R ubiquitin SGA strain_1	his3; ura3; ubi1Δ:: GPDpr-L40A; ubi2Δ:: HYGR GPDpr-L40A GPDpr-L40A; ubi3Δ:: URA3 GPDpr-3xUb(K63R)-S31-Cyc1tr GPDpr-S31; ubi4Δ:: 2X (Cyc1tr-Ub(K63R)-GDPpr) NATR; MAT a
FMGy	464	<i>hom2Δ</i> K63R ubiquitin SGA strain	his3; ura3; ubi1Δ:: GPDpr-L40A; ubi2Δ:: HYGR GPDpr-L40A GPDpr-L40A; ubi3Δ:: URA3 GPDpr-3xUb(K63R)-S31-Cyc1tr GPDpr-S31; ubi4Δ:: 2X (Cyc1tr-Ub(K63R)-GDPpr) NATR; <i>hom2Δ</i> ::KanR;

Supplementary Table 2, continued: Strains used in this study.

Strain ID	#	Description	Genotype
FMGy	466	K63R ubiquitin SGA strain_2	his3; ura3; ubi1Δ:: GPDpr-L40A; ubi2Δ:: HYGR GPDpr-L40A GPDpr-L40A; ubi3Δ:: URA3 GPDpr-3xUb(K63R)-S31-Cyc1tr GPDpr-S31; ubi4Δ:: 2X (Cyc1tr-Ub(K63R)-GDPpr) NATR; MAT a
FMGy	467	K27R ubiquitin SGA strain_2	his3; ura3; ubi1Δ:: GPDpr-L40A; ubi2Δ:: HYGR GPDpr-L40A GPDpr-L40A; ubi3Δ:: URA3 GPDpr-3xUb(K27R)-S31-Cyc1tr GPDpr-S31; ubi4Δ:: 2X (Cyc1tr-Ub(K27R)-GDPpr) NATR; MAT a
FMGy	469	<i>hom2Δ</i> K27R ubiquitin SGA strain	his3; ura3; ubi1Δ:: GPDpr-L40A; ubi2Δ:: HYGR GPDpr-L40A GPDpr-L40A; ubi3Δ:: URA3 GPDpr-3xUb(K27R)-S31-Cyc1tr GPDpr-S31; ubi4Δ:: 2X (Cyc1tr-Ub(K27R)-GDPpr) NATR; <i>hom2Δ</i> ::KanR; MAT α
FMGy	471	K29R ubiquitin SGA strain_2	his3; ura3; ubi1Δ:: GPDpr-L40A; ubi2Δ:: HYGR GPDpr-L40A GPDpr-L40A; ubi3Δ:: URA3 GPDpr-3xUb(K29R)-S31-Cyc1tr GPDpr-S31; ubi4Δ:: 2X (Cyc1tr-Ub(K29R)-GDPpr) NATR; MAT a
FMGy	473	<i>hom2Δ</i> K29R ubiquitin SGA strain	his3; ura3; ubi1Δ:: GPDpr-L40A; ubi2Δ:: HYGR GPDpr-L40A GPDpr-L40A; ubi3Δ:: URA3 GPDpr-3xUb(K29R)-S31-Cyc1tr GPDpr-S31; ubi4Δ:: 2X (Cyc1tr-Ub(K29R)-GDPpr) NATR; <i>hom2Δ</i> ::KanR; MAT α
FMGy	512	<i>hom2Δ</i> WT ubiquitin SGA strain_1	his3; ura3; ubi1Δ:: GPDpr-L40A; ubi2Δ:: HYGR GPDpr-L40A GPDpr-L40A; ubi3Δ:: URA3 GPDpr-3xUb-S31-Cyc1tr GPDpr-S31; ubi4Δ:: 2X (Cyc1tr-Ub-GDPpr) NATR; <i>hom2Δ</i> ::KanR; MAT α
FMGy	513	WT ubiquitin SGA strain_2	his3; ura3; ubi1Δ:: GPDpr-L40A; ubi2Δ:: HYGR GPDpr-L40A GPDpr-L40A; ubi3Δ:: URA3 GPDpr-3xUb-S31-Cyc1tr GPDpr-S31; ubi4Δ:: 2X (Cyc1tr-Ub-GDPpr) NATR; MAT a
FMGy	747	<i>cdc26Δ</i> K6R ubiquitin SGA strain	his3; ura3; ubi1Δ:: GPDpr-L40A; ubi2Δ:: HYGR GPDpr-L40A GPDpr-L40A; ubi3Δ:: URA3 GPDpr-3xUb(K6R)-S31-Cyc1tr GPDpr-S31; ubi4Δ:: 2X (Cyc1tr-Ub(K6R)-GDPpr) NATR; <i>cdc26Δ</i> ::KanR; MAT α
FMGy	751	<i>cdc26Δ</i> K27R ubiquitin SGA strain	his3; ura3; ubi1Δ:: GPDpr-L40A; ubi2Δ:: HYGR GPDpr-L40A GPDpr-L40A; ubi3Δ:: URA3 GPDpr-3xUb(K27R)-S31-Cyc1tr GPDpr-S31; ubi4Δ:: 2X (Cyc1tr-Ub(K27R)-GDPpr) NATR; <i>cdc26Δ</i> ::KanR; MAT α
FMGy	753	<i>cdc26Δ</i> K29R ubiquitin SGA strain	his3; ura3; ubi1Δ:: GPDpr-L40A; ubi2Δ:: HYGR GPDpr-L40A GPDpr-L40A; ubi3Δ:: URA3 GPDpr-3xUb(K29R)-S31-Cyc1tr GPDpr-S31; ubi4Δ:: 2X (Cyc1tr-Ub(K29R)-GDPpr) NATR; <i>cdc26Δ</i> ::KanR; MAT α
FMGy	755	<i>cdc26Δ</i> K33R ubiquitin SGA strain	his3; ura3; ubi1Δ:: GPDpr-L40A; ubi2Δ:: HYGR GPDpr-L40A GPDpr-L40A; ubi3Δ:: URA3 GPDpr-3xUb(K33R)-S31-Cyc1tr GPDpr-S31; ubi4Δ:: 2X (Cyc1tr-Ub(K33R)-GDPpr) NATR; <i>cdc26Δ</i> ::KanR; MAT a
FMGy	757	<i>cdc26Δ</i> K48R ubiquitin SGA strain	his3; ura3; ubi1Δ:: GPDpr-L40A; ubi2Δ:: HYGR GPDpr-L40A GPDpr-L40A; ubi3Δ:: URA3 GPDpr-2xUb(K48R)-Ub-S31-Cyc1tr GPDpr-S31; ubi4Δ:: 2X (Cyc1tr-Ub(K48R)-GDPpr) NATR; <i>cdc26Δ</i> ::KanR; MAT a
FMGy	758	<i>cdc26Δ</i> K63R ubiquitin SGA strain	his3; ura3; ubi1Δ:: GPDpr-L40A; ubi2Δ:: HYGR GPDpr-L40A GPDpr-L40A; ubi3Δ:: URA3 GPDpr-3xUb(K63R)-S31-Cyc1tr GPDpr-S31; ubi4Δ:: 2X (Cyc1tr-Ub(K63R)-GDPpr) NATR; <i>cdc26Δ</i> ::KanR; MAT a
FMGy	759	<i>cdc26Δ</i> WT ubiquitin SGA strain_1	his3; ura3; ubi1Δ:: GPDpr-L40A; ubi2Δ:: HYGR GPDpr-L40A GPDpr-L40A; ubi3Δ:: URA3 GPDpr-3xUb-S31-Cyc1tr GPDpr-S31; ubi4Δ:: 2X (Cyc1tr-Ub-GDPpr) NATR; <i>cdc26Δ</i> ::KanR; MAT a
FMGy	763	<i>ubc4Δ</i> WT ubiquitin SGA strain	his3; ura3; ubi1Δ:: GPDpr-L40A; ubi2Δ:: HYGR GPDpr-L40A GPDpr-L40A; ubi3Δ:: URA3 GPDpr-3xUb-S31-Cyc1tr GPDpr-S31; ubi4Δ:: 2X (Cyc1tr-Ub-GDPpr) NATR; <i>ubc4Δ</i> ::KanR; MAT

Supplementary Table 2, continued: Strains used in this study.

Strain ID	#	Description	Genotype
FMGy	769	<i>ubc4Δ</i> K27R ubiquitin SGA strain	his3; ura3; ubi1Δ:: GPDpr-L40A; ubi2Δ:: HYGR GPDpr-L40A GPDpr-L40A; ubi3Δ:: URA3 GPDpr-3xUb(K27R)-S31-Cyc1tr GPDpr-S31; ubi4Δ:: 2X (Cyc1tr-Ub(K27R)-GDPpr) NATR; ubc4Δ::KanR; MAT α
FMGy	771	<i>ubc4Δ</i> K29R ubiquitin SGA strain	his3; ura3; ubi1Δ:: GPDpr-L40A; ubi2Δ:: HYGR GPDpr-L40A GPDpr-L40A; ubi3Δ:: URA3 GPDpr-3xUb(K29R)-S31-Cyc1tr GPDpr-S31; ubi4Δ:: 2X (Cyc1tr-Ub(K29R)-GDPpr) NATR; ubc4Δ::KanR; MAT α
FMGy	773	<i>ubc4Δ</i> K33R ubiquitin SGA strain	his3; ura3; ubi1Δ:: GPDpr-L40A; ubi2Δ:: HYGR GPDpr-L40A GPDpr-L40A; ubi3Δ:: URA3 GPDpr-3xUb(K33R)-S31-Cyc1tr GPDpr-S31; ubi4Δ:: 2X (Cyc1tr-Ub(K33R)-GDPpr) NATR; ubc4Δ::KanR; MAT α
FMGy	775	<i>ubc4Δ</i> K48R ubiquitin SGA strain	his3; ura3; ubi1Δ:: GPDpr-L40A; ubi2Δ:: HYGR GPDpr-L40A GPDpr-L40A; ubi3Δ:: URA3 GPDpr-2xUb(K48R)-Ub-S31-Cyc1tr GPDpr-S31; ubi4Δ:: 2X (Cyc1tr-Ub(K48R)-GDPpr) NATR; ubc4Δ::KanR; MAT α
FMGy	777	<i>ubc4Δ</i> K63R ubiquitin SGA strain	his3; ura3; ubi1Δ:: GPDpr-L40A; ubi2Δ:: HYGR GPDpr-L40A GPDpr-L40A; ubi3Δ:: URA3 GPDpr-3xUb(K63R)-S31-Cyc1tr GPDpr-S31; ubi4Δ:: 2X (Cyc1tr-Ub(K63R)-GDPpr) NATR; ubc4Δ::KanR; MAT a
FMGy	810	<i>cdc26Δ</i> K11R ubiquitin SGA strain_1	his3; ura3; ubi1Δ:: GPDpr-L40A; ubi2Δ:: HYGR GPDpr-L40A GPDpr-L40A; ubi3Δ:: URA3 GPDpr-3xUb(K11R)-S31-Cyc1tr GPDpr-S31; ubi4Δ:: 2X (Cyc1tr-Ub(K11R)-GDPpr) NATR; cdc26Δ::KanR; MAT a
FMGy	811	<i>cdc26Δ</i> WT ubiquitin SGA strain_2	his3; ura3; ubi1Δ:: GPDpr-L40A; ubi2Δ:: HYGR GPDpr-L40A GPDpr-L40A; ubi3Δ:: URA3 GPDpr-3xUb-S31-Cyc1tr GPDpr-S31; ubi4Δ:: 2X (Cyc1tr-Ub-GDPpr) NATR; cdc26Δ::KanR; MAT a
FMGy	813	<i>cdc26Δ</i> K11R ubiquitin SGA strain_2	his3; ura3; ubi1Δ:: GPDpr-L40A; ubi2Δ:: HYGR GPDpr-L40A GPDpr-L40A; ubi3Δ:: URA3 GPDpr-3xUb(K11R)-S31-Cyc1tr GPDpr-S31; ubi4Δ:: 2X (Cyc1tr-Ub(K11R)-GDPpr) NATR; cdc26Δ::KanR; MAT a
FMGy	836	<i>cdc26Δ</i> Galpr-Clb2-6xhis33xFlag K11R ubiquitin SGA strain	his3; ura3; Prs413-Galpr-Clb2-6xhis33xFlag; ubi1Δ:: GPDpr-L40A; ubi2Δ:: HYGR GPDpr-L40A GPDpr-L40A; ubi3Δ:: URA3 GPDpr-3xUb(K11R)-S31-Cyc1tr GPDpr-S31; ubi4Δ:: 2X (Cyc1tr-Ub(K11R)-GDPpr) NATR; cdc26Δ::KanR; MAT a
FMGy	839	<i>cdc26Δ</i> Galpr-Clb2-6xhis33xFlag WT ubiquitin SGA strain	his3; ura3; Prs413-Galpr-Clb2-6xhis33xFlag; ubi1Δ:: GPDpr-L40A; ubi2Δ:: HYGR GPDpr-L40A GPDpr-L40A; ubi3Δ:: URA3 GPDpr-3xUb-S31-Cyc1tr GPDpr-S31; ubi4Δ:: 2X (Cyc1tr-Ub-GDPpr) NATR; cdc26Δ::KanR; MAT a
SK1 deletion array		SK1 non-essential single gene deletion library	his3; ura3; can1::STE2pr-SpHIS5 ; XXXX::KanMX4; MAT a

Supplementary Table 3: Oligonucleotides used in this study.

Oligonucleotide sequences		
Name	Description	Sequence
DS268	GPD promoter Fw	GGTTGAAACCAGTTCCTGA
DS270	Ubi1 genotyping primer Rev with DS268	CCGGAGGTAAGAAGTAAAGGTAA
DS180	Ubi2 genotyping primer Fw with DS187	AGGTTGACCCATCCCTCAAT
DS187	Ubi2 genotyping primer Rev with DS180	TGAAATCGTTTATTATGTCCATT
DS193	Ubi3 genotyping primer Fw with DS194	CCCATGCATGTGGAGTCATA
DS194	Ubi3 genotyping primer Rev with DS193	TTGCGAGAACGCTAAAAAGG
DS195	Ubi4 genotyping primer Fw with DS198	GGCAACCtATGATAGGAAAT
DS196	Ubi4 genotyping primer Rev with DS198RC	TGACTCAATTGGTTCGGCTTA
DS198	Sequencing primer between Cyt1tr and GDPpr	AGTGGCCAGCTAGCGAGTTTA
DS198R C	Sequencing primer between Cyt1tr and GDPpr RC	TAAACTCGCTAGCTGGCCACT
DS199	3X WTUb	AAGCTTATGCAGATTTTTGTTAAGACACTAACC GGAAAAACAATAACTTTGGAAGTAGAATCTAGT GATACGATTGATAATGTTAAGTCTAAAATTCAA GACAAAGAGGGCATCCCTCCTGACCAGCAAAG ACTGATTTTCGCTGGTAAACAATTGGAAGATGG TAGAACACTGTCAGATTACAACATTCAAAAAGA GTCCACATTGCATCTTGTATTGAGATTAAGGGG TGGTATGCAAATTTTCGTCAAAACATTAACAGG AAAAACTATCACGCTAGAAGTTGAATCTTCTGA TACTATCGATAATGTGAAATCAAAGATCCAGGA TAAGGAGGGTATAACCACCAGACCAACAAAGAC TAATCTTTGCCGGTAAACAGCTCGAAGATGGAC GAACCCTTTCAGATTATAACATCCAAAAGGAAA GTACTCTTCACCTTGTGCTAAGATTGAGAGGAG GCATGCAAATCTTTGTAAAGACTTTAACAGGCA AGACAATCACATTAGAAGTTGAGAGCTCAGATA CTATTGACAATGTCAAATCTAAAATCCAAGACA AGGAAGGTATTCCACCAGATCAACAAAGATTG ATATTTGCAGGGAAACAATTAGAAGATGGTCGT ACCTTGTCCGACTACAATATACAAAAGGAATCT ACTCTCCATTTGGTTTTAAGACTGAGAGGGGGC aacTAAGTCGAC

Supplementary Table 3, continued: Oligonucleotides used in this study.

Name	Description	Sequence
DS200	3X K6R Ub	AAGCTTATGCAGATTTTTGTTAGAACACTAACC GGAAAAACAATAACTTTGGAAGTAGAATCTAGT GATACGATTGATAATGTTAAGTCTAAAATTCAA GACAAAGAGGGCATCCCTCCTGACCAGCAAAG ACTGATTTTCGCTGGTAAACAATTGGAAGATGG TAGAACACTGTCAGATTACAACATTCAAAAAGA GTCCACATTGCATCTTGTATTGAGATTAAGGGG TGGTATGCAAATTTTCGTCAGAACATTAACAGG AAAA ACTATCACGCTAGAAGTTGAATCTTCTGA TACTATCGATAATGTGAAATCAAAGATCCAGGA TAAGGAGGGTATACCACCAGACCAACAAAGAC TAATCTTTGCCGGTAAACAGCTCGAAGATGGAC GAACCCTTTCAGATTATAACATCCAAAAGGAAA G TACTCTTCACCTTGTGCTAAGATTGAGAGGAG GCATGCAAATCTTTGTAAGAACTTTAACAGGCA AGACAATCACATTAGAAGTTGAGAGCTCAGATA CTATTGACAATGTCAAATCTAAAATCCAAGACA AGGAAGGTATTCCACCAGATCAACAAAGATTG ATATTTGCAGGGAAACAATTAGAAGATGGTCGT ACCTTGCCGACTACAATATACAAAAGGAATCT ACTCTCCATTTGGTTTTAAGACTGAGAGGGGGC aacTAAGTCGAC
DS201	3X K11R Ub	AAGCTTATGCAGATTTTTGTTAAGACACTAACC GGAAGAACAATAACTTTGGAAGTAGAATCTAGT GATACGATTGATAATGTTAAGTCTAAAATTCAA GACAAAGAGGGCATCCCTCCTGACCAGCAAAG ACTGATTTTCGCTGGTAAACAATTGGAAGATGG TAGAACACTGTCAGATTACAACATTCAAAAAGA GTCCACATTGCATCTTGTATTGAGATTAAGGGG TGGTATGCAAATTTTCGTCAAAACATTAACAGG AAGAACTATCACGCTAGAAGTTGAATCTTCTGA TACTATCGATAATGTGAAATCAAAGATCCAGGA TAAGGAGGGTATACCACCAGACCAACAAAGAC TAATCTTTGCCGGTAAACAGCTCGAAGATGGAC GAACCCTTTCAGATTATAACATCCAAAAGGAAA G TACTCTTCACCTTGTGCTAAGATTGAGAGGAG GCATGCAAATCTTTGTAAGAACTTTAACAGGCA GAACAATCACATTAGAAGTTGAGAGCTCAGATA CTATTGACAATGTCAAATCTAAAATCCAAGACA AGGAAGGTATTCCACCAGATCAACAAAGATTG ATATTTGCAGGGAAACAATTAGAAGATGGTCGT ACCTTGCCGACTACAATATACAAAAGGAATCT ACTCTCCATTTGGTTTTAAGACTGAGAGGGGGC aacTAAGTCGAC

Supplementary Table 3, continued: Oligonucleotides used in this study.

Name	Description	Sequence
DS203	3X K29R Ub	AAGCTTATGCAGATTTTTGTTAAGACACTAACC GGAAAAACAATAACTTTGGAAGTAGAATCTAGT GATACGATTGATAATGTTAAGTCTAGAATTCAA GACAAAGAGGGCATCCCTCCTGACCAGCAAAG ACTGATTTTCGCTGGTAAACAATTGGAAGATGG TAGAACACTGTCAGATTACAACATTCAAAAAGA GTCCACATTGCATCTTGTATTGAGATTAAGGGG TGGTATGCAAATTTTCGTCAAAACATTAACAGG AAAA ACTATCACGCTAGAAGTTGAATCTTCTGA TACTATCGATAATGTGAAATCAAGAATCCAGGA TAAGGAGGGTATAACCACCAGACCAACAAAGAC TAATCTTTGCCGGTAAACAGCTCGAAGATGGAC GAACCCTTTCAGATTATAACATCCAAAAGGAAA GTACTCTTCACCTTGTGCTAAGATTGAGAGGAG GCATGCAAATCTTTGTAAAGACTTTAACAGGCA AGACAATCACATTAGAAGTTGAGAGCTCAGATA CTATTGACAATGTCAAATCTAGAATCCAAGACA AGGAAGGTATTCCACCAGATCAACAAAGATTG ATATTTGCAGGGAAACAATTAGAAGATGGTCGT ACCTTGTCGGACTACAATATACAAAAGGAATCT ACTCTCCATTTGGTTTTAAGACTGAGAGGGGGC aacTAAGTCGAC
DS204	3X K33R Ub	AAGCTTATGCAGATTTTTGTTAAGACACTAACC GGAAAAACAATAACTTTGGAAGTAGAATCTAGT GATACGATTGATAATGTTAAGTCTAAAATTCAA GACAGAGAGGGCATCCCTCCTGACCAGCAAAG ACTGATTTTCGCTGGTAAACAATTGGAAGATGG TAGAACACTGTCAGATTACAACATTCAAAGAGA GTCCACATTGCATCTTGTATTGAGATTAAGGGG TGGTATGCAAATTTTCGTCAAAACATTAACAGG AAAA ACTATCACGCTAGAAGTTGAATCTTCTGA TACTATCGATAATGTGAAATCAAAGATCCAGGA TAGAGAGGGTATAACCACCAGACCAACAAAGAC TAATCTTTGCCGGTAAACAGCTCGAAGATGGAC GAACCCTTTCAGATTATAACATCCAAAGAGAAA GTACTCTTCACCTTGTGCTAAGATTGAGAGGAG GCATGCAAATCTTTGTAAAGACTTTAACAGGCA AGACAATCACATTAGAAGTTGAGAGCTCAGATA CTATTGACAATGTCAAATCTAAAATCCAAGACA GAGAAGGTATTCCACCAGATCAACAAAGATTG ATATTTGCAGGGAAACAATTAGAAGATGGTCGT ACCTTGTCGGACTACAATATACAAAAGAGAATCT ACTCTCCATTTGGTTTTAAGACTGAGAGGGGGC aacTAAGTCGAC

Supplementary Table 3, continued: Oligonucleotides used in this study.

Name	Description	Sequence
DS205	2X K48R Ub 1X WT Ub	AAGCTTATGCAGATTTTTGTTAAGACACTAACC GGAAAAACAATAACTTTGGAAGTAGAATCTAGT GATACGATTGATAATGTTAAGTCTAAAATTCAA GACAAAGAGGGCATCCCTCCTGACCAGCAAAG ACTGATTTTCGCTGGTAGACAATTGGAAGATGG TAGAACACTGTCAGATTACAACATTCAAAAAGA GTCCACATTGCATCTTGTATTGAGATTAAGGGG TGGTATGCAAATTTTCGTCAAAACATTAACAGG AAAA ACTATCACGCTAGAAGTTGAATCTTCTGA TACTATCGATAATGTGAAATCAAAGATCCAGGA TAAGGAGGGTATAACCACCAGACCAACAAAGAC TAATCTTTGCCGGTAGACAGCTCGAAGATGGAC GAACCCTTTCAGATTATAACATCCAAAAGGAAA GTACTCTTCACCTTGTGCTAAGATTGAGAGGAG GCATGCAAATCTTTGTAAAGACTTTAACAGGCA AGACAATCACATTAGAAGTTGAGAGCTCAGATA CTATTGACAATGTCAAATCTAAAATCCAAGACA AGGAAGGTATTCCACCAGATCAACAAAGATTG ATATTTGCAGGGAAACAATTAGAAGATGGTCGT ACCTTGCCGACTACAATATACAAAAGGAATCT ACTCTCCATTTGGTTTTAAGACTGAGAGGGGGC aacTAAGTCGAC
DS206	3X K6R K11R Ub	AAGCTTATGCAGATTTTTGTTAGAACACTAACC GGAAGAACAATAACTTTGGAAGTAGAATCTAGT GATACGATTGATAATGTTAAGTCTAAAATTCAA GACAAAGAGGGCATCCCTCCTGACCAGCAAAG ACTGATTTTCGCTGGTAAACAATTGGAAGATGG TAGAACACTGTCAGATTACAACATTCAAAGAGA GTCCACATTGCATCTTGTATTGAGATTAAGGGG TGGTATGCAAATTTTCGTGAGAACATTAACAGG AAGAACTATCACGCTAGAAGTTGAATCTTCTGA TACTATCGATAATGTGAAATCAAAGATCCAGGA TAAGGAGGGTATAACCACCAGACCAACAAAGAC TAATCTTTGCCGGTAAACAGCTCGAAGATGGAC GAACCCTTTCAGATTATAACATCCAAAGAGAAA GTACTCTTCACCTTGTGCTAAGATTGAGAGGAG GCATGCAAATCTTTGTAAAGACTTTAACAGGCA GAACAATCACATTAGAAGTTGAGAGCTCAGATA CTATTGACAATGTCAAATCTAAAATCCAAGACA AGGAAGGTATTCCACCAGATCAACAAAGATTG ATATTTGCAGGGAAACAATTAGAAGATGGTCGT ACCTTGCCGACTACAATATACAAAAGAGAATCT ACTCTCCATTTGGTTTTAAGACTGAGAGGGGGC aacTAAGTCGAC

Supplementary Table 3, continued: Oligonucleotides used in this study.

Name	Description	Sequence
DS207	3X K6R K29R Ub	AAGCTTATGCAGATTTTTGTTAAGACACTAACC GGAAAAACAATAACTTTGGAAGTAGAATCTAGT GATACGATTGATAATGTTAGATCTAGAATTCAA GACAGAGAGGGCATCCCTCCTGACCAGCAAAG ACTGATTTTCGCTGGTAAACAATTGGAAGATGG TAGAACACTGTCAGATTACAACATTCAAAAAGA GTCCACATTGCATCTTGTATTGAGATTAAGGGG TGGTATGCAAATTTTCGTCAAACATTAACAGG AAAAATATCACGCTAGAAGTTGAATCTTCTGA TACTATCGATAATGTGAAATCAAGAATCCAGGA TAGAGAGGGTATAACCACCAGACCAACAAAGAC TAATCTTTGCCGGTAGACAGCTCGAAGATGGAC GAACCCTTTCAGATTATAACATCCAAAAGGAAA GACTCTTCACCTTGTGCTAAGATTGAGAGGAG GCATGCAAATCTTTGTAAAGACTTTAACAGGCA AGACAATCACATTAGAAGTTGAGAGCTCAGATA CTATTGACAATGTCAGATCTAGAATCCAAGACA GAGAAGGTATTCCACCAGATCAACAAAGATTG ATATTTGCAGGGAAACAATTAGAAGATGGTCGT ACCTTGTCGGACTACAATATACAAAAGGAATCT ACTCTCCATTTGGTTTTAAGACTGAGAGGGGGC aacTAAGTCGAC
DS208	3X K11R K29R Ub	AAGCTTATGCAGATTTTTGTTAAGACACTAACC GGAAGAACAATAACTTTGGAAGTAGAATCTAGT GATACGATTGATAATGTTAAGTCTAGAATTCAA GACAAAGAGGGCATCCCTCCTGACCAGCAAAG ACTGATTTTCGCTGGTAAACAATTGGAAGATGG TAGAACACTGTCAGATTACAACATTCAAAAAGA GTCCACATTGCATCTTGTATTGAGATTAAGGGG TGGTATGCAAATTTTCGTCAAACATTAACAGG AAGAATATCACGCTAGAAGTTGAATCTTCTGA TACTATCGATAATGTGAAATCAAGAATCCAGGA TAAGGAGGGTATAACCACCAGACCAACAAAGAC TAATCTTTGCCGGTAAACAGCTCGAAGATGGAC GAACCCTTTCAGATTATAACATCCAAAAGGAAA GACTCTTCACCTTGTGCTAAGATTGAGAGGAG GCATGCAAATCTTTGTAAAGACTTTAACAGGCA GAACAATCACATTAGAAGTTGAGAGCTCAGATA CTATTGACAATGTCAAATCTAGAATCCAAGACA AGGAAGGTATTCCACCAGATCAACAAAGATTG ATATTTGCAGGGAAACAATTAGAAGATGGTCGT ACCTTGTCGGACTACAATATACAAAAGGAATCT ACTCTCCATTTGGTTTTAAGACTGAGAGGGGGC aacTAAGTCGAC

Supplementary Table 3, continued: Oligonucleotides used in this study.

Name	Description	Sequence
DS209	3X K11R K33R Ub	AAGCTTATGCAGATTTTTGTTAAGACACTAACC GGAAGAACAATAACTTTGGAAGTAGAATCTAGT GATACGATTGATAATGTTAAGTCTAAAATTCAA GACAGAGAGGGCATCCCTCCTGACCAGCAAAG ACTGATTTTCGCTGGTAAACAATTGGAAGATGG TAGAACACTGTCAGATTACAACATTCAAAAAGA GTCCACATTGCATCTTGTATTGAGATTAAGGGG TGGTATGCAAATTTTCGTCAAACATTAACAGG AAGAACTATCACGCTAGAAGTTGAATCTTCTGA TACTATCGATAATGTGAAATCAAAGATCCAGGA TAGAGAGGGTATAACCACCAGACCAACAAAGAC TAATCTTTGCCGGTAAACAGCTCGAAGATGGAC GAACCCTTTCAGATTATAACATCCAAAAGGAAA GTACTCTTCACCTTGTGCTAAGATTGAGAGGAG GCATGCAAATCTTTGTAAAGACTTTAACAGGCA GAACAATCACATTAGAAGTTGAGAGCTCAGATA CTATTGACAATGTCAAATCTAAAATCCAAGACA GAGAAGGTATTCCACCAGATCAACAAAGATTG ATATTTGCAGGGAAACAATTAGAAGATGGTCGT ACCTTGCCGACTACAATATACAAAAGGAATCT ACTCTCCATTTGGTTTTAAGACTGAGAGGGGGC aacTAAGTCGAC
DS210	3X K27R K33R Ub	AAGCTTATGCAGATTTTTGTTAAGACACTAACC GGAAAACAATAACTTTGGAAGTAGAATCTAGT GATACGATTGATAATGTTAGATCTAAAATTCAA GACAAAGAGGGCATCCCTCCTGACCAGCAAAG ACTGATTTTCGCTGGTAAACAATTGGAAGATGG TAGAACACTGTCAGATTACAACATTCAAAGAGA GTCCACATTGCATCTTGTATTGAGATTAAGGGG TGGTATGCAAATTTTCGTCAAACATTAACAGG AAAA ACTATCACGCTAGAAGTTGAATCTTCTGA TACTATCGATAATGTGAGATCAAAGATCCAGGA TAAGGAGGGTATAACCACCAGACCAACAAAGAC TAATCTTTGCCGGTAAACAGCTCGAAGATGGAC GAACCCTTTCAGATTATAACATCCAAAGAGAAA GTACTCTTCACCTTGTGCTAAGATTGAGAGGAG GCATGCAAATCTTTGTAAAGACTTTAACAGGCA AGACAATCACATTAGAAGTTGAGAGCTCAGATA CTATTGACAATGTCAGATCTAAAATCCAAGACA AGGAAGGTATTCCACCAGATCAACAAAGATTG ATATTTGCAGGGAAACAATTAGAAGATGGTCGT ACCTTGCCGACTACAATATACAAAGAGAATCT ACTCTCCATTTGGTTTTAAGACTGAGAGGGGGC aacTAAGTCGAC

Supplementary Table 3, continued: Oligonucleotides used in this study.

Name	Description	Sequence
DS211	3X K29R K33R Ub	AAGCTTATGCAGATTTTTGTTAAGACACTAACC GGAAAAACAATAACTTTGGAAGTAGAATCTAGT GATACGATTGATAATGTTAAGTCTAGAATTCAA GACAGAGAGGGCATCCCTCCTGACCAGCAAAG ACTGATTTTCGCTGGTAAACAATTGGAAGATGG TAGAACACTGTCAGATTACAACATTCAAAAAGA GTCCACATTGCATCTTGTATTGAGATTAAGGGG TGGTATGCAAATTTTCGTCAAACATTAACAGG AAAAATATCACGCTAGAAGTTGAATCTTCTGA TACTATCGATAATGTGAAATCAAGAATCCAGGA TAGAGAGGGTATAACCACCAGACCAACAAAGAC TAATCTTTGCCGGTAAACAGCTCGAAGATGGAC GAACCTTTTCAGATTATAACATCCAAAAGGAAA GTACTCTTCACCTTGTGCTAAGATTGAGAGGAG GCATGCAAATCTTTGTAAAGACTTTAACAGGCA AGACAATCACATTAGAAGTTGAGAGCTCAGATA CTATTGACAATGTCAAATCTAGAATCCAAGACA GAGAAGGTATTCCACCAGATCAACAAAGATTG ATATTTGCAGGGAAACAATTAGAAGATGGTCGT ACCTTGTCGGACTACAATATACAAAAGGAATCT ACTCTCCATTTGGTTTTAAGACTGAGAGGGGGC aacTAAGTCGAC
DS212	1X K11R K48R Ub 2x K11R Ub	AAGCTTATGCAGATTTTTGTTAAGACACTAACC GGAAGAACAATAACTTTGGAAGTAGAATCTAGT GATACGATTGATAATGTTAAGTCTAAAATTCAA GACAAAGAGGGCATCCCTCCTGACCAGCAAAG ACTGATTTTCGCTGGTAGACAATTGGAAGATGG TAGAACACTGTCAGATTACAACATTCAAAAAGA GTCCACATTGCATCTTGTATTGAGATTAAGGGG TGGTATGCAAATTTTCGTCAAACATTAACAGG AAGAACTATCACGCTAGAAGTTGAATCTTCTGA TACTATCGATAATGTGAAATCAAAGATCCAGGA TAAGGAGGGTATAACCACCAGACCAACAAAGAC TAATCTTTGCCGGTAAACAGCTCGAAGATGGAC GAACCTTTTCAGATTATAACATCCAAAAGGAAA GTACTCTTCACCTTGTGCTAAGATTGAGAGGAG GCATGCAAATCTTTGTAAAGACTTTAACAGGCA GAACAATCACATTAGAAGTTGAGAGCTCAGATA CTATTGACAATGTCAAATCTAAAATCCAAGACA AGGAAGGTATTCCACCAGATCAACAAAGATTG ATATTTGCAGGGAAACAATTAGAAGATGGTCGT ACCTTGTCGGACTACAATATACAAAAGGAATCT ACTCTCCATTTGGTTTTAAGACTGAGAGGGGGC aacTAAGTCGAC

Supplementary Table 3, continued: Oligonucleotides used in this study.

Name	Description	Sequence
DS213	1X K29R K48R K Ub 2x K29R Ub	AAGCTTATGCAGATTTTTGTTAAGACACTAACC GGA AAAACAATAACTTTGGAAGTAGAATCTAGT GATACGATTGATAATGTTAAGTCTAGAATTCAA GACAAAGAGGGCATCCCTCCTGACCAGCAAAG ACTGATTTTCGCTGGTAGACAATTGGAAGATGG TAGAACACTGTCAGATTACAACATTCAAAAAGA GTCCACATTGCATCTTGTATTGAGATTAAGGGG TGGTATGCAAATTTTCGTCAAACATTAACAGG AAAACTATCACGCTAGAAGTTGAATCTTCTGA TACTATCGATAATGTGAAATCAAGAATCCAGGA TAAGGAGGGTATAACCACCAGACCAACAAAGAC TAATCTTTGCCGGTAAACAGCTCGAAGATGGAC GAACCCTTTCAGATTATAACATCCAAAAGGAAA GTACTCTTCACCTTGTGCTAAGATTGAGAGGAG GCATGCAAATCTTTGTAAAGACTTTAACAGGCA AGACAATCACATTAGAAGTTGAGAGCTCAGATA CTATTGACAATGTCAAATCTAGAATCCAAGACA AGGAAGGTATTCCACCAGATCAACAAAGATTG ATATTTGCAGGGAAACAATTAGAAGATGGTCGT ACCTTGCCGACTACAATATACAAAAGGAATCT ACTCTCCATTTGGTTTTAAGACTGAGAGGGGGC aacTAAGTCGAC
DS214	3X K11R K27R K29R Ub	AAGCTTATGCAGATTTTTGTTAAGACACTAACC GGAAGAACAATAACTTTGGAAGTAGAATCTAGT GATACGATTGATAATGTTAGATCTAGAATTCAA GACAAAGAGGGCATCCCTCCTGACCAGCAAAG ACTGATTTTCGCTGGTAAACAATTGGAAGATGG TAGAACACTGTCAGATTACAACATTCAAAAAGA GTCCACATTGCATCTTGTATTGAGATTAAGGGG TGGTATGCAAATTTTCGTCAAACATTAACAGG AAGAACTATCACGCTAGAAGTTGAATCTTCTGA TACTATCGATAATGTGAGATCAAGAATCCAGGA TAAGGAGGGTATAACCACCAGACCAACAAAGAC TAATCTTTGCCGGTAAACAGCTCGAAGATGGAC GAACCCTTTCAGATTATAACATCCAAAAGGAAA GTACTCTTCACCTTGTGCTAAGATTGAGAGGAG GCATGCAAATCTTTGTAAAGACTTTAACAGGCA GAACAATCACATTAGAAGTTGAGAGCTCAGATA CTATTGACAATGTCAGATCTAGAATCCAAGACA AGGAAGGTATTCCACCAGATCAACAAAGATTG ATATTTGCAGGGAAACAATTAGAAGATGGTCGT ACCTTGCCGACTACAATATACAAAAGGAATCT ACTCTCCATTTGGTTTTAAGACTGAGAGGGGGC aacTAAGTCGAC

Chapter 2

A genetic approach to study polyubiquitination in *Saccharomyces cerevisiae*

1. Introduction

Protein polyubiquitination is a highly conserved posttranslational modification that can alter the stability, localization, and function of substrates [1]. This functional versatility arises from the structural diversity of ubiquitination. Indeed, lysine residues on substrates can be modified with single ubiquitins, known as monoubiquitination, or with a chain of polyubiquitin, consisting of ubiquitin protomers linked to each other through one of ubiquitin's seven acceptor lysines (K6, K11, K27, K29, K33, K48, and K63) or the N-terminal amino group of methionine 1 of ubiquitin. While all ubiquitin linkages exist *in vivo* in widely varying amounts [2], the functional significance of most remains enigmatic.

A large number of studies over the last four decades since the discovery of ubiquitin have elucidated some functions of specific ubiquitin linkage types. K48-linked chains were the first to be studied in detail and are considered the canonical ubiquitin chain that leads to proteasomal degradation [3]. K63 linkages have been the subject of intense study following the recognition of their non-degradative functions in various signaling pathways including the DNA damage response [2,4–7], protein trafficking [8,9], mitophagy [10], inflammation [11–13], and immune responses [14]. The importance of K11-linked polyubiquitin chains has only emerged in the last decade with the discovery of their degradative functions during mitotic progression in metazoans [15]. Proteomics studies suggest that K6, K27, K29, and K33 ubiquitin linkages are rare in cells [2,16]. Nonetheless, some pioneering studies have identified specific physiological

functions of those linkages [17]. K6-linked chains, for example, are reportedly synthesized by the BRCA1-BARD1 E3 ligase to regulate the DNA damage response in a proteolysis-independent manner [18,19]. These linkages, along with K27-linked chains, are also generated by the E3 ligase Parkin, which functions in mitophagy [10,20–22]. In an interesting mechanism, K29-linked chains on the mRNA-binding protein, HuR, are recognized by UBXD8, an adaptor for the p97 ATPase, thereby promoting the release of HuR from its association with specific mRNAs [23]. Finally, a study of post-Golgi protein trafficking provided an elegant example of how polyubiquitin linked through K33 can mediate a protein-protein interaction between Coronin-7 and Eps15 [24].

A comprehensive examination of the functional significance of all ubiquitin linkage types is lacking and would serve to accelerate the pace of discovery of the physiologically important functions of ubiquitin chain types and the ubiquitin-proteasome system. This is particularly necessary for the poorly understood polyubiquitin chains linked through K6, K11, K27, K29, and K33 of ubiquitin. The analysis of genetic interactions is a powerful tool for establishing functional relationships between genes and uncovering novel gene functions [25–32]. When two genes function in parallel or redundant pathways, mutating or deleting both genes in a cell can lead to a negative (synthetic) genetic interaction, wherein the double mutant strain has a more severe phenotype than each of the single mutant parent strains. In contrast, mutation of two genes that function in the same pathway would not lead to phenotypic enhancement in the double mutant (epistasis).

Here we describe a high-throughput method to uncover genetic interactions of individual ubiquitin linkage types by combining lysine-to-arginine (K-to-R) ubiquitin mutations with single gene deletions. A general approach to validate novel genetic interactions arising from the screen is also detailed. Aside from its utility for the study of ubiquitin in yeast, we propose that the methodology we have developed will prove

broadly applicable to the analysis of complex relationships between genes, including multigenic redundancies, in many biological pathways.

2. Strain Engineering

Previous high-throughput genetic interaction screens have examined the synthetic phenotype of two [27–29,31,33,34], or in a few cases three [35], mutations. The genetic analysis of ubiquitin, however, is challenging due to the fact that ubiquitin is encoded at four genomic loci, *UBI1-4*, in *Saccharomyces cerevisiae*. At *UBI1*, 2, and 3, ubiquitin is expressed as a fusion to ribosomal proteins RPL40A, RPL40B, and RPS31, respectively. An additional five copies of ubiquitin are encoded at *UBI4* as head-to-tail fusions. In all cases, the ubiquitin fusion proteins are proteolytically processed to release mature ubiquitin protomers that are competent to be conjugated to lysine residues of proteins. The analysis of genetic interactions normally requires the deletion of two genes in the same cell. In contrast, to study the genetic interactions of ubiquitin mutants, along with deletion of a gene of interest, all four ubiquitin genes must be modified to express the desired ubiquitin variant while also preserving expression of the ribosomal proteins encoded at *UBI1-3*. The relatively large number of loci that must be modified to carry out genetic analyses of ubiquitin mutants required key optimizations of the conventional SGA protocol described below.

Most genetic interaction screens have utilized the S288C yeast strain, which exhibits poor sporulation efficiency. In those studies, the low efficiency of sporulation was acceptable because only a total of five loci were under selection, the two loci of interest and three haploid selectable markers necessary to generate the desired haploid double mutant cells. In contrast, to study ubiquitin, eight total loci must be selected to generate haploid cells that carry modified *ubi1-4*, a given gene deletion, as well as all necessary haploid selectable markers. The efficiency of sporulation becomes a limiting factor, as an exceedingly small percentage of spores will have the final desired genotype.

The SK1 yeast strain naturally has a high sporulation efficiency of about 92%, a stark contrast to the 12% efficiency exhibited by S288C [36]. This key advantage led us to generate all the ubiquitin mutant strains and a novel single gene deletion library in the SK1 strain background.

While the SK1 strain provided a crucial advantage over S288C, two further modifications were made to decrease the number of loci under selection, thereby increasing the percentage of spores with the final desired genotypes. First, the *UBII* locus was replaced with a construct expressing Rpl40A, a ribosomal protein, under the control of the constitutive GPD promoter in the entire SK1 deletion library and all K-to-R ubiquitin mutant strains. Because the locus is equally modified in the ubiquitin mutant strains and gene deletion array, no marker was necessary (**See below, 2.1**). Second, unsporulated diploid cells are a significant source of background in SGA studies that is eliminated with two separate selections for haploid cells. The high sporulation efficiency of SK1 leads to significantly less unsporulated diploid cells, thus permitting the omission of one haploid selection step, *Iyp1*Δ selection. Ultimately, in the SK1 ubiquitin SGA 6 loci are selected: 3 ubiquitin loci, 1 gene deletion, and 2 haploid and mating type selection markers.

2.1 Deletion of *UBI1*

Strain DS1 of the genotype Mat alpha; *his3*; *ura3*; *CAN1*; *ubi1*Δ::LoxP-GAL1pr-Cre-URA3-LoxP-GPDpr-RPL40A was cultured in liquid overnight and spread on a C-uracil plate to generate a lawn. The cells were then pinned into the 384 colony format to allow mating to the SK1 gene deletion library on YPAD plates using a Singer Instruments pinning Robot (Robot: Singer Instruments PLU-001; Pinning pads: Singer Instruments RePad384A; Plates: Singer Instruments PlusPlates). The GAL1pr-Cre construct was amplified from yeast genomic DNA because it could not be maintained in bacteria, likely due to promoter leakiness. The mating mixes were transferred to C-uracil

+ G418 plates to select for diploids. Diploids were then pinned onto sporulation plates and cultured for 2 days. Haploids were then selected first on C-uracil for 24 hours, then on C-uracil containing G418 for 2 days. To induce the Cre recombinase and haploids were plated on 2% galactose containing plates for 2 days. The positions of the LoxP sites in the construct led to deletion of the *URA3* marker and Cre recombinase. The cells were transferred to plates containing 5-fluoro-orotic acid (FOA) plates and incubated at 30°C for 24 hours to select against cells carrying the *URA3* marker [37]. This negative selection was performed a total of three consecutive times to ensure deletion of *URA3*. The final plates were replicated onto C-uracil plates. To confirm the successful recombination event, the modified *ubi1* locus was amplified by PCR and sequenced. No significant changes in ubiquitin levels or doubling time were observed following deletion of *UBI1*, as has been previously reported [38].

2.2 Design of ubiquitin loci encoding ubiquitin variants

The endogenous *UBI3* locus encodes a fusion protein consisting of ubiquitin fused to *RPS31*, a ribosomal protein. Deletion of *UBI3* with a construct expressing a triple ubiquitin fusion protein along with expression of *RPS31* from a separate GPD promoter resulted in a doubling time of 7 hours. Multiple modifications to *UBI3* were attempted to ameliorate the observed growth defect. Increasing the expression of *RPS31* by including in the construct up to 5 copies of GPDpr-*RPS31* could not decrease the doubling time below 3 hours. It has been suggested that ubiquitin acts as a folding chaperone for Rps31. To address this possibility, the triple-ubiquitin sequence was fused to *RPS31*, thereby leading to expression of a triple ubiquitin-Rps31 hybrid protein. In addition, a GPDpr-*RPS31* cassette was included in the *URA3*-marked construct. The resulting strains exhibited growth rates similar to wild type.

The *UBI4* locus encodes 5 copies of ubiquitin expressed as single polypeptide that is proteolytically processed to release free ubiquitin. *UBI4* was replaced with a 2 copies

of a construct expressing ubiquitin from the constitutive GPD promoter , including the C-terminal asparagine found in endogenous *UBI4* that is proteolytically processed to release mature ubiquitin [1,40]. This locus was marked with a Nourseothricin (NAT) resistance cassette.

At the modified *ubi2* locus, two copies a cassette driving expression of the ribosomal protein Rpl40 from the GPD promoter are inserted and marked with the Hygromycin resistance gene. The modified *ubi2* locus exhibited a normal doubling time.

At all modified loci, the constitutive GPD promoter was used as it resulting in the highest level of ubiquitin expression relative to other tested promoters, including *TEF1*, *HYP2*, *PYK1*, and *PDC1* [41].

To control for the potential effects of altered ubiquitin levels, a strain expressing low levels of ubiquitin was constructed by replacing *UBI4* only with the NAT resistance cassette. In this strain, ubiquitin is only expressed from the modified *ubi3* locus.

Because lysine 48 of ubiquitin is essential, strains expressing K48R mutant ubiquitin had to be supplemented with wild type ubiquitin. In these strains, two of the ubiquitins in the triple ubiquitin fusion encoded at *ubi3* are mutated at K48. At *ubi4*, both ubiquitins are mutated at K48. Strains expressing ubiquitin mutated at K48 and another lysine were express one copy of double mutant ubiquitin (K29R K48R, for example) and two copies of single mutant ubiquitin (K29R, for example) at *ubi3*. Double mutant ubiquitin is expressed from *ubi4*.

2.3 Construction of strains expressing ubiquitin variants

The endogenous *UBI2-4* loci were replaced with the constructs detailed above as follows: A diploid strain homozygous for modified *ubi1* was transformed with the engineered *ubi2* cassette. Transformants were selected by their resistance to hygromycin and then transformed with the panel of ubiquitin mutant *ubi3* constructs. Transformants were selected upon growth on plates lacking uracil. These diploid *ubi1;ubi2;ubi3* mutants

were sporulated to generate haploid cells of mating type alpha carrying all three modified loci. In parallel, the panel of mutant ubiquitin *ubi4* constructs were used to transform diploid SK1 cells. Following sporulation of transformants that were resistant to nourseothricin and of mating type a were crossed to the haploid *ubi1-3* mutants. Diploids were sporulated to generate haploids of mating type alpha that carried all modified ubiquitin loci, which were genotyped by PCR.

3. Modification of the conventional SGA method to establish an SK1 4-marker ubiquitin SGA protocol

The 4-marker SGA was largely carried out as has been previously reported for conventional 2-marker SGA screening in the S288C strain. As detailed SGA protocols have been published elsewhere, a brief overview of the 4-marker ubiquitin SGA method is provided here with attention to notable modifications to the conventional SGA protocol that were key to establish a robust SGA process in the SK1 strain background and permit the simultaneous analysis of multiple mutant loci.

3.1 Drug concentrations

G418: Selection with G418 is required to select for the specific gene deletion that comes from the SK1 deletion library. Previous SGA studies in the S288C strain used up to 200mg/L of G418, although 100mg/L was found to be sufficient [34]. The SK1 strain requires higher concentrations of the drug. Careful titration of G418 revealed that a concentration of 350mg/L is optimal for SGA screening using the SK1 strain.

Canavanine: Resistance to canavanine is a recessive marker that is useful to kill unsporulated diploid cells. Previous screens in S288C have used canavanine at a concentration of 50mg/L [7]. This concentration of canavanine proved excessive when

combined with other selection steps (e.g. 350mg/L G418) for SK1 as the cells showed obvious growth defects. Titration of canavanine was done in combination with other drugs in the screen. The much lower concentration of 10mg/L was sufficient to kill diploids and did not cause obvious growth defects. Nonetheless, 50mg/L of canavanine was used for haploid selection following sporulation to ensure complete selection against unsporulated diploids, but the lower concentration of 10mg/L was included in all subsequent selection plates.

Nourseothricin (NAT): 100 mg/L, as used in conventional S288C SGA screening.

Hygromycin: During conventional SGA screening, hygromycin is not normally used. In this screen, *ubi2* is marked with a hygromycin-resistance. The drug was successfully used at the commonly used concentration of 200 mg/L.

3.2 Sporulation

Sporulation of the SK1 strain is about 92% efficient compared to the approximately 12% sporulation efficiency of S288C strain [42]. The poor sporulation efficiency of S288C necessitates a long sporulation time of 5 days. In contrast, sufficient sporulation of SK1 is obtained after only 2 days at 25°C. This significantly decreases the duration of the genetic screen.

3.3 Robot settings

To maximize the number of cells transferred at each pinning step, a mixed pinning used with the Singer ROTOR robot.

3.4 Overview of the 4-Marker SGA workflow

Two biological replicates of the screen were carried out on different days. Each biological replicate also had three technical replicates. Lawns of each query strain were

mated to the SK1 deletion array using the Singer Pinning Robot system for one day at 30°C. Diploids were selected on plates lacking uracil and containing NAT, G418, and HYG. The colonies were then transferred to sporulation plates for 2 days at 25°C. Haploids of mating type a were selected on plates lacking histidine and containing canavanine. Haploid mutant selections were performed in the following order: 1) C-uracil plates (*ubi3*), 200 mg/L hygromycin (*ubi2*); 2) 100mg/L Nourseothricin (*ubi4*); 3) 350 mg/L G418 (single gene deletions). To ensure effective mutant selections, in each step, the previous selection condition was included. Of note is the fact that quality control analysis revealed that the ubiquitin loci must be selected prior to the gene deletion to achieve precise mutant selections. The final plates were grown at 30°C for 48 hours, and then photographed.

4. Analysis of data quality

4.1 Calculation and characterization of genetic interaction scores

Using established SGA protocols and methods, colony sizes were recorded and normalized to calculate genetic interaction scores (S-scores) [34,43]. S-scores were averaged among replicates to obtain the final SGA dataset. As has been observed in previous SGA studies, and given that genetic interactions are rare, the S-scores in the 4-marker SGA were centered around zero, with about 53% of scores being negative and 47% positive values and 95% of scores lying within 2 standard deviations of the mean S-score of -0.21. Strong negative S-scores were more common than positive S-scores. The strongest S-score in the screen was -20.97 while the largest positive S-Score value was 6.68.

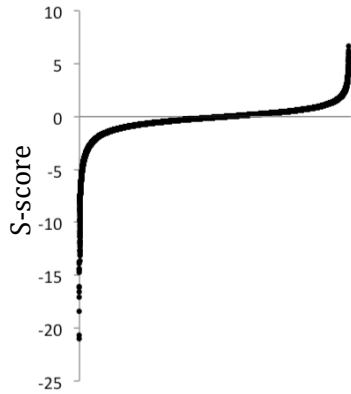


Figure 1: *A plot of all the S-scores in the 4-marker ubiquitin SGA. All the S-scores in the 4-marker ubiquitin SGA were plotted in increasing order from left to right along the X-axis.*

4.2 Quality Determination

To determine the reproducibility and robustness of the data, the Pearson correlation coefficient between two biological replicates of the screen was calculated and found to be within the range of previous SGA screens, albeit somewhat lower than some SGA studies. This fact is an important consideration for the design and interpretation of SGA screens. In contrast to many previously reported SGA studies which analyze the genetic interactions of hundreds or thousands of functionally-related gene deletions in a symmetrical fashion, the 4-marker SGA described here consisted of only 17 query strains that were mated to an unbiased array of deletion strains. Both of these peculiarities of the screen have the effect of diminishing the number of true genetic interactions and increasing noise in the dataset relative to other SGA studies, thereby leading to a slightly smaller Pearson correlation coefficient.

An additional comprehensive approach to evaluate the quality was therefore employed. Genes whose protein products physically interact are more likely have similar genetic interactions due to their related biological functions. The enrichment of genetic interaction similarities was compared between gene pairs that are known to interact physically and those that do not have reported physical interactions. Proteins were

considered to physically interact if they had a 'PE' score greater than 2 in Collins *et al*, 2007. As expected, the genetic interactions of physically interacting gene pairs is significantly higher than among non-interacting gene pairs. This is striking result when the relative small size of the ubiquitin SGA is taken into account. Although the genetic interaction profiles of gene deletions in the ubiquitin SGA include only 17 scores, the screen is similarly enriched for genetic similarity within physically interacting gene pairs as the published chromosome biology E-MAP [44], wherein the genetic interaction profiles contain over 700 scores and is biased for genes with known related functions.

Unbiased hierarchical clustering orders the mutant strains relative to each other based on the similarity of their genetic interactions. Typically, hierarchical clustering is visualized with a dendrogram tree diagram, where the most similar strains are placed next to each other. Genes that function in the same pathway or have similar functions are expected to have similar genetic interactions due to their related biological function. They are therefore more likely to cluster in the dataset. Evaluation of the degree to which known gene modules are clustered in the SGA can serve as a qualitative measure of the robustness and biological significance of the data. The ubiquitin SGA dataset was clustered using the open source software, Cluster 3.0 (Settings: uncentered correlation, average linkage), which is freely available for download at <http://bonsai.hgc.jp/~mdehoon/software/cluster/software.htm#ctv> for use with Windows, Macintosh, and Linux operating systems.

5. Identification and characterization of genetic interactions

Large screens such as the one described here uncover thousands of candidate genetic interactions. Comprehensive approaches to estimate the quality and biological significance of the dataset as whole are described above, in Section 4. It can be an overwhelming endeavor to interpret the biological significance of the myriad of

interactions for each mutant in the screen. Approaches to extract functional and biological significance from genetic interaction datasets are proposed below.

5.1 Identification of hits specific to individual ubiquitin lysine mutants

We were most interested in genes whose deletions had genetic interactions with individual ubiquitin lysine mutants, rather than with multiple lysines. To identify those gene deletions, all the S-scores for each single ubiquitin lysine mutants were compared to the average S-scores for all other ubiquitin mutants not carrying the individual lysine mutation being analyzed. For example, the S-scores of the K11R ubiquitin mutant were compared to the average the S-scores of every other ubiquitin mutant not carrying mutations of K11 (K6R, K27R, K27, 33R, etc.). This analysis revealed gene whose deletions led to genetic interactions specifically with the K11R ubiquitin mutation.

5.2 Functional characterization of individual genetic interactions

A powerful method to rapidly characterize the genetic interactomes of the ubiquitin mutants is the use of Gene Ontology (GO) Enrichment analysis. An arbitrary cutoff of S-scores of -2 or smaller was applied, and all gene deletions having S-scores meeting that criterion for each ubiquitin mutant were analyzed for the enrichment of biological process GO terms (BP-Direct) using the Database for Annotation, Visualization and Integrated Discovery (DAVID) tool which is freely available and can be accessed online at <https://david.ncifcrf.gov/> [45,46].

5.3 Functional analysis of genetic interactomes

The analysis of individual genetic interactions can be a powerful approach to generate hypotheses about the functions of ubiquitin linkage types. For example, a negative genetic interaction between a gene deletion and a specific ubiquitin lysine mutant would point to functional redundancy between the gene and ubiquitin linkage type. However, the interpretation of isolated genetic interactions can be complicated due to pleiotropy and non-specific effects of the mutations being studied. Thus, an approach that takes into account all the genetic interactions for a particular ubiquitin mutant in the screen would provide a more comprehensive functional analysis. The deletions of genes that function with a specific ubiquitin linkage in a given pathway are likely to have genetic interactions that are similar to that linkage type. To identify gene deletions that had similar genetic interactions to the ubiquitin mutants in the 4-marker SGA, the genetic interactomes of the ubiquitin mutants were compared to a large yeast genetic interaction network containing comprehensive interactomes of thousands of gene deletions in yeast [47]. Genes that have the most similar genetic interactomes to a given ubiquitin linkage type are likely to function in the same pathway as that chain type. Likewise, genes that are most similar to a particular ubiquitin linkage types may reveal the major, or at least the most phenotypic functions of a given lysine of ubiquitin.

6. Validation of genetic interactions

Prior to investing time and resources to study the molecular basis of any given genetic interaction, it is advisable to independently validate genetic interactions of interest. While high throughput methods to independently validate interactions are possible, a low throughput approach to validate a small number of genetic interactions of interest by is outlined below.

6.1 Mating

To recreate the double mutant strains (carrying a gene deletion and ubiquitin mutant) that exhibited a genetic interaction of interest in the screen, ubiquitin mutant strains were crossed to the relevant gene deletions from the SK1 deletion array. This was done by mixing roughly equal amounts of cells onto YM-1 plates (supplemented with 2% dextrose) and incubating at 30°C overnight. Importantly, prior to mating, cells were taken directly from frozen stocks and grown at 30°C on YM-1 plates supplemented with 3% glycerol to avoid petites which occur at a high rate in the SK1 strain. As in the screen, single colonies were not used for mating.

6.2 Sporulation

The high efficiency of sporulation exhibited by the SK1 strain obviates the need to select for diploids when looking at individual genetic interactions (assuming sufficient mating occurs), and also simplifies the sporulation protocol relative to other common laboratory yeast strains. Following overnight incubation of mating mixes as described above, a small patch of the mixture was transferred to 2ml of sporulation media. Sporulation cultures were incubated at 23°C with light rotation. Spores appear in the cultures relatively quickly, and in sufficient numbers to allow tetrad dissection in as little as 16 hours in our experience. However, usually, the cultures were incubated at 23°C for 3 days prior to tetrad dissection to facilitate the dissection process.

6.3 Tetrad dissection

The efficiency of sporulation was determined by examining the cultures under a light microscope. Tetrads are easily identifiable by their characteristic shape, which includes four small spores attached to each other, usually in tetrahedral organization.

200ul of each sporulation culture were centrifuged on a tabletop microcentrifuge at maximum speed for 30 seconds. 180ul of supernatant were removed, and the cell pellet was resuspended in the remaining 20ul of media. 2ul of zymolase (20mg/ml stock) was mixed with the cell suspension to digest the ascus that contains the 4 spores. The mixtures were incubated at room temperature for 10 minutes. 1ml of cold water was then added to halt digestion. 30ul of the mixture were spread in a straight line across the middle of a YM-1 plate supplemented with 2% dextrose. The liquid was allowed to dry prior to manually dissecting tetrads. Dissection plates were incubated at 30°C for 3 days.

The final haploid spores needed to carry all the modified ubiquitin loci and a gene deletion (when analyzing double mutants). In addition to those loci, a mating type and haploid selectable marker also segregated in the crosses. To simplify analysis and facilitate downstream experiments, only spores carrying all modified ubiquitin loci and the gene deletion (when desired) were analyzed, and any spores also the carrying mating type and haploid selectable marker cassette (disruption of the *CAN1* locus with the spHis5 driven by the Mat a-specific STE2 promoter) were discarded. A small percentage of spores carried the desired genotype, which was determined by replica-plating onto appropriate plates. Importantly, the dissection plates were also replica-plated onto glycerol-containing YM-1 plates to discard petites.

Because such a small percentage of spores have desired genotypes, the work of dissecting tetrads can rapidly become overwhelming and tedious. We therefore took an alternative approach when validating multiple interactions rapidly. We generated diploid strains homozygous for the modified ubiquitin loci engineered for the screen by mating strains of the opposite mating type and selecting diploids. Because the parent haploid ubiquitin mutant strains were isogenic (except for the mating type), diploids were selected manually by their distinctive appearance under a light microscope and confirmed by their lack of an ability to mate to mating type-tester strains. Gene deletion cassettes were then amplified by PCR from the SK1 deletion array and used to transform desired

homozygous ubiquitin mutant diploids. Mutants were selected on YM-1 plates containing 2% dextrose and the appropriate selection drug (usually G418). *UBI4* is known to be essential for meiotic progression. Surprisingly, the engineered ubiquitin loci, which express high levels of ubiquitin under the control of the GPD promoter, were unable to support meiotic progression. This was true even for diploids expressing wild type ubiquitin. To allow the diploids to undergo meiosis, the diploids were transformed with a 2-micron plasmid that carried the *UBI4* ORF and promoter. Following sporulation, the cells rapidly lost the plasmid in non-selective media.

6.4 Spot dilution assays to validate genetic interactions

Genetic interactions are defined as a deviation from the expected double mutant phenotype, which is estimated by taking the product of the single mutant parent phenotypes. In the SGA protocol, the phenotypes of all the single mutant strains are not actually measured as that would be labor intensive and introduce significant error. Instead, the phenotypes of the single mutant parent strains are estimated by taking into account the growth phenotypes of all double mutant strains in the screen carrying any given mutation. This estimate is valid due to the empirical fact that genetic interactions are rare. For example, the phenotype of the K11R ubiquitin mutant can be estimated by determining the typical phenotype of the thousands of double mutants in the screen carrying a gene deletion along with mutation of K11. When validating a specific genetic interaction, however, it is possible to compare the double mutant strain of interest to the single mutant parent strains.

For any given genetic interaction of interest, the appropriate double mutant strain, carrying all the mutant ubiquitin loci and a gene deletion, was generated as described above. Likewise, the corresponding single mutant strains (i.e. a strain carrying only the mutant ubiquitin loci, and a strain carrying the gene deletion and modified ubiquitin loci

expressing wild type ubiquitin) were generated as described above. To compare the growth phenotype of the double mutant strain to the single mutant phenotypes, overnight cultures were grown at 30°C. The optical density of the saturated cultures was then measured, and their densities normalized to OD600 of 1. 5-fold dilutes were then generated, and a small volume (3-6ul) was transferred onto agar plates using a multichannel micropipette. Plates were then allowed to dry prior to placing in a 30°C incubator. Images of the plates were recorded by scanning the plates on a Hewlett-Packard scanner every 24 hours up to 3 days after initial plating.

An important consideration when validating genetic interactions from a screen such as the 4-marked ubiquitin SGA described here is the fact the genetic interactions in the screen is carried out on selective plates lacking certain nutrients and containing drugs. Even though the final cells carry all necessary markers to survive and grow on the selective media, the growth conditions are inherently stressful. Therefore, some true genetic interactions will not be detected when cells are grown on rich YM-1 plates with dextrose (2%) at 30°C. To rule out any given genetic interaction as being a false positive, it is necessary to reproduce the conditions of the screen as faithfully as possible. When validating genetic interactions, it is often convenient to plate the 5-fold dilutions of the strains of interest on several plates containing different nutrients or drugs, and also incubating various plates at different temperatures (30°C, 37°C). An example is shown in **Figure 2**, wherein the strong synthetic interaction between the K6R ubiquitin mutant and deletion of *UBP6* identified in the screen (S-score of -7.05) is detectable only with increasing amounts of canavanine.

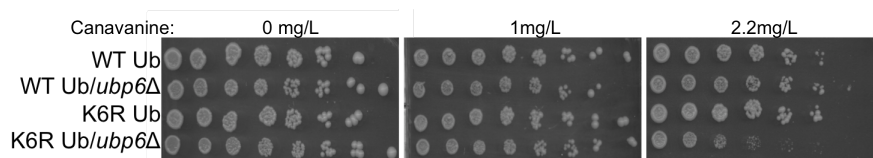


Figure 2: The conditional nature of some genetic interactions. A synthetic interaction between mutation of K6 of ubiquitin and deletion of *UBP6* was identified in the 4-marker SGA. The interaction was validated by spot dilution assays on CSM plates containing the indicated concentration of canavanine.

The interpretation of spot dilution assays is done by comparing the growth of each single mutant to the growth the double mutant strain. Because the cultures are normalized to the same number of cells prior to generating 5-fold dilutions and plating, the number of colonies observable at higher dilutions can be compared to determine whether more (or less) cell death is observed in the double mutant relative to the single mutant strains. The size of the colonies is also analyzed to determine whether the single and double mutant cells grow at different rates.

7. Concluding remarks

The redundancy between ubiquitin linkage types, the lack of biochemical tools, and their relatively low abundance have all hampered the study of atypical polyubiquitin chains [2]. The analysis of genetic interactions is a powerful approach to study functional relationships between genes that are phenotypic, thereby facilitating the discovery of physiologically important functions of genes. The synthetic genetic array (SGA) described here represents the first comprehensive genetic analysis of lysine-to-arginine ubiquitin mutant alleles. Furthermore, the methodology that was developed to carry out the SGA and follow up of hits can be applied to the study of other pathways with complex relationships between genes.

References

1. Finley D, Ulrich HD, Sommer T, Kaiser P. The Ubiquitin–Proteasome System of *Saccharomyces cerevisiae*. *Genetics*. 2012;192: 319–360.
doi:10.1534/genetics.112.140467
2. Xu P, Duong DM, Seyfried NT, Cheng D, Xie Y, Robert J, et al. Quantitative Proteomics Reveals the Function of Unconventional Ubiquitin Chains in Proteasomal Degradation. *Cell*. 2009;137: 133–145.
doi:10.1016/j.cell.2009.01.041
3. Finley D, Sadis S, Monia BP, Boucher P, Ecker DJ, Crooke ST, et al. Inhibition of proteolysis and cell cycle progression in a multiubiquitination-deficient yeast mutant. *Mol Cell Biol*. 1994;14: 5501–5509.
4. Hoegge C, Pfander B, Moldovan G-L, Pyrowolakis G, Jentsch S. RAD6-dependent DNA repair is linked to modification of PCNA by ubiquitin and SUMO. *Nature*. 2002;419: 135–141. doi:10.1038/nature00991
5. Spence J, Sadis S, Haas AL, Finley D. A ubiquitin mutant with specific defects in DNA repair and multiubiquitination. *Mol Cell Biol*. 1995;15: 1265–1273.
6. Harper JW, Elledge SJ. The DNA Damage Response: Ten Years After. *Mol Cell*. 2007;28: 739–745. doi:10.1016/j.molcel.2007.11.015

7. Wang B, Elledge SJ. Ubc13/Rnf8 ubiquitin ligases control foci formation of the Rap80/Abraxas/Brca1/Brcc36 complex in response to DNA damage. *Proc Natl Acad Sci U S A*. 2007;104: 20759–20763. doi:10.1073/pnas.0710061104
8. Lauwers E, Jacob C, André B. K63-linked ubiquitin chains as a specific signal for protein sorting into the multivesicular body pathway. *J Cell Biol*. 2009;185: 493–502. doi:10.1083/jcb.200810114
9. MacGurn JA, Hsu P-C, Emr SD. Ubiquitin and membrane protein turnover: from cradle to grave. *Annu Rev Biochem*. 2012;81: 231–259. doi:10.1146/annurev-biochem-060210-093619
10. Ordureau A, Heo J-M, Duda DM, Paulo JA, Olszewski JL, Yanishevski D, et al. Defining roles of PARKIN and ubiquitin phosphorylation by PINK1 in mitochondrial quality control using a ubiquitin replacement strategy. *Proc Natl Acad Sci U S A*. 2015;112: 6637–6642. doi:10.1073/pnas.1506593112
11. Deng L, Wang C, Spencer E, Yang L, Braun A, You J, et al. Activation of the I κ B kinase complex by TRAF6 requires a dimeric ubiquitin-conjugating enzyme complex and a unique polyubiquitin chain. *Cell*. 2000;103: 351–361.
12. Grabbe C, Husnjak K, Dikic I. The spatial and temporal organization of ubiquitin networks. *Nat Rev Mol Cell Biol*. 2011;12: 295–307. doi:10.1038/nrm3099

13. Wang C, Deng L, Hong M, Akkaraju GR, Inoue J, Chen ZJ. TAK1 is a ubiquitin-dependent kinase of MKK and IKK. *Nature*. 2001;412: 346–351.
doi:10.1038/35085597
14. Manzanillo PS, Ayres JS, Watson RO, Collins AC, Souza G, Rae CS, et al. The ubiquitin ligase parkin mediates resistance to intracellular pathogens. *Nature*. 2013;501: 512–516. doi:10.1038/nature12566
15. Matsumoto ML, Wickliffe KE, Dong KC, Yu C, Bosanac I, Bustos D, et al. K11-linked polyubiquitination in cell cycle control revealed by a K11 linkage-specific antibody. *Mol Cell*. 2010;39: 477–484. doi:10.1016/j.molcel.2010.07.001
16. Dammer EB, Na CH, Xu P, Seyfried NT, Duong DM, Cheng D, et al. Polyubiquitin Linkage Profiles in Three Models of Proteolytic Stress Suggest the Etiology of Alzheimer Disease. *J Biol Chem*. 2011;286: 10457–10465.
doi:10.1074/jbc.M110.149633
17. Akutsu M, Dikic I, Bremm A. Ubiquitin chain diversity at a glance. *J Cell Sci*. 2016;129: 875–880. doi:10.1242/jcs.183954
18. Nishikawa H, Ooka S, Sato K, Arima K, Okamoto J, Klevit RE, et al. Mass spectrometric and mutational analyses reveal Lys-6-linked polyubiquitin chains catalyzed by BRCA1-BARD1 ubiquitin ligase. *J Biol Chem*. 2004;279: 3916–3924.
doi:10.1074/jbc.M308540200

19. Christensen DE, Brzovic PS, Klevit RE. E2-BRCA1 RING interactions dictate synthesis of mono- or specific polyubiquitin chain linkages. *Nat Struct Mol Biol.* 2007;14: 941–948. doi:10.1038/nsmb1295
20. Ordureau A, Sarraf SA, Duda DM, Heo J-M, Jedrychowski MP, Sviderskiy VO, et al. Quantitative Proteomics Reveal a Feedforward Mechanism for Mitochondrial PARKIN Translocation and Ubiquitin Chain Synthesis. *Mol Cell.* 2014;56: 360–375. doi:10.1016/j.molcel.2014.09.007
21. Birsa N, Norkett R, Wauer T, Mevissen TET, Wu H-C, Foltynie T, et al. Lysine 27 ubiquitination of the mitochondrial transport protein Miro is dependent on serine 65 of the Parkin ubiquitin ligase. *J Biol Chem.* 2014;289: 14569–14582. doi:10.1074/jbc.M114.563031
22. Geisler S, Holmström KM, Skujat D, Fiesel FC, Rothfuss OC, Kahle PJ, et al. PINK1/Parkin-mediated mitophagy is dependent on VDAC1 and p62/SQSTM1. *Nat Cell Biol.* 2010;12: ncb2012. doi:10.1038/ncb2012
23. Zhou H-L, Geng C, Luo G, Lou H. The p97–UBXD8 complex destabilizes mRNA by promoting release of ubiquitinated HuR from mRNP. *Genes Dev.* 2013;27: 1046–1058. doi:10.1101/gad.215681.113
24. Yuan W-C, Lee Y-R, Lin S-Y, Chang L-Y, Tan YP, Hung C-C, et al. K33-Linked Polyubiquitination of Coronin 7 by Cul3-KLHL20 Ubiquitin E3 Ligase Regulates Protein Trafficking. *Mol Cell.* 2014;54: 586–600. doi:10.1016/j.molcel.2014.03.035

25. Dixon SJ, Costanzo M, Baryshnikova A, Andrews B, Boone C. Systematic mapping of genetic interaction networks. *Annu Rev Genet.* 2009;43: 601–625.
doi:10.1146/annurev.genet.39.073003.114751
26. Tong AH, Evangelista M, Parsons AB, Xu H, Bader GD, Pagé N, et al. Systematic genetic analysis with ordered arrays of yeast deletion mutants. *Science.* 2001;294: 2364–2368. doi:10.1126/science.1065810
27. Tong AHY, Lesage G, Bader GD, Ding H, Xu H, Xin X, et al. Global Mapping of the Yeast Genetic Interaction Network. *Science.* 2004;303: 808–813.
doi:10.1126/science.1091317
28. Schuldiner M, Collins SR, Thompson NJ, Denic V, Bhamidipati A, Punna T, et al. Exploration of the Function and Organization of the Yeast Early Secretory Pathway through an Epistatic Miniarray Profile. *Cell.* 2005;123: 507–519.
doi:10.1016/j.cell.2005.08.031
29. Braberg H, Jin H, Moehle EA, Chan YA, Wang S, Shales M, et al. From Structure to Systems: High-Resolution, Quantitative Genetic Analysis of RNA Polymerase II. *Cell.* 2013;154: 775–788. doi:10.1016/j.cell.2013.07.033
30. Costanzo M, Baryshnikova A, Bellay J, Kim Y, Spear ED, Sevier CS, et al. The genetic landscape of a cell. *Science.* 2010;327: 425–431.
doi:10.1126/science.1180823

31. Costanzo M, VanderSluis B, Koch EN, Baryshnikova A, Pons C, Tan G, et al. A global genetic interaction network maps a wiring diagram of cellular function. *Science*. 2016;353. doi:10.1126/science.aaf1420
32. Sarin S, Ross KE, Boucher L, Green Y, Tyers M, Cohen-Fix O. Uncovering Novel Cell Cycle Players Through the Inactivation of Securin in Budding Yeast. *Genetics*. 2004;168: 1763–1771. doi:10.1534/genetics.104.029033
33. Tong AHY, Boone C. Synthetic genetic array analysis in *Saccharomyces cerevisiae*. *Methods Mol Biol Clifton NJ*. 2006;313: 171–192.
34. Collins SR, Roguev A, Krogan NJ. Quantitative Genetic Interaction Mapping Using the E-MAP Approach. *Methods Enzymol*. 2010;470: 205–231. doi:10.1016/S0076-6879(10)70009-4
35. Haber JE, Braberg H, Wu Q, Alexander R, Haase J, Ryan C, et al. Systematic Triple-Mutant Analysis Uncovers Functional Connectivity between Pathways Involved in Chromosome Regulation. *Cell Rep*. 2013;3: 2168–2178. doi:10.1016/j.celrep.2013.05.007
36. Ben-Ari G, Zenvirth D, Sherman A, David L, Klutstein M, Lavi U, et al. Four Linked Genes Participate in Controlling Sporulation Efficiency in Budding Yeast. *PLoS Genet*. 2006;2. doi:10.1371/journal.pgen.0020195

37. Boeke JD, LaCroute F, Fink GR. A positive selection for mutants lacking orotidine-5'-phosphate decarboxylase activity in yeast: 5-fluoro-orotic acid resistance. *Mol Gen Genet MGG*. 1984;197: 345–346.
38. Hanna J, Leggett DS, Finley D. Ubiquitin depletion as a key mediator of toxicity by translational inhibitors. *Mol Cell Biol*. 2003;23: 9251–9261.
39. Finley D, Bartel B, Varshavsky A. The tails of ubiquitin precursors are ribosomal proteins whose fusion to ubiquitin facilitates ribosome biogenesis. *Nature*. 1989;338: 394–401. doi:10.1038/338394a0
40. Ozkaynak E, Finley D, Solomon MJ, Varshavsky A. The yeast ubiquitin genes: a family of natural gene fusions. *EMBO J*. 1987;6: 1429–1439.
41. Partow S, Siewers V, Bjørn S, Nielsen J, Maury J. Characterization of different promoters for designing a new expression vector in *Saccharomyces cerevisiae*. *Yeast Chichester Engl*. 2010;27: 955–964. doi:10.1002/yea.1806
42. Deutschbauer AM, Davis RW. Quantitative trait loci mapped to single-nucleotide resolution in yeast. *Nat Genet*. 2005;37: ng1674. doi:10.1038/ng1674
43. Collins SR, Schuldiner M, Krogan NJ, Weissman JS. A strategy for extracting and analyzing large-scale quantitative epistatic interaction data. *Genome Biol*. 2006;7: R63. doi:10.1186/gb-2006-7-7-r63

44. Collins SR, Miller KM, Maas NL, Roguev A, Fillingham J, Chu CS, et al. Functional dissection of protein complexes involved in yeast chromosome biology using a genetic interaction map. *Nature*. 2007;446: 806–810. doi:10.1038/nature05649
45. Huang DW, Sherman BT, Lempicki RA. Systematic and integrative analysis of large gene lists using DAVID bioinformatics resources. *Nat Protoc*. 2009;4: 44–57. doi:10.1038/nprot.2008.211
46. Huang DW, Sherman BT, Lempicki RA. Bioinformatics enrichment tools: paths toward the comprehensive functional analysis of large gene lists. *Nucleic Acids Res*. 2009;37: 1–13. doi:10.1093/nar/gkn923
47. Ryan CJ, Roguev A, Patrick K, Xu J, Jahari H, Tong Z, et al. Hierarchical Modularity and the Evolution of Genetic Interactomes across Species. *Mol Cell*. 2012;46: 691–704. doi:10.1016/j.molcel.2012.05.028

Chapter 3

A Top-Down Mass Spectrometry-based method to identify substrates of polyubiquitin chains

The ubiquitin field has relied heavily on proteomics methods to identify proteins that are ubiquitinated. The combination of genetics with quantitative mass spectrometry, for example, can reveal proteins that are stabilized by disruptions to ubiquitin ligases or conjugating enzymes. Proteomics can also reveal the specific lysines that are modified on a protein due to the glycine-glycine (GG) motif that remains covalently linked to ubiquitinated lysines following digestion with trypsin, a necessary step preceding protein analysis by mass spectrometry. Cell Signaling Technology Inc. developed an antibody that specifically binds the GG motif on ubiquitinated lysines. This antibody, termed the ubiquitin-remnant antibody, has been an invaluable tool in the search for ubiquitinated proteins as it permits the enrichment of modified peptides prior to analysis by mass spectrometry.

The focus of this dissertation work has been to understand the functions of atypical polyubiquitin chains in *Saccharomyces cerevisiae*. To understand their functions, it is necessary to find the substrate proteins they modify. However, current proteomics methods are limited in their ability to provide information about the type of ubiquitin chains on substrates. The typical method used to identify ubiquitinated proteins involves the digestion of proteins with trypsin, an enzyme that cleaves proteins at arginine and lysine residues. This generates peptides of an appropriate size for proteomics analysis. This process necessarily destroys information about the type of ubiquitin chain on proteins, as an arginine residue exists immediately upstream of the GG motif of ubiquitin.

A careful consideration of the primary structure of ubiquitin revealed that the use of enzymes other than trypsin, which cleaves proteins at both arginine and lysine residues, could preserve ubiquitin linkage type information for analysis by mass spectrometry. The proteases Lys-C and Lys-N cleave proteins on the carboxyl or amino terminal sides, respectively, of lysine residues only. Thus, for a protein modified with a chain of polyubiquitin, Lys-C or Lys-N cleaves at every unconjugated lysine residue of ubiquitin and the modified substrate. Lysines that are modified by ubiquitin on either the substrate or on the ubiquitin chain are not cleaved. In the specific case of a homogenous lysine 63-linked polyubiquitin chain, because there are no lysines between K63 and the C-terminus of ubiquitin, the chain will be preserved on the substrate.

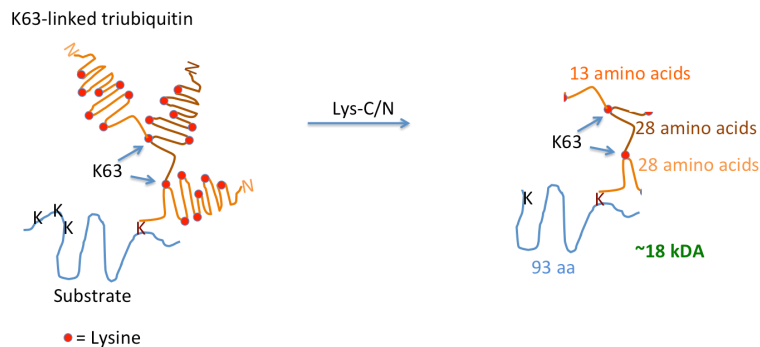


Figure 1: The proteolysis of a K63-polyubiquitinated substrate with Lys-C/N. A substrate is polyubiquitinated with a chain of three ubiquitin protomers, linked at lysine 63 of ubiquitin. Following digestion with Lys-C or Lys-N, the substrate and ubiquitins are cleaved at every available lysine residue, yielding the product shown.

While the use of Lys-C or Lys-N to preserve the linkage type information on a digested peptide solves an important theoretical hurdle in the ubiquitin field, it also generates new practical problem: The peptides arising from Lys-C/N digestion are large relative to the tryptic peptides that are conventionally analyzed by mass spectrometry. For example, the peptide corresponding to a typical protein conjugated to a tri-ubiquitin chain on a single substrate lysine will be close to 20kDA, exceedingly large for

conventional mass spectrometry. The application of ‘top-down’ or whole protein proteomics could solve this problem [1].

Top-down proteomics is an emerging methodology in the field of protein research by mass spectrometry. Important advances in mass spectrometer technology and protein separation methods have rendered the analysis of whole proteins by mass spectrometry feasible [2]. A landmark publication by the Kelleher laboratory, for example, analyzed the intact proteome of HeLa cells identified 1,043 proteins, and a multitude of post-translational modification events [3]. Importantly, the investigators identified whole proteins that were over 100kDa in mass, with the most readily identified proteins had a mass of between 10 and 30 kDa. As diagramed above, following digestion, a tri-ubiquitin chain would have an approximate mass of 7.6kDa. Each additional ubiquitin in the chain would increase the mass of the polyubiquitin chain following digestion by about 3kDa. The mass of the peptide corresponding to the polyubiquitinated substrate will vary depending on the distribution of lysine residues on the protein, with the average peptide being approximately 20kDa. Thus, a typical polyubiquitinated peptide with a chain of three ubiquitins would have a mass of about 10kDa. This mass, as well as those of peptides with much longer polyubiquitin chains, is well within the mass-ranges that have been identified successfully with top-down proteomics methods [4].

Theoretically, Lys-C and Lys-N are equal in their utility for the purposes described above—they both cleave proteins specifically at lysine residues. An important practical consideration makes Lys-N a superior choice for the methodology being developed. Glutamine and glutamate residues found on the amino terminus of a polypeptide can spontaneously convert to pyroglutamate [3,4]. Cleavage on the carboxy-

terminal side of lysine 48 of ubiquitin by Lys-C would expose a N-terminal glutamine residue. Similarly, cleavage on the C-terminal side of lysine 63 of ubiquitin would reveal an N-terminal glutamate. Incomplete or variable conversion of these N-terminal residues to pyroglutamate would severely complicate the analysis of the resulting peptides, as the same peptide would present with a different mass depending on whether each N-terminal glutamine and glutamate is converted to pyroglutamate. In contrast, the cleavage of ubiquitinated peptides with Lys-N, which cleaves on the N-terminal side of lysine residues, will always lead to lysine as the N-terminal residue on the resulting cleaved peptide. The use of Lys-N in the methodology proposed herein facilitates the identification of ubiquitinated proteins by top-down mass spectrometry by abrogating the need to enzymatically convert all N-terminal glutamine and glutamate residues to pyroglutamate to ensure complete conversion [4], or to account for the variable conversion of glutamate and glutamine to pyroglutamate computationally. Nonetheless, Lys-C was used in several proof-of-concept experiments, as pyroglutamate conversion does not affect the analysis of proteins by SDS-PAGE.

While Lys-C and Lys-N are well-characterized enzymes, they are not as broadly utilized in mass spectrometry as is the enzyme trypsin. A crucial aspect of the method proposed here is the specific cleavage of proteins exclusively at lysine residues. Off-target cleavage of ubiquitinated proteins, for example at arginine residues, would abrogate the advantages of the technique. Dr. Daniel Finley and colleagues developed a set of yeast strains and plasmids that allow for the inducible repression of wild type ubiquitin, while simultaneously expressing any variant of ubiquitin desired [5]. Using this system, ubiquitin wherein all lysines were mutated to arginine (K0), all lysines except for

K48 were mutated to arginine (K48-only), or wild type ubiquitin were expressed in cells. Total ubiquitin was purified from cell lysates using the polyubiquitin-binding reagent, Tube 1, from LifeSensors Inc., in the manufacturer-recommended buffer (50mM Tris-HCl, pH 7.5, 0.15M NaCl, 1mM EDTA, 1% NP-40, 10% glycerol). Total ubiquitin was then eluted using 0.2% Rapigest in water (w/v) and diluted to 0.1% Rapigest in a suitable buffer for digestion with Lys-C (100mM ammonium bicarbonate). To half of the elute, Lys-C enzyme was added at approximately a 1:100 ratio (enzyme:total protein) and incubated overnight at room temperature. Samples were analyzed by SDS-PAGE followed by western blotting for ubiquitin.

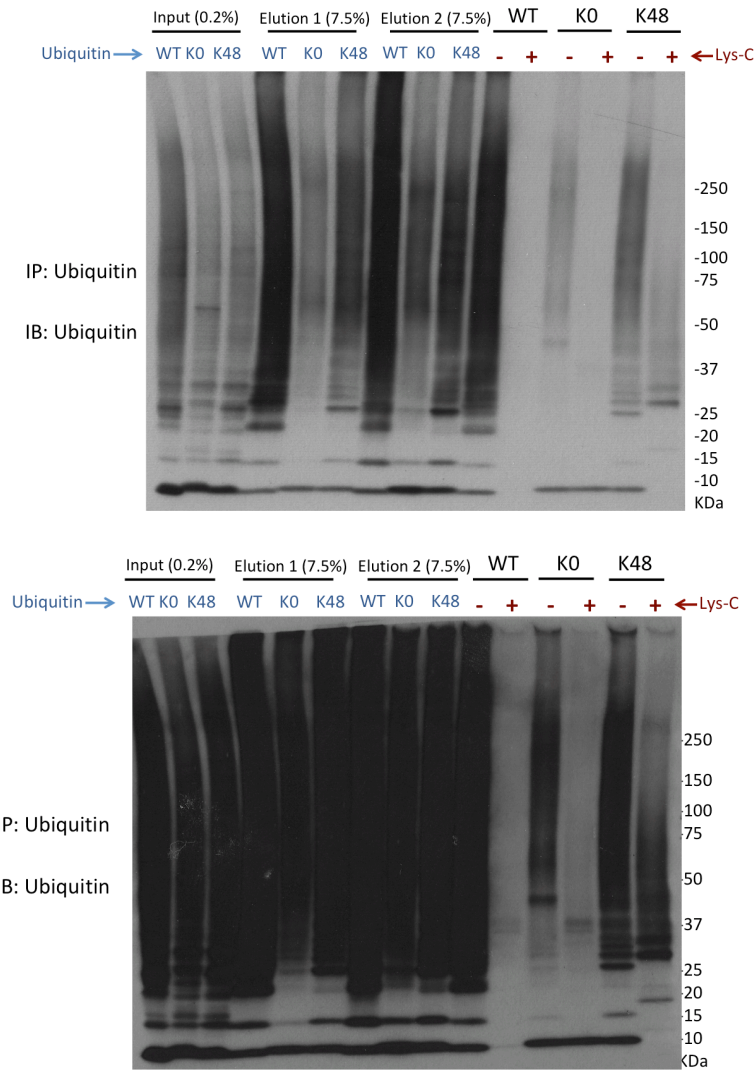


Figure 2: Digestion of total ubiquitin with Lys-C. Total ubiquitin from yeast strains expressing the indicated ubiquitin variants was isolated using a polyubiquitin-binding resin. The eluate was digested with Lys-C when noted, and analyzed by SDS-PAGE followed by western blotting for ubiquitin. Two exposures, light (top) and dark (bottom), are shown.

The Tube 2 ubiquitin-binding reagent efficiently purifies free and conjugated ubiquitin. It is evident that Lys-C efficiently cleaves the proteins in the eluate in all three tested strains (expressing WT, K0 or K48 ubiquitin). In the case of WT ubiquitin, all signal corresponding to ubiquitin is lost following digestion with Lys-C. As expected for K0 ubiquitin, free ubiquitin is not cleaved (band below 10kDa) due to the lack of lysine

residues. The ubiquitin smear is, however, lost following Lys-C digestion, as proteins that are conjugated to ubiquitin are cleaved at lysines. Crucially, an ubiquitin smear is preserved only in the sample containing K48-only ubiquitin, which likely represents chains of polyubiquitin linked to lysine-48. Importantly, as expected, free K48-only ubiquitin is cleaved by Lys-C at Lysine 48.

To confirm that Lys-N functions similarly to Lys-C, two sources of Lys-N were tested using purifications of WT ubiquitin. Thermo Scientific produces Lys-N that is purified from *Grifola frondosa*. UProtein Express produces recombinant Lys-N. Both enzymes were tested as described above in 100mM ammonium bicarbonate with a final concentration of 0.1% Rapigest. Surprisingly, the enzyme from Thermo Scientific (purified from *G. frondosa*) performs significantly better than the recombinant enzyme from UProtein Express under the stated conditions:

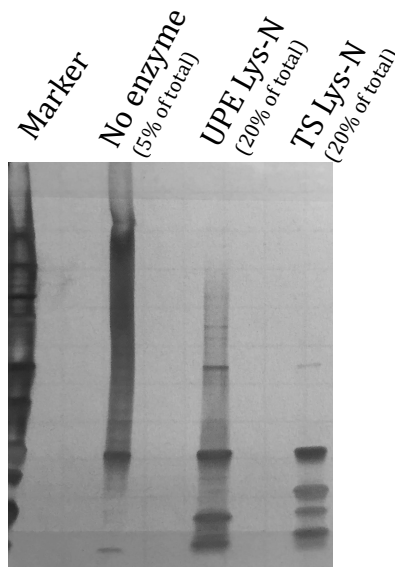


Figure 3: Determination of activity of Lys-N from commercial sources. Total ubiquitin from yeast strains expressing wild type ubiquitin was isolated using a polyubiquitin-binding resin (Tube 1, LifeSensors Inc.). The eluate was digested with Lys-N from either Thermo Scientific (TS) or UProtein Express (UPE) when noted, and analyzed by SDS-PAGE followed by Silver Staining.

The preceding experiments served to validate the activity and specificity of the enzymes Lys-C and Lys-N. The method proposed here requires analysis by mass spectrometry of complex peptide mixtures following digestion of cell lysates with Lys-N. The complexity of the samples, along with the large size of the peptides of interest, makes the analysis of the resulting mass spectrometry data challenging. In consultation with mass spectrometry collaborators in the laboratory of Dr. Neil Kelleher, the protein Sna3 was chosen to serve as a model substrate to be used in proof of principle experiments.

Sna3 is a small membrane protein, with a molecular weight of about 15KDa. Its function remains enigmatic, although it has been proposed to function as an adaptor for the E3 ubiquitin ligase, Rsp5 [6]. Importantly, Sna3 is ubiquitinated at only one of its four lysine residues (K125) with homogenous K63-linked polyubiquitin [7]. Thus, upon digestion with Lys-N, Sna3 modified with K63-linked polyubiquitin at K125 will produce a stereotypical 93-amino acid peptide (after cleavage at the most K125-proximal lysine of Sna3, K50). K125, which is conjugated to polyubiquitin, will not be cleaved by Lys-N. Because the ubiquitin chain conjugated to K125 of Sna3 is linked through lysine 63 of ubiquitin, every substrate-proximal ubiquitin will be cleaved at K48, while the terminal ubiquitin will be cleaved at K63. This yields a defined peptide corresponding to Sna3 that will remain covalently linked to a peptide corresponding to the ubiquitin modification on K125.

To characterize the ubiquitination and cleavage of Sna3 by Lys-N prior to analysis by mass spectrometry, the protein was tagged on its N-terminus with a triple Flag epitope tag. The protein was then purified using anti-Flag antibody beads and said

eluate was subjected to Lys-N-mediated proteolysis. The resulting peptide mixture was further purified using the UbiSight antibody (LifeSensors Inc.), which binds the C-terminus of ubiquitin. This final purification step allowed for the enrichment of peptides linked to ubiquitin, which is likely to significantly simplify the analysis of the peptide mixture by mass spectrometry and facilitate identification of substrates. The described experiments analyzed by SDS-PAGE followed by Silver Staining and western blotting:

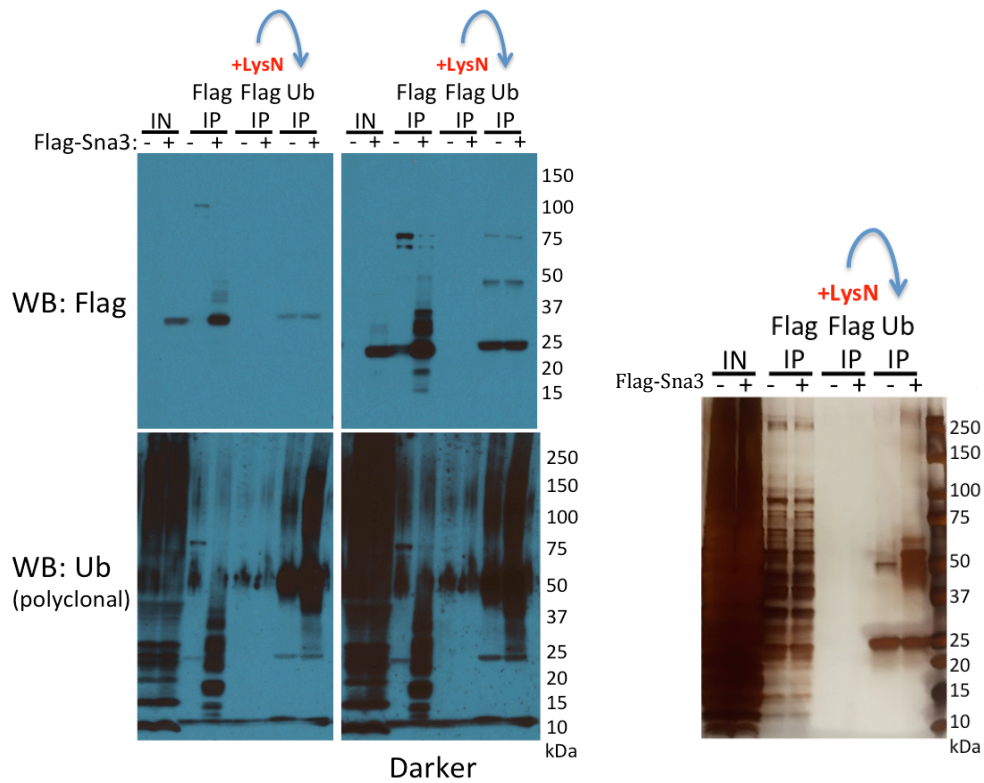


Figure 4: Digestion of purified Sna3 with Lys-N. Flag-Sna3 was purified from otherwise WT yeast strains using bead-conjugated anti-Flag antibody. The eluate was subjected to proteolysis by Lys-N (as noted) and ubiquitinated peptides were enriched using the UbiSight antibody. Samples were analyzed by SDS-PAGE followed by western blotting as indicated, or by silver staining.

References

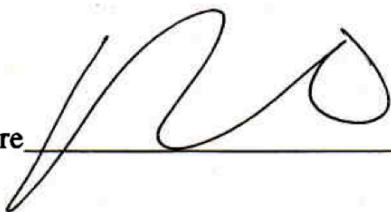
1. Catherman AD, Skinner OS, Kelleher NL. Top Down proteomics: facts and perspectives. *Biochem Biophys Res Commun.* 2014;445: 683–693.
doi:10.1016/j.bbrc.2014.02.041
2. Tran JC, Zamdborg L, Ahlf DR, Lee JE, Catherman AD, Durbin KR, et al. Mapping intact protein isoforms in discovery mode using top-down proteomics. *Nature.* 2011;480: 254–258. doi:10.1038/nature10575
3. Liu YD, Goetze AM, Bass RB, Flynn GC. N-terminal Glutamate to Pyroglutamate Conversion in Vivo for Human IgG2 Antibodies. *J Biol Chem.* 2011;286: 11211–11217. doi:10.1074/jbc.M110.185041
4. Ohtake F, Saeki Y, Ishido S, Kanno J, Tanaka K. The K48-K63 Branched Ubiquitin Chain Regulates NF- κ B Signaling. *Mol Cell.* 2016;64: 251–266.
doi:10.1016/j.molcel.2016.09.014
5. Finley D, Sadis S, Monia BP, Boucher P, Ecker DJ, Crooke ST, et al. Inhibition of proteolysis and cell cycle progression in a multiubiquitination-deficient yeast mutant. *Mol Cell Biol.* 1994;14: 5501–5509.
6. Macdonald C, Stringer DK, Piper RC. Sna3 is an Rsp5 Adaptor Protein that Relies on Ubiquitination for its MVB Sorting. *Traffic Cph Den.* 2012;13: 586–598.
doi:10.1111/j.1600-0854.2011.01326.x

7. Stawiecka-Mirota M, Pokrzywa W, Morvan J, Zoladek T, Haguenaer-Tsapis R, Urban-Grimal D, et al. Targeting of Sna3p to the Endosomal Pathway Depends on Its Interaction with Rsp5p and Multivesicular Body Sorting on Its Ubiquitylation. *Traffic Cph Den.* 2007;8: 1280–1296. doi:10.1111/j.1600-0854.2007.00610.x

Publishing Agreement

It is the policy of the University to encourage the distribution of all theses, dissertations, and manuscripts. Copies of all UCSF theses, dissertations, and manuscripts will be routed to the library via the Graduate Division. The library will make all theses, dissertations, and manuscripts accessible to the public and will preserve these to the best of their abilities, in perpetuity. I hereby grant permission to the Graduate Division of the University of California, San Francisco to release copies of my thesis, dissertation, or manuscript to the Campus Library to provide access and preservation, in whole or in part, in perpetuity.

Author Signature

A handwritten signature in black ink, consisting of a series of loops and curves, written over a horizontal line.

Date 08/30/2018